universität wien

DIPLOMARBEIT

Titel der Diplomarbeit

„The influence of the RNA helicase Mss116 on CBP2-assisted splicing of the bI5 group I intron *in vitro*“

verfasst von

Franka Debeljak

angestrebter akademischer Grad

Magistra der Naturwissenschaften (Mag.rer.nat.)

Wien, 2013

Studienkennzahl lt. Studienblatt:	A 490
Studienrichtung lt. Studienblatt:	Diplomstudium Molekulare Biologie
Betreut von:	Dr. Christina Waldsich

I would like to express my sincere gratitude to Christina Waldsich who gave me the opportunity to be part of her lab group and supported me during my work. Thank you for your encouragement, patience and supporting meetings during the time I spent in your lab and for having an open door for problems.

Thanks to Andreas, Ela, Geta, Lukas, Michael, Nora, Stefan and Verena for you help and support. I will definitely miss the discussions and fun we had not only during our lunches! Special thank to Verena for her friendship and counsel I can count on.

Especially I want to thank my parents, sister and relatives for their support. Thank you to my parents who gave me the possibility to study and supported me the whole time. Thank you for pushing me forward even when I was not confident. Without you I would not be the person I am today.

Also I want to thank my friends who are there for me. Specially Andi, Ines and Kurti whose friendship helped me through tough times and I hope we will travel to all our desired destinations! Andi, thank you for being the brother I never had to me. An extra big thank you to Ines whose friendship I can count on since childhood and who is still putting up with me!

Table of Content

Abbreviations

Amp	ampicillin
APS	ammonium persulfate
ATP	adenosine triphosphate
BSA	bovine serum albumin
CBP2	cytochrome b pre-mRNA processing protein 2 of *S. cerevisiae*
cDNA	complementary desoxyribonucleic acid
CI	chloroform-isoamyl alcohol (24:1)
cob	cytochrome b gene
CP	cell pellet
CspA and E	cold-shock protein A and E
Cyt-18 and 19	tyrosyl-tRNA synthetase
DEAD	amino acid code for D – aspartic acid, E – glutamic acid, A – alanine
DMSO	dimethyl sulfoxide
DNA	desoxyribonucleic acid
dsRNA	double-stranded ribonucleic acid
DTT	dithiothreitol
EDTA	ethylenediaminetetraacetic acid
EtBr	Ethidium bromide
fi	full intron bI5 constuct
GDP	guanosine diphosphate
GMP	guanosine monophosphate
GTP	guanosine triphosphate
GTS	glycerol tris sodiumchloride buffer
HEPES	4-(2-hydroxyethyl)-1-piperazineethanesulfonic acid
His-tag	histidine tag
IGS	internal guide sequence
IPTG	isopropyl- β -D-thiogalactopyranosid
kDa	kilo Dalton

LB	lysogeny broth medium
MMLV-RT	moloney murine leukemia virus reverse transcriptase
mRNA	messenger ribonucleic acid
Mss116	mitochondrial splicing system *S. cerevisiae* protein number 116
mt	mitochondrial
NCp7	nucleocapsid protein of the human immune deficiency virus (HIV)
Ni-NTA	nickel-nitrilotriacetic acid
nt	nucleotide
OD_{600}	optical density at a wavelength of 600 nm
o/n	overnight
ORF	open reading frame
PAGE	polyacrylamide gel electrophoresis
PCR	polymerase chain reaction
PNK	polynucleotide kinase
rc	ribozyme clone bI5 construct
RecA	*E. coli* protein essential for the repair and maintenance of DNA
RNA	ribonucleic acid
RNP	ribonucleoprotein
rpm	revolutions per minute
rRNA	ribosomal ribonucleic acid
RT	reverse transcription
SDS	sodium dodecyl sulfate
SF	super family
SN	supernatant
SOB	super optimal broth medium
ssRNA	single stranded ribonucleic acid
StpA	DNA-binding protein StpA in *E. coli*
TBE	tris borate EDTA buffer
Td	thymidylate synthase gene
TE	tris EDTA solution

TEMED	tetramethylethylendiamin
TERT	Telomerase reverse transcriptase
Tet	tetracycline
Tris	trisamine
tRNA	transfer ribonucleic acid
TSS	transformation storage solution
UTP	uridine triphosphate
wt	wild type
YP(D)	yeast extract peptone (glucose) medium
25/25	bI5 construct with 25nt exons
50/100	bI5 construct with 50nt 5’ exon and 100nt 3’ exon

Introduction

1. The RNA world

First research assumed that DNA and proteins are the important factors of evolution and RNA is just a minor player. In the 1960s this view changed as Crick (1968), Orgel (1986) and Woese (1967) hypothesized the concept of a primordial RNA molecule. However with the discovery of the catalytic ability of RNA by Thomas R.Cech and Sidney Altman, RNA became the centre of attention and its research led to the establishment of the "RNA world" (Cech, 2012). One of the most persuasive arguments for an RNA world is the ability of RNA to provide information as well as functionality. It is known that RNA can be a messenger molecule and functions as a catalyst (Cech, 2009). The RNA world model assumes that at the beginning, a variety of organic molecule complexes were present and evolved randomly, but the lack of self-replication led to their extinction (Fig. 1). RNA was able to overcome this problem by building a construct which over time developed the ability to interact with proteins, leading finally to the formation of DNA and a DNA-based genome that can be found in the last universal common ancestor (LUCA). This model of evolution is widely accepted among scientists. Nevertheless the issue of how RNA developed and whether a pre-RNA molecule existed still splits opinion.

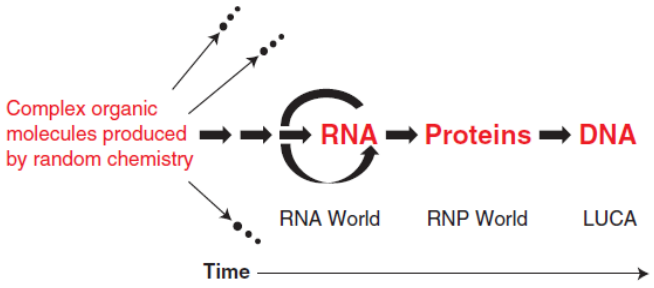

Fig. 1. Concept of the RNA world.
This figure has been adapted from Cech, 2012.

The idea that RNA only plays a role in protein synthesis is no longer accurate. In the past a variety of new RNA classes were discovered, suggesting that RNA is a significant part of the signalling pathway and gene expression. Today it is acknowledged that RNA is significant to all cellular processes playing a regulatory role, though it may also be the cause of a variety of human diseases (Clancy, 2008). A good example of RNA's and accessory protein's influence on diseases is telomerase. Telomerase is a ribonucleoprotein built up from telomerase RNA, telomerase reverse transcriptase and other components that are important for its accumulation, assembly and localization. Telomerase is crucial for the maintenance of the telomere DNA length at the end of chromosomes and is important for the aging process and cancer development. A functional protein can only be obtained if the mRNA is properly folded and correctly spliced. Similarly, the telomerase RNA needs to adopt a specific 3D architecture to be able to associate with the TERT protein. Most mutations concerning telomerase-associated diseases are located in structurally important regions. This shows the importance of RNA structure and folding (Chen & Greider, 2004; Theimer & Feigon, 2006).

2. RNA structure

In order to understand the structure and the associated folding pathway of the RNA, it is important to revisit RNA characteristics. Each RNA molecule is built on nucleotides consisting of a ribose sugar, a phosphate and one of the four bases, adenine (A), cytosine (C), guanine (G) and uracil (U). The four nucleobases can be differentiated in pyrimidines represented by cytosine and uracil and purines with adenine and guanine. The nucleobase (N1 of pyrimidines and N9 of purines) is linked to the 1' carbon atom of the ribose by an N-glycosidic bond. The nucleotides are connected through a phosphodiester bond which links the 5' phosphate group of one ribose sugar to the 3' hydroxyl group of another ribose sugar. Together the ribose sugars linked by phosphates form the RNA backbone which has a 5'→ 3' orientation and is negatively charged due to the phosphate (Doonan & Royal Society of Chemistry (Great Britain), 2004). An important difference to DNA is the presence of a hydroxyl group at the 2' carbon atom of the ribose.

Hydrogen bonds can be formed from the three different edges of the bases. Those edges are known as the Watson-Crick edge, the Hoogsteen edge and the Sugar edge. The Hoogsteen edge applies just to a purine but its equivalent for a pyrimidine is the CH edge. One possibility is that one of these edges interacts with any other edge of another base in cis or in trans orientation depending on the glycosidic bond. In total, 12 different edge-to-edge conformations are possible. One of these conformations is the interaction of the Watson-Crick-edges of two bases known as the canonical base pairing. Adenine and uracil interact by two hydrogen bonds, while guanine and cytosine are connected with three hydrogen bonds. These edge-to-edge interactions are important for the directionality of the RNA. Another way for nucleobases to interact with each other is through stacking. Stacking is crucial to the folding process as well (Leontis et al, 2002; Leontis & Westhof, 1998; Leontis & Westhof, 2001). Through determination of the primary sequence of the RNA it is possible to gain information about the secondary structure. The secondary structure consists of paired and unpaired RNA nucleobases. Watson-Crick base-pairing leads to the formation of double-stranded helices, while unpaired residues are either part of closing loops, internal loops or bulges (Fig. 2) (Abrahams et al, 1990; Moore, 1999). Today these structure motifs can be predicted with the help of different structural prediction programs, using different algorithms (Mathews et al, 2010). The motifs can again interact with each other and assemble the tertiary RNA structure, providing a 3D image. These interactions can occur also between distant RNA sequences, forming kissing loops, pseudoknots and tetraloop – receptor interactions, among others (Butcher & Pyle, 2011).

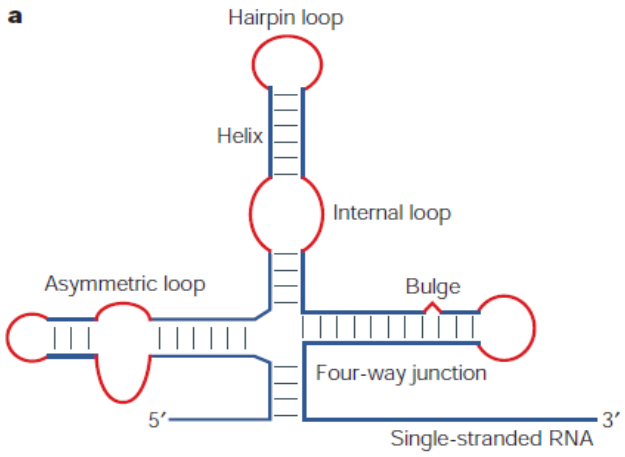

Fig. 2. Secondary structure motifs.
RNA secondary structure is built up of single stranded and double stranded RNA sequences. These regions can form helices, bulges or loops. This figure has been adapted from Schroeder et al, 2004.

3. RNA folding

RNA has to be folded in a specific 3D manner to be able to carry out its proper function. RNA folding starts with the unfolded state forming a stable secondary structure with the help of monovalent ions, reaching an intermediate state. In the presence of divalent ions, the RNA molecule can form tertiary structure and attain its folded state (Draper et al, 2005; Moghaddam et al, 2009; Woodson, 2005). However this folding pathway does not take course without problems. The RNA folding problem predicted by D. Herschlag takes the occurring problems into account. The first problem considers the ability of RNA to fold into an alternative conformation and to become kinetically trapped in it. The second problem is that the tertiary structure is not thermodynamically stable (Herschlag, 1995). Experiments showed that some RNAs, like the *Tetrahymena* group I intron, reach their native form taking different folding pathways (Woodson, 2010; Woodson, 2011). Mostly, different intermediates can form, trapping such RNAs in a stable and compact misfolded state and not being able to carry out its function. The minority of RNA population folds rapidly into their correct form, the majority misfolds to an intermediate state and tries to reach its correct form from the trapped state, which is a slow process. Escape from the misfolded state requires more energy, as the RNA has to unfold to a certain degree before folding correctly. In other words folding from an unstable extended state to a compact, but trapped intermediate state is considered to be fast, while the following unfolding and refolding steps are slow (Fig. 3) (Schroeder et al, 2004). The experiments indicate that the structural content of the unfolded population at the beginning is important to the entire folding process. Nevertheless, it seems that the unfolded RNA shows some structural elements that further decide which folding pathway will be taken (Russell et al, 2002). An aspect which should be taken in consideration is the probability that the misfolded intermediates could also have an as yet unknown function (Pan et al, 2000) and that the majority of the folding information obtained comes from *in vitro* studies that do not reproduce the conditions in the cell (Schroeder et al, 2004). Indeed, because little information is available from *in vivo* studies, it is not known how often RNAs misfold (Schroeder et al, 2004). It is assumed that *in vivo* folding is influenced by directionality of transcription and, in prokaryotes, by translation and trans-acting factors (Zemora & Waldsich, 2010). As the correctly folded

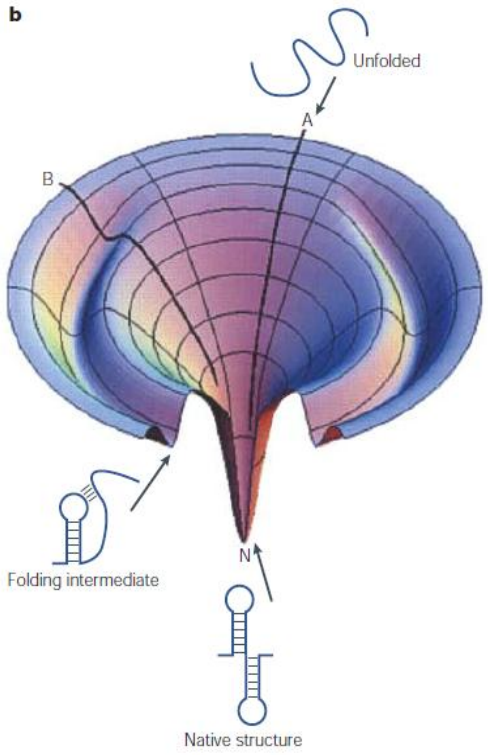

Fig. 3. RNA folding landscape.
In pathway A RNA undergoes rapid folding from the unfolded state into its native structure, whereas in pathway B the RNA is trapped in an intermediate folding state and has to unfold again before reaching the native state. This figure has been adapted from Schroeder et al, 2004.

RNAs are crucial for functions in the cell, there have to be mechanisms with the help of which the two folding problems, kinetic traps and thermo-dynamic instability, can be overcome. Two components are known that can help with this problem; metal ions and RNA binding proteins.

4. Metal ions

RNA itself is a negatively charged molecule because of the phosphate ions in the backbone. At the folding process the negative backbone would repel itself. Therefore mono- and divalent metal ions are important, as they can interact with the backbone and prevent repulsion (Moghaddam et al, 2009). The most considered metal ions are K^+ and Mg^{2+}, as a sufficient amount of it is available in the cell (Draper, 2004). An unfolded RNA sequence needs monovalent ions, e.g. K^+, to collapse, thereby forming a secondary structure (counter-ion mediated condensation). After reaching this compact state, divalent cations, mostly Mg^{2+}, are additionally needed to reach a stable, native tertiary structure. It appears that the Mg^{2+} ions help to accelerate folding and result in an even more compact state (Mg^{2+}-induced compaction), which is then followed by folding to the native state (Muller, 2010). It should be mentioned that there are considered to be two different ways as to how metal ions can interact with the RNA. First, diffuse ions mostly interact through long distance electrostatic forces with water to RNA and each other. They do not interact directly with the RNA backbone. However, these diffuse ions are necessary for the collapse of the RNA, thereby enabling the formation of the secondary structure. Second ions bind on a site-specific basis to the RNA backbone or nucleobase, inducing tertiary structure formation. These metal ions are termed chelated ions. To be able to bind directly they have to be dehydrated first, which means losing the surrounding water molecules. This requires a lot of energy (Draper, 2004).

5. RNA binding proteins

RNA binding proteins can be split in two groups; non-specific binding proteins and specific binding proteins. Non-specific binding proteins include the group of RNA chaperones among others (Herschlag, 1995; Schroeder et al, 2004), while for example splicing factors belong to the family of specific RNA binding proteins.

Specific RNA binding proteins, known as RNA co-factors, are essential to all processes involving RNA, because no function involving RNA without protein co-factor interaction is known (Fig. 4) (Schroeder et al, 2004). *In vitro* RNA co-factors not only stabilize the RNA during folding but also lower the number of metal ions required for folding (Zemora & Waldsich, 2010). Ribozymes are often taken for studying these interactions, as they are dependent on protein co-factors and their native state can be measured through catalytic activity. A well studied example is the *Neurospora crassa* group I intron-specific splicing factor Cyt-18. Cyt-18 binds to the P4-P6 domain of its cognate group I introns and stabilizes them, but does not lead to the native fold. To reach the correct fold, Cyt-18 recruits Cyt-19, which is a RNA helicase and together they facilitate intron folding and in turn splicing. Another example is the yeast protein CBP2 which enables splicing of the yeast mitochondrial bI5 intron *in vivo* and *in vitro* (see section 6.4.) (Schroeder et al, 2004; Zemora & Waldsich, 2010).

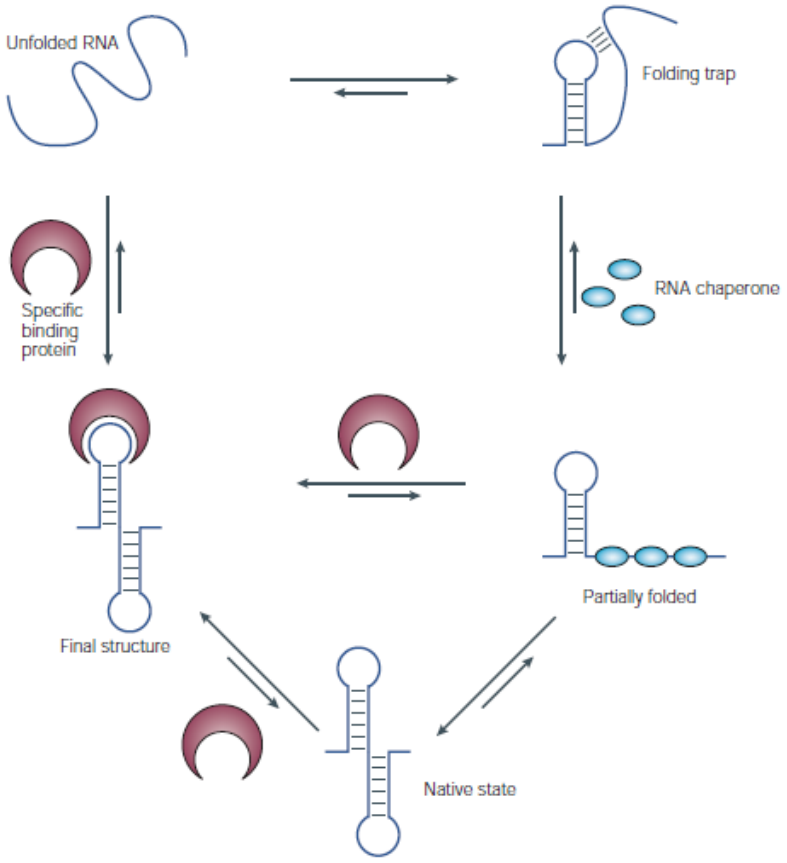

Fig. 4. RNA folding pathways in the presence of RNA co-factors and RNA chaperones.
On the left, RNA co-factor mediated folding is illustrated. They bind to the unfolded or intermediate conformation/ states and stabilize it till the RNA reaches its native state, which often needs stabilization by RNA binding proteins as well. On the right the mechanism conducted by RNA chaperones is shown. RNA chaperones bind to a misfolded state and help to reopen the RNA and allow refolding to the correct fold. This figure is has been adapted from Schroeder et al, 2004.

RNA chaperones are defined as proteins that help RNA in the folding process by refolding compact intermediates (Fig. 4) (Herschlag, 1995). One of their characteristics is that they are just needed during refolding but not to maintain their native state (Doetsch et al, 2010). Non-specific binding proteins have shown to be multifunctional. RNA chaperones do not have conserved sequences or motifs. The primary function of RNA proteins with chaperone activity involves the regulation of transcription, RNA export and RNP assembly (Rajkowitsch et al, 2007). RNA chaperones do not need ATP as an energy source to carry out their function, but the source of the energy is still not known (Rajkowitsch et al, 2007). One of the best-studied proteins with RNA chaperon activity is Stp A, a small *E. coli* protein that favours weak binding to unstructured RNA. Aside from acting as transcriptional regulator, it is also involved in strand displacement and cis- and trans-splicing of the T4 phage derived thymidylate synthase (*td*) group I intron. By conducting *in vivo* chemical probing experiments with dimethyl sulphate (DMS) it was possible to observe the structure of the *td* intron during StpA interaction (Schroeder et al, 2004; Waldsich et al, 2002a; Waldsich et al, 2002b). These experiments led to the assumption that through the binding of StpA, the bases of the RNA which are involved in the tertiary structure are more easily accessible. Therefore StpA seems to open up the RNA structure and gives the RNA another chance to

refold and to reach the native state (Doetsch et al, 2010; Schroeder et al, 2004; Waldsich et al, 2002a). Another well-studied example is the nucleocapsid protein of the human immune deficiency virus (HIV), NCp7. The protein is important for virus replication. It enables the dimerization of the two genomic RNA strands and the packaging of the viral RNA during virus assembly. However, the role of its RNA chaperone activity for viral replication remains enigmatic. Another group of RNA chaperones are the cold-shock proteins (CSP). The stability of RNA secondary structure is temperature-dependent. Therefore, RNA cannot fold properly and is trapped in one of the intermediate or misfolded states at low temperature. Cold-shock proteins, especially CspA and CspE, help by resolving the transcription-terminator stem and reducing the antitermination (Rajkowitsch et al, 2007; Russell, 2008; Schroeder et al, 2004).

5.1. RNA helicases

Another group of proteins that can influence RNA structure are RNA helicases that have the ability to remodel RNA or ribonucleoprotein (RNP) complexes by using ATP (Fairman-Williams et al, 2010). These RNA helicases can again be split into six superfamilies (SF), with SF 1 and 2 being the largest (Singleton et al, 2007). Considering RNA folding, the family of DExD/H-box proteins of the superfamily 2 are one of the most interesting. To look more specifically into the topic, the subgroup of DEAD-box proteins, which is the largest family of SF2, can be examined. The proteins can be found in all 3 domains of life and execute diverse functions, e.g. assembly of ribosomes and spliceosomes, are part of gene expression control mechanisms and folding of RNA group I and group II introns. Like all SF1 and SF2 family members, DEAD-box proteins have a core structure that includes two RecA-like domains and are centered around conserved sequence motifs. The name derives from the conserved amino acid sequence of aspartic acid – glutamic acid – alanine – aspartic acid (D-E-A-D) that is found in motif II (Jarmoskaite & Russell, 2011; Linder & Jankowsky, 2011; Pan & Russell, 2010). At the N-terminal RecA-like domain, the ATP binding motifs Q and I are accommodated as well as the ATP hydrolysis motifs II and III and the RNA binding motifs Ia, Ib and Ic. At the C-terminal RecA-like domain RNA-binding motifs IV, IVa, V and Vb, the ATP-binding motif VI and motif Va are found. Motif Va and motif III seem to couple ATP hydrolysis with RNA binding and therefore as well with unwinding (Rocak & Linder, 2004; Sachsenmaier & Waldsich, 2013). Together, both domains form a cleft into which the ATP cofactors bind (Sachsenmaier & Waldsich, 2013). While binding to ssRNA or dsRNA, DEAD-box proteins go through cycles of binding and hydrolyzing ATP which enable them to restructure the RNA. But in comparison with DNA helicases and other RNA (non DEAD-box helicases), these DEAD-box helicases show two major differences. The processivity of DEAD-box proteins is low, therefore making them poor helicases (Jarmoskaite & Russell, 2011; Russell, 2008). Experiments have shown that their unwinding ability decreased if the RNA helix was longer than 10-15 base pairs. If the sequence was longer than 20-25 base pairs, no helicase activity at all was measured (Jarmoskaite & Russell, 2011; Russell, 2008). Also it was determined that DEAD-box proteins are not able to unwind the RNA if it consists of very stable secondary structures (Jarmoskaite & Russell, 2011; Sachsenmaier & Waldsich, 2013). These characteristics make them appear as inefficient helicases, though it should be considered that the helical elements in most structured RNAs are not longer than 10 base pairs and therefore the processivity no longer seems to be of such importance (Jarmoskaite & Russell, 2011; Russell, 2008). Also

DEAD-box proteins are assumed to use a mechanism that does not involve translocation for their unwinding activity. They seem to be capable of unwinding the duplex internally by using just one cycle of ATP-dependent changes in RNA affinity (Pan & Russell, 2010). In comparison to RNA chaperones which bind to the RNA in a non-specific manner, DEAD-box proteins seem to need specific RNA features such as 5' or 3' overhang or specific secondary structures to be able to bind and carry out ATP hydrolysis (Rajkowitsch et al, 2007). A very well characterized DEAD-box protein is the *N. crassa* Cyt-19 protein. Lambowitz and his associates showed that different Cyt-19 mutants result in defects with group I intron splicing *in vivo. In vitro* experiments showed that it binds RNA in a non-specific manner and facilitates remodelling of the misfolded *Tetrahymena* group I intron, indicating that RNA helicase might act in an RNA-chaperone like fashion. Additional work indicated as well that the yeast mitochondrial DEAD-box protein Mss116 might act analogously to Cyt-19 (Halls et al, 2007). Although both proteins have a similar helical core, their N- and C-terminal extensions vary from other DEAD-box proteins (Del Campo & Lambowitz, 2009; Russell, 2008).

5.2. DEAD-box protein Mss116

Mss116 was discovered by a genetic screen of yeast nuclear mutants that were not able to splice their mitochondrial RNA and thus could not grow on non-fermentable carbon sources by respiration (Seraphin et al, 1987). Shortly after, its function as a helicase was postulated (Seraphin et al, 1989). Today, it is known that the Mss116 protein is a DEAD-box protein and closely related to *Neurospora crassa's* Cyt-19. Mss116 is needed for efficient splicing of all *Saccharomyces cerevisiae* mitochondrial group I and group II introns *in vivo* (Huang et al, 2005). The protein shares common DEAD-box protein characteristics including RNA-dependent ATPase activity, duplex unwinding and ATP-independent strand-annealing (Halls et al, 2007; Solem et al, 2006). It binds non-specifically to the RNA and through ATP hydrolysis it is able to facilitate intron folding and in turn splicing (Halls et al, 2007; Solem et al, 2006). The core region of Mss116 has the typical character of a DEAD-box helicase, though its N- and C-terminal regions differ. The C-terminal region is arginine-rich and consists of an upstream element containing α-helices and a basic tail region with few secondary structure motifs. It is supposed that the region is important for stabilizing the helicase core and its functions as well as for RNA binding (Del Campo & Lambowitz, 2009; Mohr et al, 2008). Additionally to the helical core-induced bend of the RNA, the C-terminus of Mss116 promotes a second bend of the RNA, leading to RNA crimping and in turn this has been postulated to lead to unwinding (Fig. 5) (Mohr et al, 2011).

Group II introns, their folding pathway and their splicing reactions have been studied extensively (Lehmann & Schmidt, 2003; Solem et al, 2009; Su et al, 2005). Group II introns can self-splice *in vitro* but need high amounts of magnesium, monovalent salt and an elevated temperature (Peebles et al, 1986; Schmelzer & Schweyen, 1986; van der Veen et al, 1987). *In vivo,* additional proteins are needed for efficient splicing (Lehmann & Schmidt, 2003; Michel & Ferat, 1995; Mohr et al, 2006). Solem et al. used the group II intron ai5γ to study Mss116's behaviour, as it is a natural co-factor of the intron. They showed that ai5γ can splice *in vitro* under near-physiological conditions in the presence of Mss116. They established that the splicing reaction needed binding and hydrolysis of ATP (Solem et al, 2006). Experiments conducted with ai5γ *in vivo* demonstrated that the intron was unfolded and no tertiary interactions were observed if Mss116 was absent, but most secondary

structure was formed (Liebeg et al, 2010). This suggested that Mss116 is already needed at an early folding step (Liebeg et al, 2010). Further experiments looking into the folding pathway of ai5γ showed that Mss116 is important at the first step in the folding process and is a stabilizing factor (Fedorova et al, 2010; Liebeg et al, 2010; Zemora & Waldsich, 2010). Mss116 facilitates the collapse of domain 1 of ai5γ, forming a stable intermediate that is needed for the further folding steps (Fedorova et al, 2010; Liebeg et al, 2010). It is assumed that Mss116 assist the intron on a one-way path, meaning that once the compact state is achieved it does not unfold again (Fedorova et al, 2010). Is seems that there is little influence on the later folding steps of ai5γ (Fedorova et al, 2010; Liebeg et al, 2010). Notably, Mss116 is able to unwind short duplexes (Pan & Russell, 2010; Solem et al, 2006). A study taking into account different variants of ai5γ implies that unwinding is not necessary for intron folding but for exon refolding. Also the length of the exons seems to be of importance (Zingler et al, 2010).

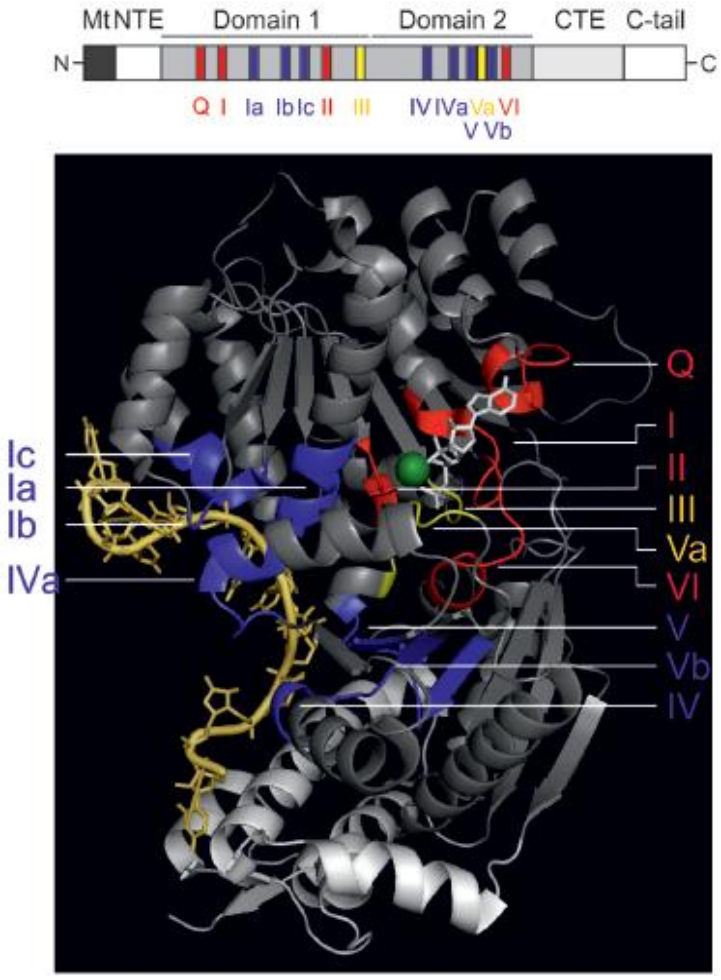

Fig. 5. Structure of the DEAD-box protein Mss116.
In the upper part, the domain organization of the DEAD-box protein Mss116 is schematically illustrated (Sachsenmaier & Waldsich, 2013). The lower panel shows the crystal structure of the Mss116 helical core region. The conserved motifs are indicated in different colours: bound RNA (light yellow), ATP binding and hydrolysis (red), RNA binding (blue), communication sites between ATP and RNA binding (yellow). The non-conserved region of the domain is shown in grey and the CTE in light grey. Non-hydrolyzable ATP analog (AMPNP) is seen in white and the Mg^{2+} ion in green. This figure has been adapted from Sachsenmaier & Waldsich, 2013.

Additional experiments revealed that Mss116 assists group I intron splicing, unwinds RNA duplexes and promotes ATP-independent strand annealing (Halls et al, 2007; Yang et al, 2007).
Two mechanisms were postulated as to how Mss116 facilitates splicing of ai5γ. One possibility is that it acts in an RNA chaperone-like manner using unwinding (Del Campo et al, 2007). The other solution is that it acts as a stabilizing factor, binding to the RNA in an ATP-dependent manner. Nevertheless this possibility would require ATP hydrolysis for the dissociation from the compact near-native folding intermediate to allow native state formation and recycling of the co-factor (Fedorova et al, 2010).

6. Group I intron

Genes are arranged in coding sequences that are interrupted by non-coding sequences. The coding sequences are known as exons and the non-coding as introns. To produce a functional mRNA, rRNA or tRNA for further cellular processes, the introns are removed from the precursor – a process termed splicing. The introns can be split in four major groups, the autocatalytic group I and group II, the spliceosomal and the tRNA introns. Those four groups differ through their splicing mechanisms, as well as their sequences and structural motifs. Only group I and group II introns are autocatalytic as their folded structure is capable of catalysing their excision from the pre-RNA (Cech, 1990; Haugen et al, 2005). These two groups differ in their splicing mechanism, in which group I introns need the 3' OH of an external guanosine and group II introns the 2' OH of an internal adenosine residue to initiate splicing (Vicens & Cech, 2006).

Group I introns are RNAs usually between 250-500nt in size after the splicing reaction, and are found in a variety of organisms. Most group I introns are self-splicing *in vitro*, though some additionally need proteins to fold stably and in turn to carry out splicing (Cech, 1990). Group I introns show very little sequence conservation, which makes them difficult to identify. Through comparison of specific secondary structures it was possible to differentiate them into several subgroups (Nielsen & Johansen, 2009). To date, 13 subgroups of group I introns are known (Michel & Westhof, 1990).
The group I ribozyme played an important role in the RNA field as it was one of the first examples of a catalytic RNA. The first example of self-splicing was discovered in the early 1980s in *Tetrahymena*. Scientists observed that the precursor of the rRNA spliced the intron and ligated the exons. Subsequent *in vitro* studies showed that purified rRNA, when put in a solution with Mg^{2+} and guanosine or GTP, acted in the same way. At first a protein was proposed to catalyse the reaction, but after failure to identify the protein, a new hypothesis was developed which saw the RNA as the catalytic unit. This can be taken as the beginning of catalytic RNAs, which were subsequently called ribozymes. Since then, a new research field of RNA biology evolved around ribozymes and is still growing as new and more specific data becomes available (Cech, 2002).

6.1. Group I intron splicing mechanism

Splicing pathway

The group I splicing reactions consist of two transesterification reactions (Fig. 6). In the first step, an exogenous guanosine binds to the G-binding site of the intron and makes a nucleophilic attack via its 3' OH on the phosphorus atom at the 5' splice site. This results in a 3'-5' phosphodiester bond at the G-cofactor with the first nucleotide of the intron, leaving the guanosine attached to the 5' end of the intron. Additionally to guanosine, any 5'-phosphorylated form of it can be used, e.g. GMP, GDP or GTP. This step also frees the 5' exon terminating with a nucleophilic 3' OH. In the second step, the 5' exon attacks the phosphorus of the 3' splice site. This attack leads to the release of the intron and the exon ligation by a phosphodiester bond (Cech, 1990; Nielsen & Johansen, 2009).

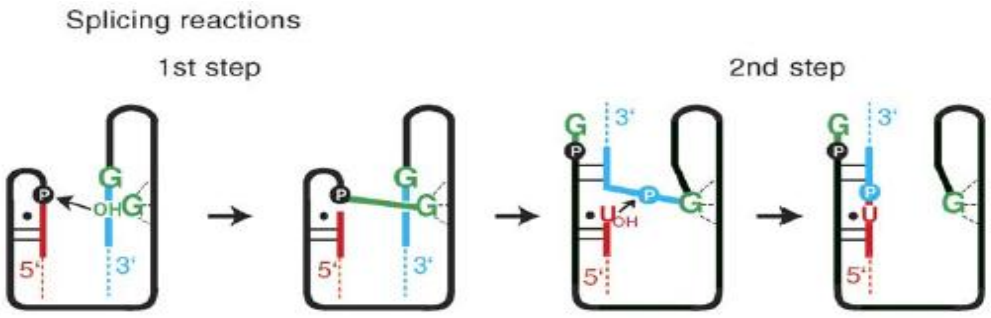

Fig. 6. Splicing mechanism of group I intron.
In the first step of the splicing reaction, the exogenous G binds to the G-binding site and attacks the 5' splice site. In the second step, the 5' exon attacks the 3' splice site, which leads to the release of the intron and exon ligation. This figure has been adapted from Stahley & Strobel, 2006.

After this splicing process, the RNA intron is linear with guanosines at both ends. There are two ways in which the intron can form circles. This happens again by transesterification that is self-catalyzed. In one of the processes, the conserved ΩG of the 3' splice site reacts with a phosphorus molecule at the 5' end. This pathway produces two products, a large circle with almost the entire intron and the small 5' exon end (Zaug et al, 1983). Further experiments showed that the circle can reopen and form another circle again on a protein-independent basis (Zaug et al, 1984). The site where the intron forms a circle differs in the intron groups, but it is assumed that it is managed by binding with the IGS site. It was not possible to determine any indication of a biological function of the circular introns (Nielsen & Johansen, 2009).

The second pathway was recently observed. There, ΩG attacks the exogenous guanosine molecule that was attached to the 5' end of the intron, resulting ultimately in a large circular intron and pyrophosphate (Vicens & Cech, 2009).

Circularization pathway

An alternative pathway to splicing consists of two reaction steps, although in this case the first step is a hydrolysis reaction followed by transesterification step (Fig. 7). At first the 3' splice site ΩG undergoes hydrolysis. This seems to depend on a nucleophilic attack on the 5' splice site on the P9 structural motif that is not important during the canonical splicing reaction. At the free 3' end, the ΩG attacks the 5' splice site. Subsequently, a full circular intron and released but not ligated exons are obtained. This second step is similar to the first step of the canonical splicing reaction, except that it does not use an exogenous guanosine. For this circularization is it important that the P1 motif is correctly folded, consisting of a base-paired IGS and a G·U wobble pair at the 5'splicing site. This pathway was observed in nuclear group I introns (Kruger et al, 1982; Nielsen et al, 2003; Vicens & Cech, 2009).

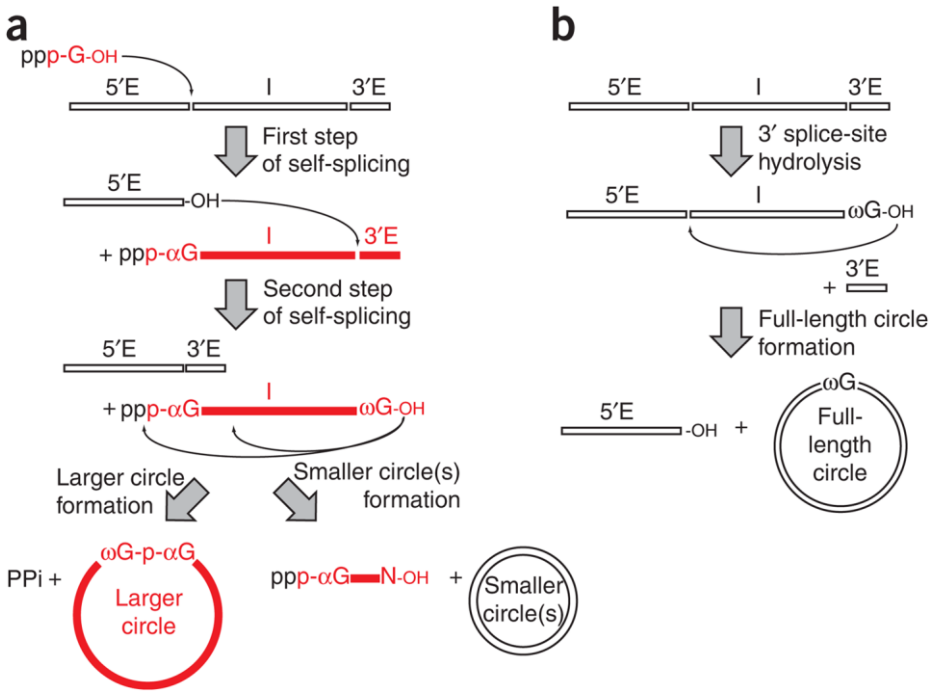

Fig. 7. Reaction pathways of group I intron.
a) The self-splicing reaction can either produce a large circle intron and as a byproduct pyrophosphate or it can form a small circle and a 5' exon end.
b) The circularization pathway consists of a hydrolysis step followed by a transesterification step. Through this pathway, a full length intron circle and exons are released, but exons are not ligated. (Guerrier-Takada et al, 1983; Kruger et al, 1982; Vicens & Cech, 2009). This figure has been adapted from Vicens & Cech, 2009.

Reverse splicing

Woodson and Cech were among the first scientists to show that the splicing reaction of the *Tetrahymena* rRNA group I intron is fully reversible *in vitro*. By using short oligonucleotides as substrates (i.e. mimicking the ligated exons) and incubating them with the linear intron, they observed that the splice sites are reformed and the precursor RNA reassembled (Fig. 8) (Woodson & Cech, 1989). To achieve this, it is necessary for the 5' exon to be able to base pair with the IGS of the intron. The mechanism consists of two steps. At the beginning, the ligated exon sequence binds the active site of the linear intron. Then the guanosine of the 3' end of the intron

(ΩG) attacks a phosphate at the splice junction of the ligated exons, adding the 3' exon to the 3' splice site. In the second step, the 3' OH of the 5' exon attacks the phosphodiester bond of the linear intron, which leads to the release of the guanosine at the 5' end and joining of the 5' exon with the intron. The reverse reaction required a higher RNA and magnesium concentration and a higher temperature, but no additional guanosine (Woodson & Cech, 1989).

Group I introns are found in genomes of different species and have conserved secondary motifs. It was consequently assumed that some genetic mobility mechanism has to exist. Through the discovery of reverse splicing it was hypothesized that reverse splicing could be part of goup I intron RNA transposition, as one intron could be released from RNA and ligate into other RNA (Birgisdottir & Johansen, 2005; Roman & Woodson, 1998; Woodson & Cech, 1989). A further indication favouring this hypothesis is the need for low target specificity of the sequence, which would make it easy to integrate into novel targets (Roman et al, 1999; Roman & Woodson, 1998). In this way the reintegrated intron could be transcribed into cDNA and inserted into chromosomes through homologous recombination (Woodson & Cech, 1989). Since then, reverse splicing has been successfully proven *in vivo*, for example by integrating a *Tetrahymena* intron into *Escherichia coli* (Roman et al, 1999; Roman & Woodson, 1998). The *in vivo* experiments also indicated that reverse splicing is less specific for integration than endonuclease-dependent intron homing which had been considered at that time and could have been used as a way for the spread of group I introns (Roman & Woodson, 1998). Nevertheless, the structure of the RNA and the accessibility of some RNA sequences seem to play a role during reverse splicing (Roman et al, 1999).

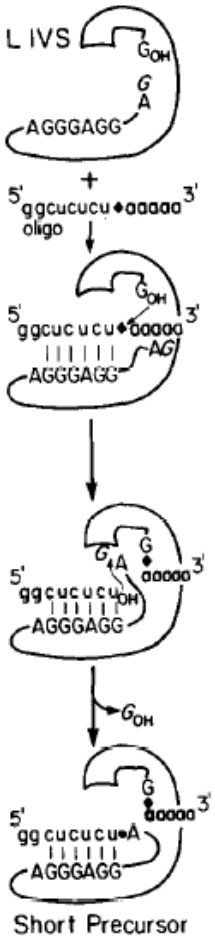

Fig. 8. Reverse splicing mechanism of *Tetrahymena* group I intron.
The ligated exons bind to the active site of the linear intron (here L IVS) and attacks the 3' end of the linear intron. In the next step the 3' OH of the 5' exon attacks the linear intron. This results in joining the 5' exon to the linear intron and the realease of guanosine. This figure has been adapted from Woodson & Cech, 1989.

Another possibility for intron mobility is through forming a circle of the intron. The truncated introns which form a circle cannot be used as they are missing the 5' end. Those that have the full intron sequence also have the exogenous guanosine included and could be taken into account for intron mobility (Nielsen & Johansen, 2009). This type of circular intron would have to reopen, remove the exogenous guanosine and split the ligated exons. In contrast, it would also have to establish the 5' splice site and the 3' splice site. For this, three phosphodiester bonds must be broken and two reformed to allow the intron to reintegrate (Nielsen &

Johansen, 2009). The formed circle products of the circularization pathways, which include the full intron, have been reintegrated successfully *in vivo* (Birgisdottir & Johansen, 2005).

Further to the above mentioned mechanisms that can be observed naturally, new mechanisms have been developed involving group I intron splicing. One of the most interesting is the use of trans-splicing (Long et al, 2003; Nielsen & Johansen, 2009; Sullenger & Cech, 1994). By targeted trans-splicing, a defective segment of RNA can be replaced by a functional (Sullenger & Cech, 1994). The trans-splicing mechanism is similar to the splicing mechanism. The major difference is that the target RNA is not attached to the ribozyme. As the modification of the RNA is posttranscriptional, gene regulation is not affected in the cell. This mechanism could play an important role in the future as it can be used as a new approach for treating genetic diseases (Long et al, 2003).

6.2. Group I intron structure

The structure of group I introns is characterized by specific Watson-Crick paired regions that are linked by loops (L) and junctions (J). Ten paired regions (P1-10) are known, which together with the loops and junctions assemble the catalytic core (Fig. 9) (Vicens & Cech, 2006).

5’ splice site

The 5’ splice site is located within stem P1. This helix is formed by base pairing of the internal guide sequence (IGS) with 4-7nts of the 5’ exon (Barfod & Cech, 1989; Cech, 1990). The sequence of P1 varies from intron to intron, except a U preceding the 5’ splice site which forms a base pair with a G which is the first nucleotide of the intron in the IGS. This base pair defines the attacking site of the exogenous guanosine during the first splicing step. After the first splicing step, P1 still stays stable and positions the 5’ exon for the second splicing step (Cech, 1990). Surprisingly, the U·G pair is needed just for the first splicing step and not for the second, unlike the P1 element which is of importance for both splicing steps (Barfod & Cech, 1989).

3’ splice site

At the 3’ splice site, there is no sequence conservation, except for a G, referred as ΩG (Vicens & Cech, 2006), which is the ultimate residue of the intron and its distance to P9 are important. Tanner and Cech suggested that at the 3’ splice site, some intron nucleotides bind to an internal site and help with the exon ligation (Tanner & Cech, 1987). This hypothesis, later confirmed by Michel as well as by Burke, showing that the nucleotides of J7/9 interact with two nucleotides preceding ΩG forming P9.0 (Fig. 9) (Burke, 1988; Cech, 1990; Michel et al, 1990).

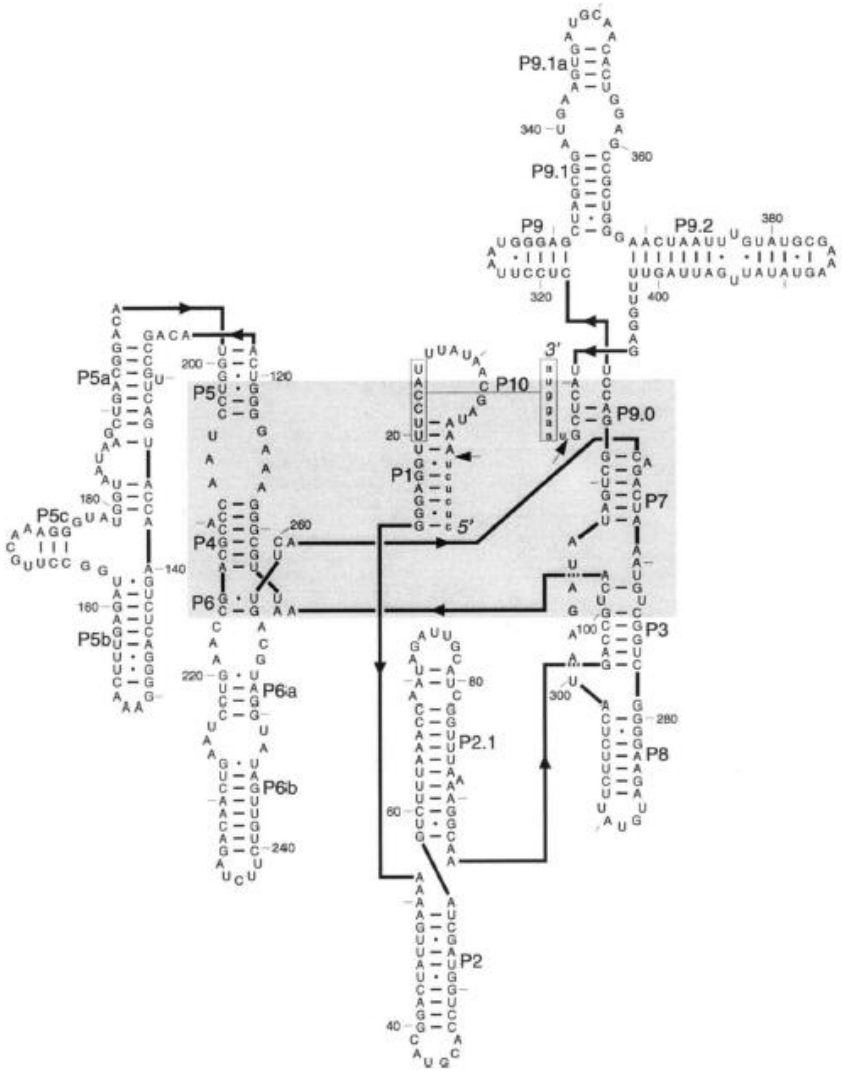

Fig. 9. Secondary structure of *Tetrahymena* group I intron.
On the left the P4-P6 domain and on the right the P3-P9 domain is shown with P1, which contains the 5' splice site in between the two domains. The grey shaded region represents the catalytic core. This figure has been adapted from Cech et al, 1994.

G-binding site

Since observations that group I splicing reactions are guanosine-dependent, it was hypothesized that the molecule has to bind to the intron in a specific manner and therefore should have a specific binding site. Initially, it was considered that the guanosine binds in a G·C base pairing manner through hydrogen bonds (Bass & Cech, 1984; Cech, 1990). Additionally, it was observed that the cyclization of the intron also involved a G-site, which seemed similar to the splicing G-site. It was therefore postulated that just one G-binding site existed that was crucial to intron splicing and cyclization and was just modified during these processes (Cech, 1990; Tanner & Cech, 1987). Michel and his colleagues confirmed that just one G-binding site exists, as their experiments showed that same mutations affected both splicing sites (Michel et al, 1989). Today it is known that the G-binding site is localized in P7, although also forming complex interactions with J6/7 and J8/7 (Golden et al, 2005). For this interaction the ΩG seems to form coplanar hydrogen bonds to the conserved G·C base pair adjacent to the semi-conserved bulge in P7 (Adams et al, 2004; Golden et al, 2005; Vicens & Cech, 2006).

Additionally, this interaction is supported by other base-triple interactions involving nucleotides of P7 and J6/7 (Adams et al, 2004; Golden et al, 2005; Vicens & Cech, 2006). As a result, guanine is stacked on purines, which facilitates a specific recognition site for guanine and at the same time leaves the sugar moiety of the guanosine accessible for catalysis (Vicens & Cech, 2006).

Core sequence

Group I introns have a conserved core that forms the catalytic centre (Fig. 10). The active site is embedded within higher order structural elements formed by P3, P4, P5, P6, P7, P8 and P9 that form two major domains (Cech et al, 1994; Michel & Westhof, 1990). The two major domains are called P4-P6 and P3-P9, consisting of coaxially stacked helices, whereby the P3-P9 domain wraps around the P4-P6 domain forming a cleft into which P1 (or P10) can dock and the active site is assembled (Cech et al, 1994; Doudna & Cech, 1995; Michel & Westhof, 1990; Tanner & Cech, 1997). This establishes a cleft in which the substrate can bind with the help of P1 and P10 (Michel & Westhof, 1990). The binding site of the guanosine is localized in the P3-P9 domain. The P4-P6 domain structurally supports the other domain and is supposed to interact with P1 during the splicing reaction (Doudna & Cech, 1995; Woodson, 2005). The two domains are connected by junctions that are 3-7nts long and form base triples with P4 and P6, respectively that are important for achieving the proper orientation of the two domains to each other for the folding process (Vicens & Cech, 2006). J3/4 and J6/7 connect P4-6 and P3-9 (Vicens & Cech, 2006). J8/7, which is located near P3, has a conserved length and sequence and plays a role in the interaction of P3-P7 region, containing the guanosine binding site with the P1 helix (Vicens & Cech, 2006). Studies showed that the two helical domains can be separated structurally as well as functionally.

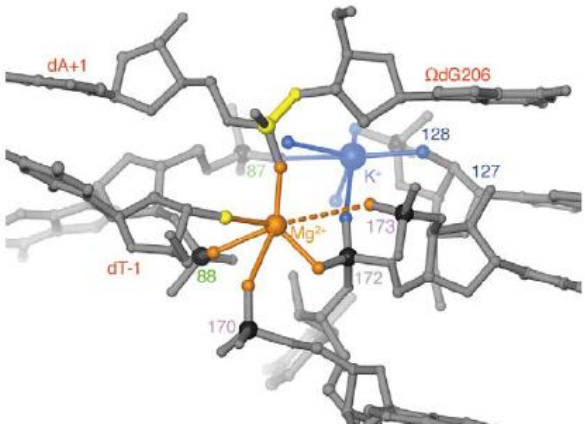

Fig. 10. Group I ribozyme active side with metal ions
Mg^{2+} (metal 1) and its ligands is indicated in orange. K^{+} (metal 2) and its ligands are shown in blue. The 3' OH nucleophile, scissile phosphorus atom and 3' O leaving group are in yellow. This figure has been adapted from Woodson, 2005.

The results also implied that the P3-P9 domain is enough to recognize the two splicing sites and bind metal ions to conduct splicing (Ikawa et al, 2000). This may indicate a separate evolution of the domains. A possibility would be that the first ribozymes consisted of just a P3-P9 structure and the addition of the P4-P6 domain leads to a stable structure and more efficient splicing (Ikawa et al, 2000; Ohuchi et al, 2002). In recent years more detailed information of the structure was identified, as three different crystallographic structures were

achieved (Fig. 11). They showed that the catalytic core and the G-binding site are more complex than previously assumed (Adams et al, 2004; Golden et al, 2005; Guo et al, 2004).

6.3. Group I intron folding

To function properly, the RNA has to be folded into its native conformation. To reach the native fold the tertiary structure has to assemble, which means that long-range interactions have to form. This applies as well to ribozymes. Probably the most well studied example is the *Tetrahymena thermophila* group I intron. This intron has a typical group I intron structure (see chapter 6.2.), arranged from two major domains. If separated, the P4-6 domain is still able to fold into the same conformation as in the intact intron. The P4-6 domain contains numerous residues in P4, P5, P6, J3/4, J4/5 and J6/7 that are part of the catalytic core. Some group I subgroups contain an additional motif, known as P5abc, that improves catalysis by stabilizing the intron core (Cate et al, 1996; Doudna & Cech, 1995; Tanner & Cech, 1997). Subgroups without the P5abc peripheral extension need additional motifs or interact with specific RNA binding proteins (Cate et al, 1996; Engelhardt et al, 2000; Thirumalai, 1998). Cate et al. showed that P4, P5, P6, P6a and P6b form a coaxial stack and P5a and P5b are coaxially stacked as well, and oriented in parallel to the P4-P6 coaxially stacked helices (Cate et al, 1996). A bending hinge region between P5 and P5a makes it possible that the two structures interact with each other, facilitated by several Mg^{2+} ions bound to their domain (Cate et al, 1996; Sclavi et al, 1998; Sclavi et al, 1997). The P5abc segment, forming a three way junction, also contains an A-rich bulge and a GAAA tetraloop closing the P5b stem (Cate et al, 1996; Engelhardt et al, 2000; Murphy & Cech, 1994; Sclavi et al, 1998). It has been suggested that the A-rich bulge interacts with the minor groove nucleotides of P4. The GAAA tetraloop interacts with the minor groove of P6a and J6a/6b of the core region (Cate et al, 1996). It is assumed that the entire P4-6 domain forms independently and early in the folding pathway and helps the second domain to fold (Sclavi et al, 1998; Zarrinkar & Williamson, 1994). The splice site is found in P1, which has to react with the G-binding site located in P7 of the P3-9 domain (Doherty & Doudna, 1997; Laggerbauer et al, 1994). Most conserved nucleotides that are essential for correct positioning of P1 and one of the core helices P7 are also found in P3-9 domain (Doherty & Doudna, 1997; Laggerbauer et al, 1994). P3 and P7 seem to interact with P9.1 and P9.2 in a similar way as P4-6 with P5abc (Laggerbauer et al, 1994). Experiments have

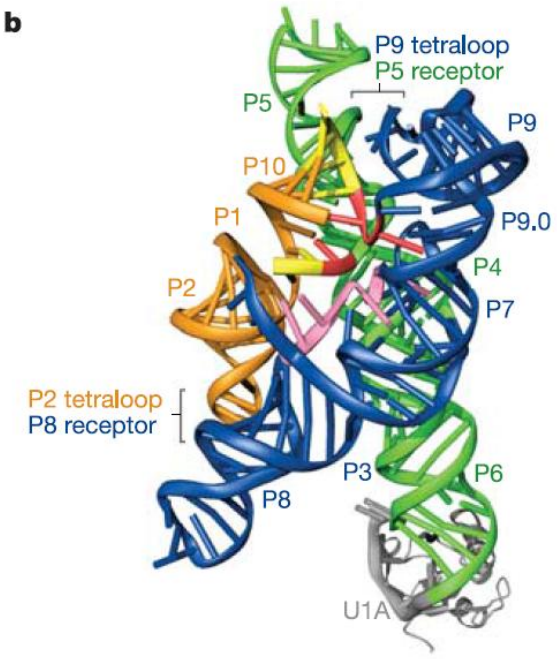

Fig. 11. Crystal structure of *Azoarcus* intron.
The intron has three stacked helical elements: P10, P1 and P2 (orange/yellow); P5, P4 and P6 (green); and P9.0, P7, P3 and P8 (blue).This figure has been adapted from Adams et al, 2004.

shown that in absence of the P4-P6 domain the P3-9 domain can form its secondary structures and some tertiary structure interactions (Doherty & Doudna, 1997). But without P4-P6 it cannot assemble stably folded structure, leading to the conclusion that the P3-P9 domain is not able to fold independently (Doherty & Doudna, 1997; Zarrinkar & Williamson, 1994). Therefore it was also proposed and then shown that after P4-P6 formed properly it induces or strengthens the interaction between P3-P7 and P9.1 and P9.2 (Doherty & Doudna, 1997; Doudna & Cech, 1995; Laggerbauer et al, 1994; Sclavi et al, 1998). Both major domains interact with each other to form the active site and the docking site of the substrate (Cate et al, 1996; Doherty & Doudna, 1997; Golden et al, 2005; Vicens & Cech, 2006). They interact with each other through long-range interactions. Biochemical experiments suggest that base pair 5 in P4 interacts with base 5 in the J8/7 region by building a base triple (Tanner & Cech, 1997). An A·C or G·C base pair is at the P4 position and a G or U at the J8/7 position. At the same time P4 is said to interact through base pairs 2 and 3 with J6/7 region. Those interactions tether the two domains, laying the foundation for the catalytic core (Tanner & Cech, 1997). It also applies that the P1 helix that is important for splicing docks into the cleft formed by the two major domains by hydrogen-bonds with ribose 2' hydroxyl groups (Pyle et al, 1992; Strobel & Cech, 1993; Strobel et al, 1998). Looking at the folding kinetics, it was shown that the P4-P6 domain folds within seconds after the addition of Mg^{2+} (Pan & Woodson, 1998; Sclavi et al, 1998; Zarrinkar & Williamson, 1994). In contrast, the P3-P9 domain misfolds easily and takes minutes to hours to fold properly (Pan & Woodson, 1998; Woodson, 2002). It seems that these misfolded nucleotides are mostly found in the P3 helix, which is then trapped in an alternative fold (Pan & Woodson, 1998). This alternative fold appears to be more favourable than the native P3 helix fold, because it forms short-range and not long-range interactions. Consequently, correct refolding takes up most of the folding time (Thirumalai & Woodson, 2000). An explanation for the kinetic differences between the domains might be that the P4-P6 domain folds rapidly as its nucleotides are near to each other in the primary structure and has a low contact order (Woodson, 2002). On the other hand, the P3-P9 domain includes residues that are 170nts apart from each other in their primary sequence and by interacting through long-range interactions misfold easily (Woodson, 2002).

Another commonly used RNA for studying the folding of group I intron *in vivo* is the thymidylate synthase (*td*) gene of the T4 phage. This RNA needs translation of the pre-mRNA before it can remove the intron, suggesting that the ribosome may have a chaperone like activity (Schroeder et al, 2004; Semrad & Schroeder, 1998; Waldsich et al, 2002b). Studies conducted on the *td* intron in the presence of antibiotics showed inhibition of translation interfered with splicing and enhanced misfolding (Schroeder et al, 2004; Waldsich et al, 1998). In this case the misfolding problem was overcome with the help of RNA chaperones (Schroeder et al, 2004; Semrad & Schroeder, 1998; Waldsich et al, 2002a). StpA is a RNA chaperone that helps *td* intron molecules which are trapped in a misfolded state. It thereby loosens the intron structure. On the other hand, an RNA co-factor studied on *td* intron is Cyt-18, which stabilizes the core structure of the intron and helps the RNA to reach the native fold state (Waldsich et al, 2002a).

6.4. bI5 group I intron and its splicing co-factor protein CBP2

Some group I introns are capable of self-splicing *in vitro*, though under high magnesium concentrations. Other group I introns need proteins as RNA co-factors to reach their native splicing competent fold (Garriga & Lambowitz, 1984; Partono & Lewin, 1988; Shaw & Lewin, 1995). These co-factors can bind on a specific basis to the RNA structure (Schroeder et al, 2004). Additionally, several groups of introns can self-splice under high magnesium concentrations *in vitro*, but need a protein as a co-factor *in vivo*. Adding recombinant co-factor protein to such group I splicing reaction lowers the Mg^{2+} requirements *in vitro* as well, as it has been observed for the yeast mitochondrial group I intron bI5 (Gampel & Cech, 1991; Weeks & Cech, 1995a; Weeks & Cech, 1995b)

The maintenance of mitochondria depends on efficient gene regulation and expression. Nuclear DNA has a specific influence on mitochondrial gene expression (McGraw & Tzagoloff, 1983). A catalytic component of the respiratory complex coenzyme QH2-cytochrome c reductase is cytochrome b, an electron transfer carrier (Gampel & Tzagoloff, 1987; Nobrega & Tzagoloff, 1980). The *Saccharomyces cerevisiae* cytochrome b is a gene consisting of 5 introns and 6 exons. The terminal intron, bI5, is A+T rich and possesses a short sequence that is homologous to a region upstream of the intron, which led to speculations of a possible involvement of the short homologous sequence during removal of the intron (Nobrega & Tzagoloff, 1980). BI5 belongs to the IA subgroup of group I introns. It lacks the structural motif P5abc, but instead has an additional peripheral extension termed P7.1/P7.2 and P9.1 (Shaw & Lewin, 1997). An additional long-range interaction between L7.1 and P6a, called P11, has been identified as well (Jaeger et al, 1991).

CBP2 promotes bI5 splicing at low salt

In vitro experiments demonstrated that the terminal intron of the cob gene can splice autocatalytically (Gampel & Tzagoloff, 1987; Garriga & Lambowitz, 1984; Partono & Lewin, 1988). To achieve efficient splicing, a high quantity of monovalent ions is needed (Partono & Lewin, 1988). The products obtained were characteristic for group I splicing, including the gain of two circles formed by the intron with the ability to open and form circles again (Partono & Lewin, 1988).

However, *in vivo S. cerevisiae* cytochrome b messenger RNA needs the nuclear-encoded cytochrome b pre-mRNA processing protein 2, CBP2, for removal of the terminal intron (Gampel et al, 1989; Gampel & Tzagoloff, 1987). From studies conducted previously, it is known that CBP2 mutants are respiratory-deficient and accumulate unspliced cytochrome b pre-mRNA (McGraw & Tzagoloff, 1983). However, other mitochondrial pre-mRNAs are unaffected by the mutations, indicating that just bI5 needs CBP2 protein for efficient splicing (Hill et al, 1985; McGraw & Tzagoloff, 1983). At the end of the 1980s, Gampel and colleagues confirmed that *in vitro*, bI5 intron depends on a protein co-factor when undergoing splicing under near-physiological concentrations of magnesium and that the required co-factor is CBP2 (Gampel et al, 1989; Gampel & Tzagoloff, 1987). It should be mentioned that they conducted the experiments using terminal intron bI2 form, a shorter cytochrome b gene which does not harbour all 5 introns (Gampel et al, 1989; Gampel & Tzagoloff, 1987). They revealed that splicing involving CBP2 does not have an impact on the basic mechanism of bI5 splicing (Gampel

et al, 1989). This was done by showing that protein-dependent splicing still needed guanosine and forms the same products as the self-splicing reaction. Notably, the guanosine factor binds with the same affinity to the CBP2-bI5 complex and to bI5 by itself (Weeks & Cech, 1995a). BI5 intron variants carrying mutations in an important structural position (e.g. base change in the catalytic active region or 5' exon mutation) showed no splicing activity due to the addition of CBP2 (Gampel et al, 1989). The CBP2 protein consists of 630 amino acids and has a calculated molecular weight of 74kDa. The DNA sequence predicts a polar protein with a high amount of positively charged and aromatic amino acids (McGraw & Tzagoloff, 1983). Self-splicing as well as the CBP2-dependent reactions require magnesium (Gampel & Cech, 1991; Gampel et al, 1989; Gampel & Tzagoloff, 1987; Weeks & Cech, 1995a; Weeks & Cech, 1995b). It was assumed that a high quantity of divalent ions is needed *in vitro* to stabilize the RNA secondary structure for autocatalytic splicing. *In vivo* and *in vitro* under near physiological conditions, the protein co-factor CBP2 lowers the Mg^{2+} requirement and stabilizes the intron structure (Gampel & Tzagoloff, 1987). This comes along with the structural requirements of group I introns. These divalent ions are essential to achieve the native, splicing-competent conformation. First experiments confirmed that *in vitro* self-splicing was stimulated by 50mM $MgCl_2$, whereas 5mM $MgCl_2$ was sufficient for CBP2-assisted splicing. The low amount of magnesium indicated that CBP2 seems to be important as a stabilizing factor, i.e. to reach and maintain the active fold of the bI5 intron (Gampel et al, 1989; Gampel & Tzagoloff, 1987; Webb & Weeks, 2001; Weeks & Cech, 1995a). In fact at 5mM $MgCl_2$, the autocatalytic reaction is approximately 1000 times slower than the protein-dependent reaction at the same $MgCl_2$ concentration (Weeks & Cech, 1995a; Weeks & Cech, 1995b). At 40mM $MgCl_2$ concentration, the autocatalytic reaction is about 8 times slower than the protein-mediated reaction, indicating that magnesium ions cannot compensate for all the functions of CBP2 (Weeks & Cech, 1995a).

Binding of CBP2 to bI5

Gampel and Cech were among the first who proposed that CBP2 must either interact with the catalytic core of the bI5 intron, or proper folding of the core is needed for binding the protein (Gampel & Cech, 1991). They constructed different variants of the intron with specific deletion, showing that L1 and L8 regions have no influence on the binding. But mutations affecting the G-binding site interfered with the protein binding (Gampel & Cech, 1991). Further research showed that CBP2 has a major influence on the secondary and tertiary structure of bI5 (Gampel & Cech, 1991; Shaw & Lewin, 1995; Weeks & Cech, 1996). Interactions between the protein and the RNA were found to affect numerous sites. The strongest effects were observed in P1, L2, P4 and P6a (Shaw & Lewin, 1995). Also, its stabilizing function was confirmed via UV cross-linking (Shaw & Lewin, 1995). Meanwhile it has been shown that P7.1 and P7.2, which are specific structural elements of subgroup IA of group I introns

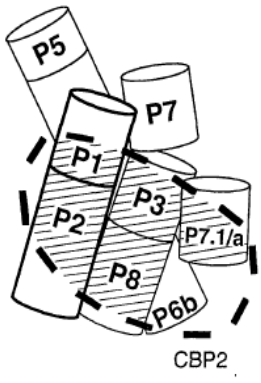

Fig. 12. Interaction sites of bI5 core and CBP2. The scheme illustrates the folded core structure of bI5 and its interactions sites with CBP2. This figure has been adapted from Weeks & Cech, 1996.

are important elements for binding of CBP2 to the bI5 intron (Weeks & Cech, 1995b). CBP2 binds across the P8 region and seems to position P1-P2 between itself and the core region (Fig. 12) (Webb et al, 2001; Weeks & Cech, 1995a).

CBP2-promoted bI5 folding

CBP2 promotes the splicing reaction by helping the preformed secondary structure to assemble into a specific tertiary fold (Shaw & Lewin, 1995; Weeks & Cech, 1996). Binding assays provided the assembly pathway for this ribonucleoprotein (RNP) complex (Fig. 13) (Weeks & Cech, 1996). At the beginning, the RNA forms secondary structures, but no tertiary interactions exist. In a first slow step, the two domains of the bI5 intron assemble the catalytic core (Weeks & Cech, 1995b; Weeks & Cech, 1996). The CBP2 protein binds fast to this catalytic core and enables stable tertiary structure formation. Ultimately, P1/P2 binds the CBP2-stabilized catalytic core and forms the active RNP complex (Weeks & Cech, 1996).

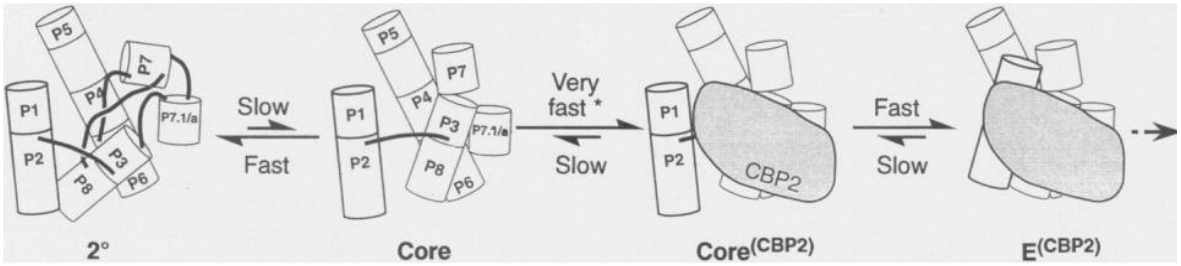

Fig. 13. Folding pathway of bI5 in the presence of CBP2.
In the graphic the bI5 RNA folding pathway at physiological Mg^{2+} concentration and in the presence of CBP2 is shown. This figure has been adapted from Weeks & Cech, 1996.

Buchmueller et al. used a bI5 variant consisting only of the core sequences, termed bI5core, to study its folding pathway (Buchmueller et al, 2000). They demonstrated that the RNA is in an expanded state when no ions are present. By the addition of magnesium, bI5 folds into a collapsed but near-native fold (Buchmueller et al, 2000). Under physiological conditions, the collapsed and the expanded state are in equilibrium (Buchmueller et al, 2000). Nevertheless, 3mM $MgCl_2$ are enough to achieve the collapsed state. At a high magnesium concentration or by the addition of CBP2, the RNA folds into its active state (Buchmueller et al, 2000). It was discovered that the collapsed state is not a kinetic trap (Webb & Weeks, 2001). It is rather an intermediate along the assembly pathways, because through the binding of CBP2 bI5 reaches its native fold. However, when CBP2 binds to the expanded state, the formed bI5-CBP2 complex is kinetically trapped (Webb et al, 2001). By gaining insight into this pathway, the most recent research has focused on the structural content of these three different states. Monovalent ions are sufficient to allow formation of the secondary structure within peripheral extensions (Fig. 14), but divalent ions are required to establish the catalytic core (Chamberlin & Weeks, 2003).

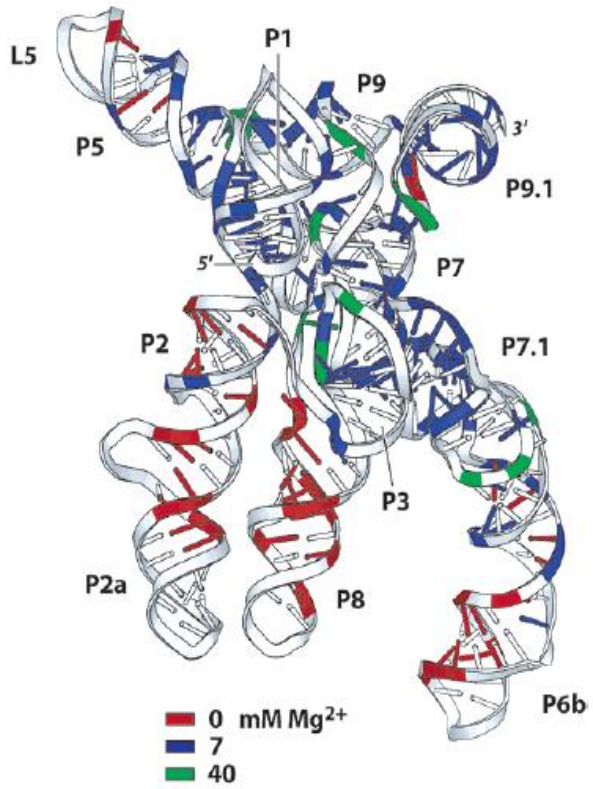

Fig. 14. Assembled bI5 core region.
The figure shows stable and protected bI5 regions at different Mg^{2+}concentrations. Red regions are observed with 0mM Mg^{2+}, blue with the addition of 7mM Mg^{2+} and green with 40mM Mg^{2+}. This figure has been adapted from Chamberlin & Weeks, 2003.

The peripheral stems P2-2a, P6b, P8 and the upper part of P5 are still more stable than the more reactive P5, P7.1a, P9 and P9.1 helices (Buchmueller & Weeks, 2003; Chamberlin & Weeks, 2003). Recent studies imply that CBP2 is needed to a far lesser extent than previously supposed (Buchmueller & Weeks, 2003). They postulate that the RNA itself is responsible for correct folding, as the collapsed state self-chaperones the RNA into the native RNP (Buchmueller & Weeks, 2003; Garcia & Weeks, 2004; Webb & Weeks, 2001). Importantly, in the collapsed state, the RNA adopts a near-native structure (Webb & Weeks, 2001). At this step, CBP2 is only needed to induce small structural changes (Buchmueller & Weeks, 2003). In other words, the CBP2 protein captures the tertiary structure of the bI5 intron, resulting in the formation of a stable, splicing competent conformation (Buchmueller & Weeks, 2003; Garcia & Weeks, 2004). By binding to the extended RNA, the complex is trapped in a stable but inactive protein RNA complex (Garcia & Weeks, 2004; Webb & Weeks, 2001). CBP2 has no preference as to binding to the expanded and the collapsed state. As such reaching the collapsed state prevents misassembling of CBP2 with the extended bI5 intermediate (Garcia & Weeks, 2004; Webb & Weeks, 2001). In addition, CBP2 recognizes RNA structure motifs rather than sequence specific binding motifs (Garcia & Weeks, 2003). Especially in the fast binding step non-specific interactions are formed, inducing the formation of stable tertiary interactions (Bokinsky et al, 2006).

To gain more information on RNP complex assembly, Webb et al. analyzed the splicing bI5 efficiency in the presence of another RNA co-factor, the *N. crassa* amino acyl-tRNA synthetase Cyt18 (Fig. 15) (Webb et al, 2001). Cyt-18 was fully capable of binding to bI5 by recognizing P4-P6 and inducing conformational changes in stem P8 and P9 as well as in J8/7, implying tertiary structure formation and active site assembly (Webb et al, 2001). However, a major difference was observed in the assembly mechanism with bI5. Similar to CBP2, which binds to a collapsed near-native state, Cyt-18 binds rapidly to the collapsed state as well, but it specifically binds to the P4-P6 region. In contrast to the CBP2, Cyt18 has a larger activation barrier for rearrangements (Webb et al, 2001). Additionally, a slow second step is required at which the catalytically active state is formed (Webb et al, 2001).

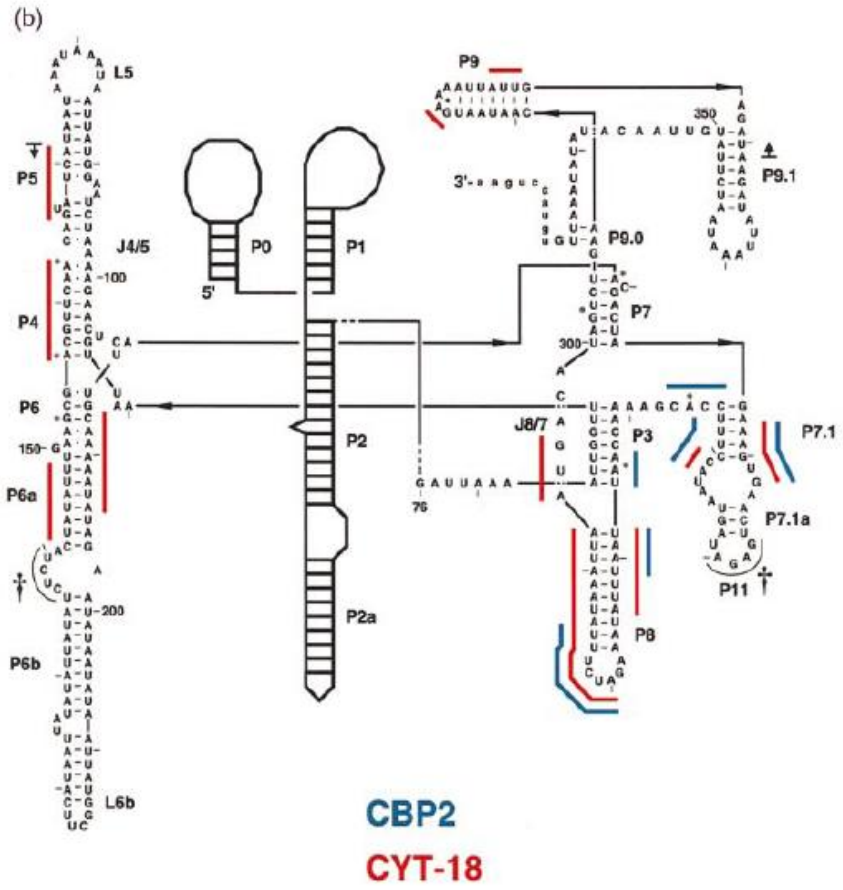

Fig. 15. Interaction sites of bI5 core intron and two different protein co-factors.
In the panel, nucleotides protected from $OH^{\bullet}$ radical cleavage in the presence of either protein are indicated. Protection upon presence of CBP2 is represented by blue lines, while those of Cyt-18 by red lines. The figure has been adapted from Webb et al, 2001.

6.5. RNA splicing co-factors and their functional similarity

Mss116 is required for efficient splicing of group I and group II introns in *S. cerevisiae* mitochondria. Extensive research focusing on DEAD-box protein facilitated functions and group II folding pathways was conducted, using Mss116 and ai5γ group II intron *in vivo* and *in vitro* (Fedorova et al, 2010; Halls et al, 2007; Huang et al, 2005; Liebeg et al, 2010; Solem et al, 2006). In contrast to ai5γ, all other mt introns need additional splicing factors, for efficient splicing. This splicing factor can either be a maturase or a nuclear encoded protein, such as for example CBP2, which is uniquely required for bI5 splicing (Huang et al, 2005).

Studies comparing *N. crassa* Cyt-19 and *S. cerevisiae* Mss116 showed that Cyt-19 complements Mss116 *in vitro* as well as *in vivo* (Del Campo et al, 2009; Huang et al, 2005). In *N. crassa*, Cyt-19 functions in an ATP-dependent, RNA chaperone-like manner with Cyt-18, a mt tyrosyl-tRNA synthetase (Mohr et al, 2002). While Cyt-18 acts as a stabilizing factor, Cyt-19 was proposed to resolve kinetic traps in *N. crassa* intron splicing (Mohr et al, 2002). By replacing Cyt-19 with Mss116 it was revealed that Mss116 can work together with Cyt-18 and support group I splicing in *N. crassa* (Del Campo et al, 2009). Given that CBP2 and Cyt-18 are both considered as stabilizing factors in different organisms, the outcome of their function is the same. Importantly, Cyt-18 successfully substitutes for CBP2 and facilitates bI5 group I intron splicing *in vitro*, although the two proteins use different mechanisms for assembly of the RNP complex (Webb et al, 2001). In spite of these results, it is still not clear how CBP2 and Mss116 co-opt to promote bI5 splicing *in vivo*. It remains enigmatic if Mss116 and CBP2 have redundant functions or if both can bind to bI5 at the same time, fulfilling different tasks in bI5 folding. Evidence for the latter comes from the fact that bI5 splicing is virtually abolished in a *cbp2*-knockout strain, while bI5 splicing is reduced to 40% in a *mss116*-knockout strain (Sachsenmaier & Waldsich, unpublished). This suggests that 60% of the bI5 population need both proteins to reach the native state. However, it needs to be shown if the protein acts simultaneously or consecutively on the bI5 intron. It will be interesting to reveal whether Mss116 applies a similar mode of action to promote group I and group II intron folding.

Scientific aims of the project

RNA folding is crucial to obtain a functional RNA. Despite metal ions which are important during the folding process, protein co-factors are also needed to establish a correctly folded RNA. During folding and splicing of group I introns *in vivo* two co-factors from *S. cerevisiae* are needed, the proteins CBP2 and Mss116. The project aim was to gain more insight into the bI5 splicing mechanism in the presence of both co-factors CBP2 and Mss116 *in vitro*. CBP2 is a specific group I co-factor, essential to bI5 intron folding and splicing (Gampel et al, 1989; Gampel & Tzagoloff, 1987; Weeks & Cech, 1995a; Weeks & Cech, 1995b). Mss116 is a DEAD-box helicase, promoting intron folding and splicing as well (Fedorova et al, 2010; Halls et al, 2007; Huang et al, 2005; Liebeg et al, 2010; Solem et al, 2006). While it is known that both proteins are needed for efficient splicing of the yeast mitochondrial bI5 intron *in vivo* (Del Campo et al, 2009; Huang et al, 2005; Mohr et al, 2002), little is known about the mechanism and pathway the proteins use to assemble a functional RNP. Interestingly, *in vitro* CBP2 is capable of promoting intron splicing efficiently without the second co-factor, Mss116. To be able to conduct the experiments, our first aim was to establish a protocol for producing recombinant CBP2. After accomplishing protein purification we addressed the question of whether Mss116 further stimulates bI5 intron splicing *in vitro* and whether such a positive influence would be dependent on CBP2. By analyzing bI5 splicing in the absence and presence of either RNA co-factor or both proteins we aimed to shed light on the role of Mss116 in CBP2-assisted folding of the intron RNA. This also required cloning of several bI5 pre-RNA constructs, as most studies were conducted with shortened bI5 pre-RNA, containing three intronic deletions. As such, we set out to create shortened and full-length bI5 introns flanked by exon sequences of different length. This constructs should help us understand, if Mss116 is required to enable proper folding of the full-length intron while CBP2 alone is sufficient for splicing of short constructs.

Materials & Methods

1. Strains and plasmids

Rosetta™ 2(DE3)pLysS Singles™ Competent Cells Novagen®

Rosetta™ 2(DE3)pLysS Singles™ Competent Cells (Novagen® Catalog.# 71401-3) are used for eukaryotic protein expression. This strain is a derivate of *E. coli* BL21 and supplies tRNAs for rare codons. The plasmid carries a chloramphenicol resistance and can be induced with IPTG (1.). Genotype: F^- ompT $hsdS_B(r_B^-m_B^-)$ gal dcm (DE3) pLysSRARE2 (Cam^R).

E. coli DH5α

DH5α cells were made competent by the Waldsich group. The strain is used for higher plasmid yield and misses the endonuclease A (endA). Genotype: F^- endA1 glnV44 thi-1 recA1 relA1 gyrA96 deoR nupG Φ80dlacZΔM15 Δ(lacZYA-argF)U169, hsdR17(r_K- m_K+), λ– (2.).

E. coli XL-1 Blue

The *E. coli* XL-1 Blue are made competent by KCM method cells. The cells were kindly provided from Georgeta Zemora and the protocol for making them competent from the laboratory of G. Wiche. Genotype: endA1 gyrA96(nal^R) thi-1 recA1 relA1 lac glnV44 F'[::Tn10 $proAB^+$ $lacI^q$ Δ(lacZ)M15] hsdR17(r_K- m_K+) (2.).

Yeast strain HRH #49

This yeast strain is a derivative strain of a 161-U7 (Phenotype: ura-, GII-0 (no group II introns - group I introns were not deleted), which has only group I introns in its mt DNA. All group II inrons were deleted. This strain is used for RNA isolation and in turn to clone different bI5 constructs. This strain is a generous gift of P.Perlman (University of Texas, Austin, USA).

Yeast strain HRH #54

This strain has been derived from HRH #49 (Phenotype: ura-, ΔMss116/GII-0 (no group II introns but group I introns with Mss116 knock out; kanR) by disrupting the *MSS116* ORF with a kanamycin cassette, and in turn knocking out *mss116*. This strain is used for RNA isolation and in turn to clone different bI5 constructs. This strain was also a generous gift of P. Perlman (University of Texas, Austin, USA).

Yeast strain yCW07

In this yeast strain, the cytochrome b pre-mRNA processing protein 2, CBP2, was knocked out by a Nat1 cassette through homologous recombination (by Nora Sachsenmaier). Again the strain HRH #49 was used as the starting strain. The strain is resistant to clonat. This strain is used for RNA isolation and in turn to clone different bI5 constructs.

pBS-ΔT7

The pBlueSkript vector used lacks the original T7 promoter and carries an ampicillin resistance gene. This plasmid was obtained from A. Pyle (Yale University).

pCBP2

This plasmid encodes the cytochrome b pre-mRNA processing protein 2, CBP2, fused to 6 x His-tag, at C-terminus, although the first His is part of the protein itself. The plasmid carries ampicillin and tetracycline resistance genes. This plasmid was kindly provided by K. M. Weeks (University of North Carolina, Chapel Hill, USA).

pbI5

The plasmid contains truncated version of the bI5 intron. It contains a deletion of 207nts in L1. Two segments were additionally removed. Nucleotides 387-410 were deleted and L6 was closed with a with a C(UUCG)G tetraloop. Similarly, nts 502-653 were deleted and L8 was closed with the sequence AGAUCU. As such the intron was downsized to 368nts from 738nts (Fig. 15). This construct was also named bI5core and in contrast to the full-length bI5 intron, this truncated variant can be folded to the native splicing competent state (Weeks & Cech, 1995a). This plasmid was kindly provided by K. M. Weeks (University of North Carolina, Chapel Hill, USA).

pΔbI5

ΔbI5 is derived from the bI5core variant by shortening P6b (deleting nts 168 – 180 and nts 187- 197). This plasmid was kindly provided by K. M. Weeks (University of North Carolina, Chapel Hill, USA).

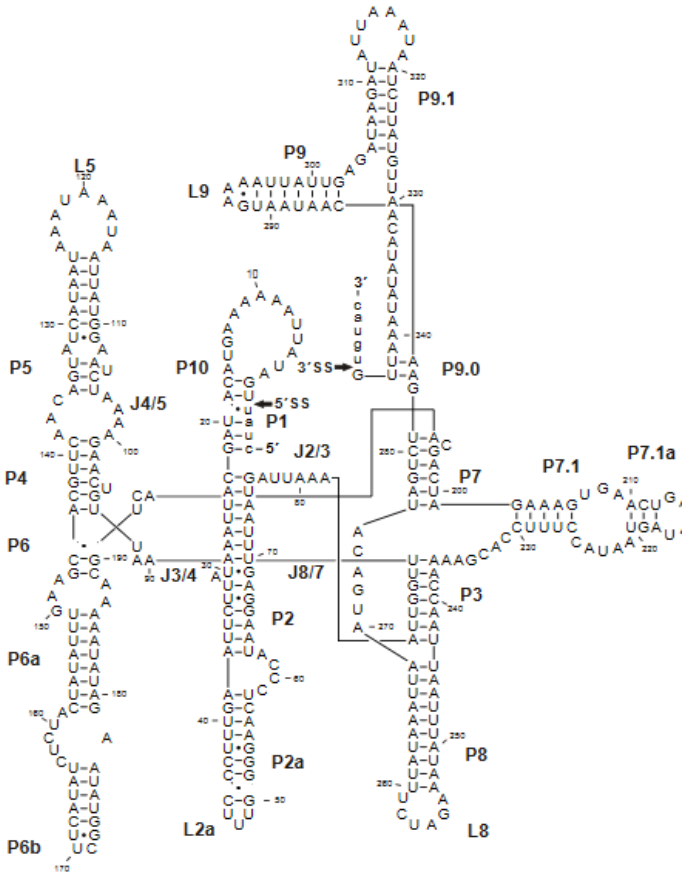

Fig. 16. bI5core construct
The sequencing results from the construct which we received from K. M. Weeks, were used to create the secondary structure of the bI5 intron. The figure was prepared by Stefan Handl.

2. Consumables and equipment

Enzymes, Buffers & Markers

Enzyme / Buffer /Marker	Company	Catalog #
Alkaline Phosphatase, Calf intestinal (CIP)	NEB	M0290S
T4 Polynukleotide kinase (500 U)	NEB	M0201S
NEB 4 buffer	NEB	B7004S
EcoRI	NEB	R0101S
EcoRI buffer	NEB	B0101S
XbaI	NEB	R0145S
BamHI	NEB	R0136L
100 x BSA	NEB	B9001S
Rnase Inhibitor (10000 U)	Promega	N2515
M-MLV Reverse Transcriptase (10000 U)	Promega	M3682
Random hexamers, 20µg	Promega	C1181
Rnase H (50 U)	Promega	M4281
T4 ligase	NEB	19827715
T4 ligase buffer	NEB	B0202B
dNTP set (Li-salt - RT grade)	Roche	11277049001
dNTP set (Na-salt - PCR grade)	Roche	11969064001
GoTaq DNA polymerase (2500 U)	Promega	M3178
Pfu DNA polymerase (500 U)	Promega	M7745
PfuTurbo DNA Polymerase	Agilent/ Stratagene	600250
PfuUltra II Fusion HotStart DNA Polymerase	Agilent/ Stratagene	600670
ProSieve QuadColor Protein Marker	Biozym	830537
RiboRuler Low Range RNA Ladder	Thermo Scientific	SM1831
100bp DNA ladder	NEB	N3231S
1kb DNA ladder	NEB	N3232S

Chemicals

Chemical	Company	Catalog #
DMSO	Sigma	D8418
Bacto tryptone	BD	211684
Yeast extract	BD	12750
NaCl	VWR	APPCA2942.5000
NaN_3	Sigma Aldrich	S2002-25G
KCl	VWR	A2939.1000
$MgCl_2$	VWR	A4425.1000
$MgSO_4$	VWR	A6287.0250
PIPES Sodium-salt	Applichem	A1080.0100
$CaCl_2$	VWR	A4689.1000
$MnCl_2$	VWR	APPCA2087.0100
KOH	VWR	A3871.0500

Polyethylenglycol (PEG)	VWR	A1249.1000
Ampicillin	VWR	A0839.0100
EDTA	VWR	A5097.1000
Glycogen	AL Labortechnik	23550.03
Ethanol p.a.	VWR	A3678.2500
NaOAc	VWR	A5268.1000
Peptone	BD	211684
L-tyrosine	Sigma-Aldrich	-
L-adenine	Sigma-Aldrich	-
Glucose	Applichem	A3730.1000
Raffinose-pentahydrat	VWR	APLIA6882.0100
Clonat	Werner Bioreagents	5002000
Agarose	VWR	733-1562
Ethidiumbromid	VWR	A1152.0025
Tris base	VWR	A2264.5000
Boric acid	VWR	A2940.5000
Phenol, TE-saturated (pH 8)	VWR	A1153.0500
Phenol, water-saturated (pH 4)	VWR	A1624.0500
Chloroform	VWR	A1585.1000
Isoamylalcohol	VWR	A2610.1000
Urea	VWR	APPCA1049.5000
SDS	VWR	A0676.0500
Bromophenol blue	VWR	A3640.0005
β –mercaptoethanol	VWR	A1108.0100
IPTG	VWR	A4773.0025
Hepes	VWR	A3724.1000
ATP	Applichem	-
Imidazole	VWR	A1378.0250
Glycerol	VWR	A2926.1000
DTT	VWR	A2948.0010
40% Acrylamide / bisacrylamide (19:1)	Applichem	A3857.1000
40% Acrylamide / bisacrylamide (37.5:1)	Applichem	A4989.1000
APS	VWR	A2941.0100
TEMED	VWR	A1148.0100
Tris	VWR	A2264.5000
Formamid	VWR	A2156.0500
Methanol	VWR	A3493.2500GL
Acetic acid	VWR	A3686.2500
Coomassie Brillant Blue	VWR	A1092.0100
Tween 20	VWR	A4974.0100
Sucrose	VWR	A2211.1000
Xylene cyanol	VWR	A4976.0005
Bradford reagent	VWR	A6932.0250

Kits

Kits	Company	Catalog #
Amersham ECL Prime Western Blotting Detection Reagent	GE Healthcare	RPN2232
MEGAscript ® T7 kit	Life Technologies	AM1334
MEGAclear™ kit	Life Technologies	AM1908
RiboPure™- Yeast kit	Life Technologies	AM1926
PureYield™ Plasmid Midiprep System	Promega	A2495
Malachite Green Phosphate Detection Kit	R&D Systems	DY996
Wizard® SV Gel and PCR Clean-Up System	Promega	A9282

Devices & Software

Device	Company	Catalog #
PerfectPro Ni-NTA (Nickel-nitrilotriacetic acid) Agarose nickel-charged resin	5prime	2400000
Amicon® Ultra-4 Centrifugal Filter Units	Merck Millipore	UFC803024
Slide-A-Lyzer Dialysis Casette 10K (orange)	Thermo Scientific	66380
illustra MicroSpin G-25 Columns	GE Healthcare	27-5325-01
Amersham Hybond-P	GE Healthcare	RPN303F
Storage Phosphor Screen & Cassette	GE Healthcare	-
Amersham Hyperfilm ECL	GE Healthcare	28906836
Image Eraser	Amersham Biosciences	-
Storm Phosphorimager 820	Molecular Dynamics	-
U-2000 Spectrophotometer	Hitachi	-
NanoDrop (ND-1000)	Thermo Scientific	-
Gel Dryer Model GD-5040	SCIE-PLAS	-
Dual Gel Caster	Hoefer	SE245
Mini vertical gel electrophoresis unit	Hoefer	SE250
µCLEAR plate, chimney, 96 well – black, clear bottom	Greiner Bio-one	655087
Nunc® MicroWell® MiniTrays	Thermo Scientific	470378
Infinite F500 microplate reader	Tecan	-
Storm Scanner Software	Molecular Dynamics	-
Image Quant™	GE Healthcare	-
KaleidaGraph Version 4.1.1.	Synergy Software	-

3. Oligonucleotids

All oligonucleotids were ordered from Sigma-Aldrich®.

The melting temperature of each oligonucleotide was calculated using the approximation of 2°C for A/T base pairs and 4°C for G/C base pairs.

Primer name	primer name	use	sequence (5'→ 3')	length (bp)	Temp. (°C)
CW75F	bI5-rc-fw	PCR	cggaattccgtaatacgactcactatacagtagcattaaatattcttaagt	51	60
CW75R	bI5-rc-rev	PCR	cgggatcccgcaatttatatatgttaacataagatta	37	62
CW75F_2	long-bI5-rc-fw	PCR	cggaattccgtaatacgactcactatagggcagtagcattaaatattcttaagt	54	60
CW75R_2	long-bI5-rc-rev	PCR	cgggatcccaatttatatatgttaacataagatta	35	62
CW75F_3	short-bI5-rc-fw	RT	cagtagcattaaatattcttaagt	24	60
CW75R_3	short-bI5-rc-rev	RT	caatttatatatgttaacataagatta	27	62
CW76F	bI5-fi-fw	PCR	cggaattccgtaatacgactcactatatgatattaaaaaagtacagtagc	50	58
CW76R	bI5-fi-rev	PCR	cgggatccccaatttatatatgttaacataagat	34	58
CW76F_2	long-bI5-fi-fw	PCR	cggaattccgtaatacgactcactatagggctattgatattaaaaatattaataaaa	57	58
CW76F_3	bI5-fi-wt-fw	RT	ctattgatattaaaaatattaataaaa	27	58
CW76F_4	bI5-fi-fw-wt2	RT	cggaattccgtaatacgactcactatactattgatattaaaaatattaataaaa	54	58
CW76R_2	RT-short-bI5-fi-rev	RT	caatttatatatgttaacataagat	25	58
CW76F_5	short-bI5-fi-fw	RT	ctattgatattaaaaatattaataaaa	27	58
CW77F	bI5-preRNA 25/25 fw	PCR	cggaattccgtaatacgactcactatatcctttagtaacaccagcatc	48	60
CW77R	bI5-preRNA 25/25 rev	PCR	cgggatcccggaatggtaataagtatcattcag	33	60
CW77F_2	long-bI5-25/25-fw	PCR	cggaattccgtaatacgactcactatagggtcctttagtaacaccagcatc	51	60
CW77R_2	long-bI5-25/25-rev	PCR	cgggatccgaatggtaataagtatcattcag	31	60
CW77F_3	short-bI5-25/25-fw	RT	tcctttagtaacaccagcatc	21	60
CW77R_3	short-bI5-25/25-rev	RT	gaatggtaataagtatcattcag	23	60
CW78F	bI5-preRNA 50/100 fw	PCR	cggaattccgtaatacgactcactatacatcctgataactatattcctg	49	60
CW78R	bI5-preRNA 50/100 rev	PCR	cgggatcccgctaaaatagctgcaaacattaga	33	60
CW78F_2	long-bI5-50/100-fw	PCR	cggaattccgtaatacgactcactatagggcatcctgataactatattcctg	52	60
CW78R_2	long-bI5-50/100-rev	PCR	cgggatccctaaaatagctgcaaacattaga	31	60
CW78F_3	50/100 fw 2	PCR	catcctgataactatattcctggtaatcctttagtaacaccagcatc	47	73
CW78R_3	50/100 rev 1	PCR	cgggatcccgtaaaatagctgcaaacattagaataactcctaataatttatc	52	73
CW78R_4	50/100 rev 2	PCR	gaataactcctaataatttatcaggaatagatcttaaaatagcatagaatg	51	68
CW78R_5	50/100 rev 3	PCR	aggaatAgatcttaaaatagcatagaatggtaataagtatcattcag	47	68
CW78F_4	short-bI5-50/100-fw	RT	catcctgataactatattcctg	22	60
CW78R_6	short-bI5-50/100-rev	RT	ctaaaatagctgcaaacattaga	23	60

4. Preparation of competent cells

4.1. Preparation of DH5α competent cells using $CaCl_2$/PIPES method

- The DH5α cells from the stock were struck out on a LB-plate and incubated at 37°C overnight.
- The next day 10-12 colonies of *E. coli* DH5α were inoculated in 250ml SOB medium.
- The cell culture was grown at 22°C on a shaker, till an OD_{600} between 0.6-0.8 was reached.
- The cells were put on ice for 10 minutes. Afterwards the cells were centrifuged at 4°C at 2500 x g for 10 minutes.
- The cell pellet was resuspended in 80ml ice-cold TB-buffer.
- Again the resuspended cells were centrifuged at 4°C at 2500 x g for 10 minutes and resuspended in 20ml ice-cold TB-buffer.
- 1.4ml DMSO [f.c. 7%] was added while swirling and cell mixture was put on ice for 10 minutes.
- 500µl aliquots were pipette into tubes and shock frozen in liquid nitrogen before storage at -80°C.

Materials:

- LB - Plates

  10 g bacto tryptone
  5 g yeast extract
  5 g NaCl
  15 g agar

  Fill up to 1L with ddH_2O and autoclave. After cooling media down, pour the plates in a sterile environment. After solidification, the plates are stored at 4°C.

- SOB-medium

  20 g tryptone
  5 g yeast extract
  0.6 g NaCl
  0.2 g KCl

  Fill up to 1L with ddH_2O and autoclave. After autoclaving add 1M $MgCl_2$ [f.c. 10mM] and 1M $MgSO_4$ [f.c. 10mM].

- TB-buffer

  10 mM PIPES Na-salt
  215 mM $CaCl_2$
  250 mM KCl
  255 mM $MnCl_2$

  Adjust the pH to 6.7 with 1M KOH before adding Mn^{2+} and fill up to 1L with ddH_2O. Pass the buffer through a sterile filter.

- Additional reagents: DMSO

4.2. Preparation of *E. coli* XL-1 Blue competent cells using KCM method

- The XL-1 Blue cells from the stock were struck out on a LB-plate and incubated at 37°C overnight.
- The next day a colony was picked and inoculated in 5ml LB-medium at 37°C overnight shaking (220 rpm).
- The following day 1ml of the o/n culture was inoculated in 100ml LB-medium and shaken at 37°C until an OD_{600} between ~0.5-0.6 was reached.
- The culture was put on ice for 20 minutes, followed by harvesting the cells. Therefore the cells were centrifuged at 4000 rpm for 10 minutes at 4°C.
- The cell pellet was resuspended in 5ml ice-cold TSS solution and put on ice for 15 minutes.
- 100µl aliquots were pipetted into tubes and shock frozen in liquid nitrogen before storage at -80°C.

Materials:

- LB-Medium

  10 g bacto tryptone
  5 g yeast extract
  5 g NaCl

  Fill up to 1L with ddH_2O and autoclave.

- LB - Plates

  10 g bacto tryptone
  5 g yeast extract
  5 g NaCl
  15 g agar

  Fill up to 1L with ddH_2O and autoclave. After cooling media down, pour the plates in a sterile environment. After solidification, the plates are stored at 4°C.

- TSS solution

37.5 ml LB-medium
5 g 10% PEG 3350
2.5 ml 5% DMSO
5 ml 1M $MgSO_4$
5 ml 1M $MgCl_2$

Mix together and pass through sterile-filter.

5. Midi-Prep PureYield™ Plasmid Midiprep System

The Midi-Prep Pure Yield™ Plasmid Kit was used for plasmid extraction from bacteria cultures (*E. coli*) following the manufacturer's manual.

6. Transformation

6.1 Transformation into *E. coli* Rosetta

x µl plasmid DNA [c]= ~30ng/µl
40 µl competent cells

For the negative control, 10µl of competent cells were used.

- The cells and the plasmid were mixed together and were put on ice for 5 minutes and then heat shocked at 42°C for 30 seconds.
- 250µl of LB-medium was added and cells were incubated at 37°C for 1 hour shaking (200 rpm).
- After the incubation the cells were centrifuged at 6000 rpm for 2 minutes.
- The supernatant was discarded, except for ~200µl in which the pellet was resuspended.
- ~130µl of the sample was plated on selective plates (e.g. LB-Amp) and incubated at 37°C o/n.

Materials:

- LB-Medium

10 g bacto tryptone
5 g yeast extract
5 g NaCl

Fill up to 1L with ddH_2O and autoclave.

- LB - Amp Plates

  10 g bacto tryptone
  5 g yeast extract
  5 g NaCl
  15 g agar

  Fill up to 1L with dH_2O and autoclave. After cooling media down, add 1ml of ampicillin and pour the plates in a sterile environment. After solidification, the plates are stored at 4°C.

- Additional reagents: 1000 x ampicillin stock solution (100mg/ml)

6.2 Transformation into *E. coli* DH5α

x µl plasmid DNA [c]= ~10-30ng/µl
100 µl competent cells

For the negative control, 100µl of competent cells were used.

- The cells and the plasmid were mixed gently together and were put on ice for at least 20 minutes.
- In the next step, the cells were heat shocked at 42°C for 1 minute and put on ice for 30 seconds.
- 1ml of LB- medium was added and cells were incubated at 37°C for 1 hour in order to regenerate the cells.
- After incubation, the cells were centrifuged at 6000 rpm for 2 minutes.
- The supernatant was discarded, except for ~200µl in which the pellet was resuspended.
- The cells were plated on selective plates (e.g. LB-Amp) and incubated at 37°C o/n.

Materials:

- LB-Medium

  10 g bacto tryptone
  5 g yeast extract
  5 g NaCl

  Fill up to 1L with ddH_2O and autoclave.

- LB - Amp Plates

  10 g bacto tryptone
  5 g yeast extract
  5 g NaCl
  15 g agar

  Fill up to 1L with dH_2O and autoclave. After cooling media down, add 1ml of ampicillin and pour the plates in a sterile environment. After solidification, the plates are stored at 4°C.

- Additional reagents: 1000 x ampicillin stock solution (100mg/ml)

6.3. Transformation into *E. coli* KCM cells

E. coli XL-1 blue cells are made competent (see section 4.2.) and transformed using the KCM method which is based on a solution containing potassium, calcium and magnesium. With these cells, higher transformation efficiency is achieved.

10 µl ligation mix
20 µl 5 x KCM buffer
100 µl competent cells

For the negative control, 100µl of competent cells were used.

- The components were mixed gently together and put on ice for 20 minutes.
- In the next step the cells were heat shocked at 37°C for 5 minutes.
- 200µl of LB-medium was added and cells were incubated at 37°C for 1 hour in order to regenerate them.
- After the incubation the cells were centrifuged at 6000 rpm for 2 minutes.
- The supernatant was discarded, except for ~150µl in which the pellet was resuspended.
- The cells were plated on selective plates (e.g. LB-Amp) and incubated at 37°C o/n.

Materials:

- LB-Medium

  10 g bacto tryptone
  5 g yeast extract
  5 g NaCl

  Fill up to 1L with ddH_2O and autoclave.

- LB - Amp Plates

  10 g bacto tryptone
  5 g yeast extract
  5 g NaCl
  15 g agar

  Fill up to 1L with dH_2O and autoclave. After cooling media down, add 1ml of ampicillin and pour the plates in a sterile environment. After solidification, the plates are stored at 4°C.

- 5 x KCM buffer

  0.5 M KCl
  0.15 M $CaCl_2$
  0.25 M $MgCl_2$

  Fill up to 30ml with ddH_2O and store at 4°C.

- Additional reagents: 1000 x ampicillin stock solution (100mg/ml)

7. RNA isolation

A colony was inoculated in an o/n-culture (4ml YP-Medium + 1ml 10% glucose + 5µl Clonat (100mg/ml)) at 30°C. The following day, a main culture (40ml YP-medium + 10ml 10% raffinose + 50µl Clonat (100mg/ml)) was prepared adding 2.5ml of o/n-culture and shaken at 30°C until it reached an OD_{600} ~0.7-1. 35ml were put in a falcon and centrifuged for 4000 x g at room temperature for 5 minutes. The supernatant was discarded and the pellet was resuspended in 1ml of YPD. The sample was again centrifuged at 6000 x g at room temperature for 2 minutes and the supernatant was discarded. The pellet was stored at -80°C for 1 hour. Subsequently, total RNA was isolated using the RiboPure^{TM}-Yeast Kit from Ambion, following the manufacturer's manual.
After RNA isolation, the RNA was precipitated.

RNA precipitation: 2 µl 0.5M EDTA (pH 8)
1 µl glycogen (10mg/ml)
2.5 x vol. EtOH/ 0.3M NaOAc

The sample was stored at -20°C o/n. The next day the sample was centrifuged at full speed at 4°C for 30 minutes. After discarding the supernatant, the pellet was washed with 70% EtOH, dried for 10 minutes at room temperature and resuspended in 11µl of ddH_2O. The RNA concentration was measured with a UV/VIS spectrometer (e.g. Nanodrop).

Materials:

- YP-Medium

  1 % yeast extract
  2 % peptone
  55 mg/ L-tyrosine
  55 mg/ L-adenine

  Fill up to 1L with ddH_2O.

- YPD-Medium

  1 % yeast extract
  2 % peptone
  55 mg/ L tyrosine
  55 mg/ L adenine

  Fill up to 800mL with ddH_2O. After autoclaving, add 200mL of sterile filtered 10 % glucose [f.c. 2%].

- Additional reagents: 10 % glucose
  10 % raffinose
  1000 x clonat stock solution (100mg/ml)
  EtOH / 0.3M NaOAc (pH 5)
  glycogen (10mg/ml)
  0.5M EDTA (pH 8)
  70 % EtOH

8. Two-step reverse transcription – PCR

This method is based on two steps. The first one consists of a randomly primed reverse transcription, followed by a gene specific PCR.

8.1. Reverse transcription

Denaturing RNA: 0.5 µl RNA (2µg)
1 µl random hexamers (500ng/µl)
12.5 µl dH_2O
14 µl

- To denature the RNA, the sample was incubated at 70°C for 5 minutes, followed by cooling on ice for 5 minutes. The sample was spun down and the remaining reverse transcription components were added:

5 µl	5 x M-MLV RT buffer
1.3 µl	10mM dNTP mix
1 µl	RNase inhibitor (40U/µl)
0.5 µl	MMLV-RT (200U/µl)
3.2 µl	dH_2O
25 µl	

- The sample was mixed gently and spun down. The sample was incubated at room temperature for 10 minutes before incubating at 40°C for 50 minutes. To remove RNA, 1µl of RNase H (2U/µl) was added and incubated at 37°C for 20 minutes.
- Afterwards the tube was incubated at 70°C for 15 minutes to inactivate the RNase H and the reverse transcriptase.

Materials:

- 10mM dNTP mix (RT grade)

10 µl	100mM dATP [f.c. 10mM]
10 µl	100mM dCTP [f.c. 10mM]
10 µl	100mM dGTP [f.c. 10mM]
10 µl	100mM dTTP [f.c. 10mM]

Add 60µl of ddH_2O and store at -20°C.

8.2. PCR

The following PCR mixtures were used:

	Gotaq (2mM Mg^{2+})	**Gotaq** (3mM Mg^{2+})	**Gotaq** (after RT)	**Gotaq** colony PCR	**Pfu/Gotaq mix** (3.25mM Mg^{2+})
5 x Gotaq buffer (7.5mM $MgCl_2$)	10µl	10µl	10µl	10µl	5µl
10 x Pfu buffer (20mM $MgSO_4$)					2.5µl
DMSO	2.5µl	2.5µl	2.5µl	2.5µl	2.5µl
10mM dNTPs	1µl	1µl	1µl	1µl	1µl
100µM Primer F	0.5µl	0.5µl	0.5µl	0.5µl	0.5µl
100µM Primer R	0.5µl	0.5µl	0.5µl	0.5µl	0.5µl
10mM $MgCl_2$	2.5µl	7.5µl			
10mM $MgSO_4$					7.5µl
Taq polymerase (5U/µl)	0.25µl	0.25µl	0.25µl	0.25µl	0.25µl
Pfu polymerase (3U/µl)					0.4µl
DNA template (50ng/µl)	1µl	1µl			1µl
cDNA			5µl		
dH_2O	31.75µl	26.75µl	30.25µl	35.25µl	28.85µl

	Pfu (2mM Mg^{2+})	**Pfu - DMSO** (2mM Mg^{2+})	**Pfu** (2.5mM Mg^{2+})	**Pfu** (3mM Mg^{2+})	**Pfu** (3.5mM Mg^{2+})
10 x Pfu buffer (20mM $MgSO_4$)	5µl	5µl	5µl	5µl	5µl
DMSO	2.5µl		2.5µl	2.5µl	2.5µl
10mM dNTPs	1µl	1µl	1µl	1µl	1µl
100µM Primer F	0.5µl	0.5µl	0.5µl	0.5µl	0.5µl
100µM Primer R	0.5µl	0.5µl	0.5µl	0.5µl	0.5µl
10mM $MgSO_4$			2.5µl	5µl	7.5µl
Pfu polymerase (3U/µl)	0.4µl	0.4µl	0.4µl	0.4µl	0.4µl
DNA template (50ng/µl)	1µl	1µl	1µl	1µl	1µl
dH_2O	39.1µl	41.6µl	36.6µl	34.1µl	31.6µl

	Pfu Turbo	**Pfu Ultra II Fusion HS**	**Pfu Ultra II Fusion HS** with DMSO
10 x cloned Pfu buffer	5µl		
10 x Pfu Ultra II buffer		5µl	5µl
DMSO			1µl
10mM dNTPs	1µl	1.25µl	1.25µl
100µM Primer F	1µl		
100µM Primer R	1µl		
10µM Primer F		1µl	1µl
10µM Primer R		1µl	1µl
Pfu Turbo polymerase (2.5U/µl)	1µl		
Pfu Ultra II Fusion HS polymerase		1µl	1µl
Plasmid template (50ng/µl)	2µl		
Plasmid template (25ng/µl)		1µl	1µl
dH_2O	39µl	39.75µl	38.78µl

The following PCR programs were used:

The annealing temperature of the primers was adjusted by the gradient PCR. The elongation time had to be adjusted, depending on the length of the PCR product and the polymerase used.

- The PCR program used after reverse transcription and using PCR reaction mixes GoTaq polymerase 2mM Mg^{2+} / 3mM Mg^{2+} / 3.25mM Mg^{2+} , Pfu polymerase 2mM Mg^{2+} / 3mM Mg^{2+} / 3.25mM Mg^{2+}, GoTaq/Pfu polymerases mix and for colony PCR:

	95°C	2 minutes
30 cycles	95°C	1 minute
	Tm of oligo - 5°C	1 minute
	72°C	2 minutes
	72°C	15 minutes
store at 4°C		

- The PCR program used for Pfu and GoTaq/Pfu polymerase mixes:

	95°C	2 minutes
30 cycles	95°C	1 minute
	Tm of oligo - 5°C	30 seconds
	72°C	1.5 minutes
	72°C	5 minutes
store at 4°C		

- The PCR program used for Pfu Turbo polymerase:

	95°C	2 minutes
30 cycles	95°C	30 seconds
	Tm of oligo - 5°C	30 seconds
	72°C	1 minute
	72°C	10 minutes
store at 4°C		

- The PCR program used for Pfu Ultra II Fusion HotStart:

	95°C	2 minutes
30 cycles	95°C	20 seconds
	Tm of oligo - 5°C	20 seconds
	72°C	15 seconds
	72°C	3 minutes
store at 4°C		

Materials:

- 10mM dNTP mix (PCR grade)

  10 µl 100mM dATP [f.c. 10mM]
  10 µl 100mM dCTP [f.c. 10mM]
  10 µl 100mM dGTP [f.c. 10mM]
  10 µl 100mM dTTP [f.c. 10mM]

  Add 60µl of ddH_2O and store at -20°C.

- Additional reagents: 1M $MgCl_2$
  1M $MgSO_4$
  DMSO

8.3. Native agarose gel

To analyze the size of the PCR product and to estimate concentrations (ng/µl), DNA samples were loaded on an agarose gel. 4µl of samples were mixed with 1µl of suitable 10 x loading dye. The gel chamber is filled with 1 x TBE and the 5µl samples were run on the gel at 100V for 1 hour.

Gel preparation:

	big agarose gel	small agarose gel
0.8 % agarose	80 ml	40 ml
EtBr (10mg/ml)	0.8µl	0.4µl

Materials:

- 0.8 % agarose

  3.2 g agarose

  Fill up with 400ml of 1 x TBE and heat in the microwave to dissolve it. Keep at 60°C.

- 10 x TBE

  540 g Tris base [f.c. 890mM]
  275 g boric acid [f.c. 890mM]
  29.2 g EDTA [f.c. 20mM]

  Fill up to 5L with ddH_2O and autoclave. For 1 x TBE dilute with ddH_2O.

- Additional reagents: ethidium bromide (10mg/ml)

9. Wizard® SV Gel and PCR Clean-Up System

The PCR fragments were cleaned up using the Wizard® SV Gel and PCR Clean-Up System kit from Promega following the manufacturer's manual.

10. Ligation

10.1. Restriction digest

Before the ligation the PCR fragments as well as the vector pBS-ΔT7 into which the fragments were ligated had to be cut with the restriction enzymes BamHI and EcoRI.

Reaction mix:

	inserts	vector
PCR products	50µl	
pBS-ΔT7 (100µg)		24.4µl
10 x NEB EcoRI buffer	10µl	12µl
100 x BSA	1µl	1.2µl
BamHI (20U/µl)	4µl	4µl
EcoRI (20U/µl)	4µl	4µl
ddH_2O	31µl	74.4µl
	100µl	120µl

The reaction mix was incubated at 37°C for 4 hours. As BamHI cannot be heat inactivated, a phenol extraction needs to be carried out.

10.2. Dephosphorylation of the vector

Before ligation could be carried out, the vector pBS-ΔT7 had to be dephosphorylated. As the CIP enzyme is active in 1 x NEB EcoRI buffer, 1µl of CIP (10U/µl) was added to the vector digest and incubated at 37°C for 1 hour. As the CIP enzyme (and BamHI) cannot be heat-inactivated, a phenol extraction was subsequently performed.

10.3. Phenol extraction

Because the inserts and the vector are DNA, it was important to use the TE-saturated phenol with a pH of 8. The reaction volume was increased up to a total of 200µl with ddH_2O. 200µl of phenol/CI (1:1) mixture was added and vortexed well. The sample was centrifuged at 4°C at full speed for 3 minutes. The upper phase was

transferred to a new tube (~200µl) and mixed with an additional 200µl of CI. This was followed by vortexing and centrifugation as before. At the end, the upper phase was pipetted into a new tube and precipitated.

RNA precipitation:
2µl 0.5M EDTA (pH 8)
1µl glycogen (10mg/ml)
2.5 x vol. EtOH/ 0.3M NaOAc

The sample was stored at -20°C o/n. The following day the sample was centrifuged at full speed for 30 minutes at 4°C, washed with 70% EtOH and dried for 10 minutes at room temperature. The pellet was resuspended in 20µl of ddH_2O. Instead of a phenol extraction, the Wizard® SV Gel and PCR Clean-Up System (Promega) can be used.

Materials:

- Additional reagents: TE-saturated phenol (pH 8)
  chloroform/ isoamyl alcohol mixture (24:1)
  glycogen (10mg/ml)
  0.5M EDTA (pH 8)
  70% EtOH

10.4. Ligation reaction

With ligation, a 1:3 molar ratio between the vector and insert is required.

Ligation mix:

10 x T4-ligation buffer	2µl
T4 ligase (400U/µl)	1µl
insert (100ng)	0.52µl
vector (200ng)	4.46µl
ddH_2O	12.02µl
	20µl

The ligation was incubated at 16°C o/n. The next day transformation into *E. coli* KCM cells was carried out.

11. CBP2 purification

11.1. CBP2 expression

As it is advisable to start the expression of CBP2 with an o/n culture, a colony was inoculated in 5ml of LB-medium with 5µl of ampicillin (100mg/ml). The next day the main growth culture consisting of 1L of LB-medium, 1ml of ampicillin (100mg/ml) and 500µl of o/n culture were grown at 37°C until it reached an OD_{600} ~0.8. The OD_{600} was measured with a UV/VIS spectrometer. After reaching the required OD_{600}, 1ml of sample of the growth culture was withdrawn and centrifuged at 6500 rpm for 2 minutes. The pellet was resuspended in 100µl of SDS PAGE sample buffer and stored at -20°C for subsequent further analysis on an SDS PAGE. At the same time 1ml of 1M IPTG [f.c. 1mM] was added to the main growth culture, inducing the protein expression. IPTG is a lactose derivate and acts as an inducer of the lac operon, by binding to the lac repressor. At binding to the tetrameric lac repressor it releases the repressor from the lac operator, making the promoter accessible for the RNA polymerase and enabling the transcription of genes downstream of the lac promoter. It cannot be metabolized or degraded by cells, leading to a constant concentration in the cell. CBP2 is regulated by a lac promoter and therefore its expression is induced by IPTG. The induced culture was incubated at 22°C o/n. The next day 1ml of the culture was removed again, centrifuged at 6500 rpm for 2 minutes and resuspended in 100µl of the SDS PAGE sample buffer.

Materials:

- LB-Medium

  10 g bacto tryptone
  5 g yeast extract
  5 g NaCl

  Fill up to 1L with ddH_2O and autoclave.

- SDS PAGE sample buffer

  10 ml 0.5M Tris·HCl (pH 6.8) [f. c. 0.1M]
  10 ml glycerol [f. c. 20%]
  10 ml 10% SDS [f. c. 2%]
  10 mg bromophenol blue [f. c. 0.02%]

  Fill up to 50ml with ddH_2O and add fresh ß-mercaptoethanol before use [f. c. 5%].

- 1M IPTG

  238 mg IPTG

  Fill up to 1ml with ddH_2O and store at -20°C

- Additional reagents: 1000 x ampicillin stock solution (100mg/ml)

11.2. Cell harvesting

From this point onwards, all procedures had to be performed on ice and at 4°C.

The cells were harvested at 4°C at 6500 x g for 20 minutes. The obtained pellet was resuspended in 10ml of ice-cold column buffer and the cells were lysed by sonication with 6 x 15 seconds bursts with 10 seconds cooling time in-between. The lysate was centrifuged at 10000 rpm at 4°C for 30 minutes. After centrifugation the supernatant was transferred into a new falcon.
20µl of the supernatant were removed and mixed with 80µl of the SDS PAGE sample buffer. In addition, the cell pellet was slightly resuspended with 5ml of column buffer. 20µl of the cell pellet were withdrawn and 80µl of the SDS PAGE sample buffer was added. Both samples were stored at -20°C for further analysis on a SDS-PAGE gel at a later time point.

Materials:

- Column buffer

  7.5 ml 1M Hepes (pH 7.6) [f.c. 50mM]
  52.5 ml 2M NaCl [f.c. 700mM]
  15 ml 10% glycerol
  524.47 µl β-mercaptoethanol [f.c. 5mM]
  0.03 g NaN_3 [f.c. 0.02%]

  Fill up to 150ml with ddH_2O and store at 4°C.

- SDS PAGE sample buffer

  10 ml 0.5M Tris·HCl (pH 6.8) [f. c. 0.1M]
  10 ml glycerol [f. c. 20%]
  10 ml 10% SDS [f. c. 2%]
  10 mg bromophenol blue [f. c. 0.02%]

  Fill up to 50ml with ddH_2O and add fresh ß-mercaptoethanol before use [f. c. 5%].

11.3. Batch purification

The supernatant was stirred together with 4ml of Ni^{2+} agarose resin (1ml of Ni^{2+} agarose resin for 4ml of supernatant) and put on a rotation wheel for 1 hour at 4°C. Before pouring the resin into a polypropylene column, 20µl of imidazole [f.c. 1mM] were added to the resin. The resin was left to set down. Afterwards the flow through was collected. It is important that the resin is never dry or is not covered with solution.

The purification was performed as follows:

- The column was washed with 4 x 10ml of column buffer.
- Next the column was washed with 5 x 5ml of column buffer containing 20mM imidazole.
- Followed by elution of 5 x 5ml of column buffer containing 80mM imidazole.
- And finally by eluting 5 x 5ml of column buffer containing 200mM imidazole.

A 10µl sample of each fraction was taken and mixed with 10µl of SDS PAGE sample buffer. All samples were run on a 10% SDS PAGE and analysed.

Materials:

- 1M Imidazole

  6.8 g imidazole

  Resuspend in 100 ml of ddH_2O and store at 4°C.

- Column buffer + 20mM imidazole

  24.5 ml column buffer

  0.5 ml 1M imidazole [f.c. 20mM]

- Column buffer + 80mM imidazole

  23 ml column buffer

  2 ml 1M imidazole [f.c. 80mM]

- Column buffer + 200mM imidazole

  20 ml column buffer

  5 ml 1M imidazole [f.c. 200mM]

- SDS PAGE sample buffer

  10 ml 0.5M Tris·HCl (pH 6.8) [f. c. 0.1M]

  10 ml glycerol [f. c. 20%]

  10 ml 10% SDS [f. c. 2%]

  10 mg bromophenol blue [f. c. 0.02%]

  Fill up to 50ml with ddH_2O and add fresh ß-mercaptoethanol before use [f. c. 5%].

11.4. Dialysis

The fractions which contain most of the protein were pooled and concentrated at 7500 x g using a Millipore Centrifugal Unite (30K cut off). The concentrated solution was put in a dialysis cassette and dialyzed at 4°C o/n in 1L of protein storage buffer, changing the buffer once.
The next day the protein solution was removed from the cassette and the protein was aliquoted and stored at -20°C.

Materials:

- Protein storage buffer

  40 ml 1M Hepes (pH 7.6) [f.c. 20mM]
  400 ml 1M NaCl [f.c. 200mM]
  400 µl 0.5M EDTA (pH 8) [f.c. 0.1mM]
  800 ml glycerol [f.c. 40%]
  4 ml 1M DTT [f.c. 2mM]

  Fill up to 2L with ddH_2O.

- 1M Dithiothreitol (DTT)

  154 mg DTT

  Add 1ml of ddH_2O, resuspend and store at -20°C.

11.5. Bradford assay

The protein concentration was measured with the Bradford assay.
A BSA [100ng/µl] standard curve was consequently first conducted using 0/10/20/40/50/75/100 ng/µl as reference points.

BSA concentration [ng/µl]	BSA(10mg/ml)	dH_2O
0	-	20µl
10	2µl	18µl
20	4µl	16µl
40	6µ	14µl
50	10µl	10µl
75	15µ	5µl
100	20µl	-

In addition, a protein dilution series was carried out as well using 20µl as the dilution volume.

The samples were pipetted into a µCLEAR 96-well plate and 200µl Bradford reagent was pipetted into each well. The samples were incubated for 20 minutes at room temperature. The absorption was measured at 595nm with the Infinite F500 microplate reader (Tecan).

Materials

- Additional reagent: Bradford reagent
  100 x BSA (10mg/ml)

11.6. SDS-PAGE

Sodium dodecyl sulphate polyacryalmide gel electrophoresis (SDS-PAGE) separates proteins according to their molecular mass.

Preparations for 2 x SDS-Gels:

	10% separating gel	4% stacking gel
ddH_2O	3.79ml	2.975ml
1.5M Tris HCl (pH 8.8)	2.6ml	-
0.5M Tris HCl (pH 6.8)	-	1.25ml
10 % SDS	100µl	50µl
30 % Acrylamide/bisacrylamide (37.5:1)	3.4ml	670µl
10 % APS	100µl	50µl
TEMED	10µl	5µl

At the beginning it is important to make sure that the glass plates are clean and washed.
First the separating gel was poured into a gel caster. The gel was covered with a layer of EtOH and left to polymerise. After the polymerisation the EtOH was discarded and the stacking gel was poured on top of the separating gel and a comb was inserted. After the separating gel polymerised, the gel was put in a gel electrophoresis unit and the comb was removed. The samples were denatured for 5 minutes at 95°C and 1 x GTS buffer was poured into the electrophoresis unit. 10-15µl of the sample was loaded on the gel and run at 140V till the loading buffer dye reached the bottom of the gel. After the gel run, the gel electrophoresis unit was dissembled and the stacking gel was cut off. The separating gel was stained with Coomassie solution for ~15 minutes while shaking on a suitable platform. The Coomassie solution can be reused. After staining, the gel was placed in de-staining solution and left in it till protein bands were clearly visible against the background. It is advisable to change the de-staining solution in-between.

Materials

- 1.5M Tris (pH 8.8)

  45.4 g Tris

  Adjust pH with HCl. Afterwards fill up to 250ml with ddH_2O and autoclave.

- 0.5M Tris (pH 6.8)

  15.1 g Tris

  Adjust pH with HCl. Afterwards fill up to 250ml with ddH_2O and autoclave.

- 10 % APS

  1.5 g APS

  Dissolve in 15ml ddH_2O and store at 4°C protected from light.

- 10 x GTS buffer

  60 g TRIS base [f. c. 250mM]

  288 g glycine [f. c. 1.92M]

  20 g SDS [f. c. 1%]

  Add ddH_2O up to 2L and filter but do not autoclave.

- Coomassie solution

  125 ml methanol [f. c. 50%]

  25 ml acetic acid [f. c. 10%]

  625 mg Coomassie Brilliant Blue R250 [f. c. 0.25%]

  Fill up to 250ml with ddH_2O.

- De-staining solution

  50 ml Methanol [f. c. 5%]

  75 ml Acetic acid [f. c. 7.5%]

  Fill up to 1L with ddH_2O.

- Addtional reagents: 10% SDS

  30% acrylamide/ bisacrylamide solution (37.5:1)

  TEMED

11.7. Western blot

A SDS-PAGE gel was run as described in section 11.6. The stacking gel was cut off and just the separating gel was used for blotting.

A nitrocellulose membrane was cut out in the size of the gel and placed for 10 minutes in 100% EtOH. The transfer buffer was prepared and 6 Whatman paper sheets, the nitrocellulose membrane and the separating gel were placed in it. 3 Whatman paper sheets were placed on the western blot apparatus. At every step it was important that no air bubbles were in-between the layers. The membrane was placed carefully on top of the Whatman paper sheets, followed by the gel and the other 3 Whatman paper sheets at the end. The transfer was run at 100mA for 1 hour. After the transfer the membrane was placed in a 50ml falcon and blocked with ~5ml of 5% BSA in TBS-T for 2 hours at room temperature or o/n at 4°C using a rotary wheel. Next the membrane was washed with TBS-T for 1-2 minutes. The primary antibody (a mouse α-His tag) was diluted 1:2000 with TBS-T in a total volume of 4ml and the membrane was incubated with the antibody o/n at 4°C (or for 2 hours at room temperature). Before incubation with the secondary antibody, the membrane was washed 3 x for 15 minutes with TBS-T. The secondary antibody (anti-mouse) was diluted 1:10000 in 2.5 % BSA/TBS-T in a total of 5ml. The membrane was incubated with the secondary antibody for 1 hour at room temperature on the rotary wheel. Again it was washed 3 x for 15 minutes with TBS-T.

The secondary antibody was then detected by chemiluminescence using the Amersham ECL Prime Western Blotting Detection Reagent kit (GE Healthcare) following the manufacturer's manual.

Materials

- Transfer buffer

  20 % EtOH

  1 x GTS

- 10 x GTS buffer

  60 g TRIS base [f. c. 250mM]

  288 g glycine [f. c. 1.92M]

  20 g SDS [f. c. 1%]

  Add ddH_2O up to 2L and filter but do not autoclave. For 1 x GTS buffer dilute with ddH_2O.

- 10 x TBS

  30 g Tris [f.c. 25mM]

  80 g NaCl [f.c. 150mM]

  2 g KCl [f.c. 2mM]

  Adjust the pH to 7.4 and fill up to 1L with ddH_2O.

- 1 x TBS-T

  100 ml 10 x TBS
  1 ml Tween 20
  900 ml ddH_2O

- 5 % BSA + TBS-T

  2.5 g BSA in 50ml TBS-T

- Additional reagents: EtOH abs.
  Whatman paper
  Tween 20
  BSA (10mg/ml)
  mouse α-His tag antibody (provided by the laboratory of G. Wiche)
  anti-mouse antibody

12. Splicing assay

12.1. Restriction digest

The splicing assays were performed using the pbI5 construct received from K. M. Weeks's laboratory.
To be able to transcribe the plasmid it had to be cut with the restriction enzyme XbaI.

Reaction mix:

psbI5 (100µg)	30.15µl
10 x NEB 4 buffer	12µl
100 x BSA	1.2µl
XbaI (20U/µl)	7µl
ddH_2O	69.65µl
	120µl

The reaction mix was incubated at 37°C o/n. XbaI can be inactivated through heat inactivation. The mix was consequently incubated at 65°C for 20 minutes. Afterwards it was precipitated.

Precipitation: 2 µl 0.5M EDTA (pH 8)
1 µl glycogen (10mg/ml)
2.5 x vol. EtOH/ 0.3M NaOAc

The sample was stored at -20°C for at least 1 hour. Next the sample was centrifuged at full speed at 4°C for 30 minutes. After discarding the supernatant the pellet was washed with 70 % EtOH, dried for 10 minutes at room temperature and resuspended in 20µl of ddH_2O. The RNA concentration was measured with a UV/VIS spectrometer (e.g. Nanodrop).

Materials:

- Additional reagents: EtOH / 0.3M NaOAc (pH 5)
  0.5M EDTA (pH 8)
  glycogen (10mg/ml)
  70 % EtOH

12.2. *In vitro* transcription (body labelling)

This step was performed using the MEGAscript® T7 Kit (Ambion). Before starting the UTP solution was diluted 1:10 with dH_2O.

Reaction mix:

ATP (75mM)	4µl
CTP (75mM)	4µl
GTP (75mM)	4µl
1:10 UTP (7.5mM)	4µl
α-^{32}P-UTP (10µCi/µl)	6µl
10 x reaction buffer	4µl
enzyme mix	4µl
template DNA (2µg)	0.5µl
dH_2O	9.5µl
	40µl

The reaction mix was incubated at 37°C for 1 ½ hours. 2µl of TURBO DNase were added and incubated at 37°C for further 15 minutes. The cleanup was performed using the MEGAclear® Kit (Ambion), following the manufacturer's manual. Alternatively, the cleanup was performed using illustra MicroSpin G-25 columns (GE Healthcare), following the manufacturer's manual.

Materials:

- Additional reagent: α-^{32}P-UTP (6000 Ci/mmol; 10µCi/µl; Hartman Analytics)

12.3. Self-splicing kinetics

With the kinetic assays different conditions were analysed.

CBP2-assisted bI5 splicing and controls

		pos. con.	neg. con.	25nM CBP2	50nM CBP2
	RNA	0.25µl	0.25µl	0.25µl	0.25µl
	0.1 x TE	14µl	14µl	14µl	14µl
	→ 90°C for 1'				
	→ put on ice for 2'				
+	10 x reaction buffer I	2µl	-	-	-
	10 x reaction buffer II	-	2µl	2µl	2µl
	0.25µM CBP2	-	-	2µl	-
	0.5µM CBP2	-	-	-	2µl
	RNA inhibitor (40U/µl)	2µl	2µl	2µl	2µl
	Protein storage buffer	1.75µl	1.75µl	-	-
	incubate at 35°C for 30'				
+	20mM GTP	1µl	1µl	1µl	1µl
	at indicated time points 1µl aliquots were taken and treated as follows				
+	Proteinase K (20mg/ml)	1µl	1µl	1µl	1µl
	incubate for 1'				
+	STOP buffer	3 µl	3µl	3µl	3µl
	→ put samples on ice				

Adding Mss116 to the denatured bI5 pre-RNA

		50nM Mss116	25nM CBP2 + 25nM Mss116	25nM CBP2 + 50nM Mss116	50nM CBP2 + 100nM Mss116
	RNA	0.25µl	0.25µl	0.25µl	0.25µl
	0.1 x TE	14µl	14µl	14µl	14µl
	→ 90°C for 1'				
	→ put on ice for 2'				
+	10 x reaction buffer II	2µl	2µl	2µl	2µl
	0.5µM CBP2	-	1µl	1µl	-
	1µM CBP2	-	-	-	1µl
	0.5µM Mss116	2µl	1µl	-	-
	1µM Mss116	-	-	1µl	-
	2µM Mss116	-	-	-	1µl
	RNA inhibitor (40U/µl)	2µl	2µl	2µl	2µl
	Protein storage buffer	-	-	-	-
	incubate at 35°C for 30'				
+	20mM GTP	1µl	1µl	1µl	1µl
	at indicated time points 1µl aliquots were taken and treated as follows				
+	Proteinase K (20mg/ml)	1µl	1µl	1µl	1µl
	incubate for 1'				
+	STOP-buffer	3µl	3µl	3µl	3µl
	→ put samples on ice				

Adding Mss116 to the native bI5-CBP2 complex

		25nM CBP2 + 25nM Mss116	25nM CBP2 + 50nM Mss116	50nM CBP2 + 50nM Mss116	50nM CBP2 + 100nM Mss116
	RNA	0.25µl	0.25µl	0.25µl	0.25µl
	0.1 x TE	14µl	14µl	14µl	14µl
	→ 90°C for 1'				
	→ put on ice for 2'				
+	10 x reaction buffer II	2µl	2µl	2µl	2µl
	0.5µM CBP2	1µl	1µl	-	-
	1µM CBP2	-	-	1µl	1µl
	RNA inhibitor (40U/µl)	2µl	2µl	2µl	2µl
	Protein storage buffer	-	-	-	-
	incubate at 35°C for 30'				
+	0.5µM Mss116	1µl	-	-	-
	1µM Mss116	-	1µl	1µl	-
	2µM Mss116	-	-	-	1µl
	incubate at 35°C for 30'				
+	20mM GTP	1µl	1µl	1µl	1µl
	at indicated time points 1µl aliquots were taken and treated as follows				
+	Proteinase K (20mg/ml)	1µl	1µl	1µl	1µl
	incubate for 1'				
+	STOP-buffer	3µl	3µl	3µl	3µl
	→ put samples on ice				

The samples were analysed on a 5 % denaturing polyacrylamide gel.

Materials:

- 0.1 x TE

  1 µl 1M Tris (pH 7.5) [f.c. 1mM]

  0.2 µl 0.5M EDTA (pH 8) [f.c. 0.1mM]

  Fill up to 1ml with ddH_2O.

- 10 x reaction buffer I (400mM Mg^{2+})

  0.5 ml 1M Hepes (pH 7.6) [f.c. 500mM]

  0.166 ml 3M KCl [f.c. 500mM]

  400 µl 1M $MgCl_2$ [f.c. 400mM]

  Fill up to 1ml with ddH_2O.

- 10 x reaction buffer II (70mM Mg^{2+})

  0.5 ml 1M Hepes (pH 7.6) [f.c. 500mM]

  0.166 ml 3M KCl [f.c. 500mM]

  70 µl 1M $MgCl_2$ [f.c. 70mM]

  Fill up to 1ml with ddH_2O.

- Protein storage buffer

  40 µl 1M Hepes (pH 7.6) [f.c. 20mM]

  400 µl 1M NaCl [f.c. 200mM]

  0.4 µl 0.5M EDTA (pH 8) [f.c. 0.1mM]

  800 µl glycerol [f.c. 40%]

  4 µl 1M DTT [f.c. 2mM]

  Fill up to 2mL with ddH_2O.

- STOP buffer

  Solution 1: 500 µl 50% sucrose [f. c. 25%]

  100 µl 10 x TBE [f. c. 1 x TBE]

  500 µl ddH_2O

  + crumbs of bromophenol blue and xylene cyanol

  Solution 2: 800 µl formamide [80%]

  200 µl solution1 [20%]

  Solution 3: 100 µl 0.5M EDTA (pH 8) [f. c. 50mM]

  900 µl solution 2

- 10 x TBE

  540 g Tris base [f.c. 890mM]

  275 g boric acid [f.c. 890mM]

  29.2 g EDTA [f.c. 20mM]

  Fill up to 5L with ddH_2O and autoclave.

- Additional reagents: 20mM GTP
  Proteinase K (20mg/ml)
  RNA inhibitor (40U/µl)

12.4. Denaturing PAGE

To separate the splicing products of the kinetic assay, a 5 % denaturing polyacrylamide gel is used.

- Acrylamide solution:

	5%
7M Urea	210g
40 % acrylamide/bisacrylamide solution (19:1)	62.5ml
10 x TBE	50ml

Fill up with ddH_2O to 500ml.

- Acrylamide gels:

Size	20cm x 22cm
5 % acrylamide solution	30ml
10 % APS	300µl
TEMED	30µl

After polymerization the gel was adjusted on the gel apparatus and the chambers were filled with 1 x TBE. Before the samples were loaded, the wells were rinsed out with running buffer. The gel was run at 23W until the xylene cyanol dye has reached the last third of the gel.

The gel was then transferred to Whatman paper and covered with saran wrap. It was placed on a gel drier at 80°C for at least 1 hour under vacuum. The dried gel was placed for exposure into a phosphor imager cassette o/n. The following day the screen was scanned using a STORM Phosphorimager 820 and analyzed with Image Quant and Kaleidagraph.

To achieve more accurate results, we took into account the number of Us in the different RNA molecules (precursor and products) during analysis.

Materials:

- 10 x TBE

  540 g Tris base [f.c. 890mM]

  275 g boric acid [f.c. 890mM]

  29.2 g EDTA [f.c. 20mM]

  Fill up to 5L with ddH_2O and autoclave.

- 10 % APS

  1.5 g APS

  Dissolve in 15 ml of ddH_2O and store at 4°C protected from light.

- Additional reagents: 40 % acrylamide/bisacrylamide solution (19:1)
  TEMED

12.5. 5' end labeling of RNA ladder

To determine the fragment size of the splice products, an RNA ladder was radioactively labeled. First the ladder had to be dephosphorylated.

The following reaction mix was prepared:

RNA ladder	8µl
Rnase inhibitor (40U/µl)	0.5µl
10 x NEB 4 buffer	2µl
CIP (10U/µl)	2µl
ddH_2O	7.5µl
	20µl

The sample was incubated at 37°C for 30 minutes, followed by a phenol extraction. After increasing the volume of the sample to 200µl, 200µl of phenol/CI (1:1) mixture was added (note that water-saturated phenol at pH~4 is used for RNA) and vortexed well. The sample was centrifuged at 4°C at full speed for 3 minutes. The upper phase was transferred in a new tube and mixed with additional 200µl of CI. This was followed by vortexing and centrifugation as before. Finally, the upper phase was pipetted into a new tube and precipitated with 2.5 x vol. EtOH/ 0.3M NaOAc for 15-30 minutes at
-20°C. The sample was then centrifuged at full speed for 20 minutes at 4°C, washed with 70 % EtOH and dried for 10 minutes at room temperature. The pellet was resuspended in 10µl of dH_2O.

For labeling, the following reaction mix was prepared:

dephos. RNA ladder	1µl
Rnase inhibitor (40U/µl)	0.25µl
10 x T4 PNK buffer	1µl
T4 polynucleotide kinase (10U/µl)	1µl
γ-^{32}P-ATP (10µCi/µl)	5µl
ddH_2O	1.75µl
	20µl

The sample was incubated at 37°C for 30 minutes. The reaction was stopped by adding 1µl of 0.5M EDTA (pH 8). An equal amount of chloroform was added and the sample centrifuged at full speed for 3 minutes at 4°C. The upper phase was transferred into a new tube. Before loading it onto the gel, the RNA ladder was diluted 1:2 with ddH_2O.

Materials:

- Additional reagents: water-saturated phenol (pH 4)
  chloroform / isoamyl alcohol (24:1)
  EtOH / 0.3M NaOAc (pH 5)
  70 % EtOH
  0.5M EDTA (pH 8)
  chloroform
  γ- ^{32}P-ATP (6000 Ci/mmol; 10µCi/µl; Hartman Analytics)

13. ATPase assay

To determine if the recombinant Mss116 produced in our lab is functional, an ATPase assay was performed.

13.1. Restriction digest

To be able to carry out a run-off *in vitro* transcription, the pbI5 plasmid had to be cut with XbaI.

Reaction mix:

pbI5 (100µg)	30.15µl
10 x NEB 4 buffer	12µl
100 x BSA	1.2µl
XbaI (20U/µl)	7µl
ddH_2O	69.65µl
	120µl

The reaction mix was incubated at 37°C o/n. As XbaI can be inactivated through heat inactivation, the mix was stored for 20 minutes at 65°C. Afterwards it was precipitated.

Precipitation: 2µl 0.5M EDTA (pH 8)
1µl glycogen (10mg/ml)
2.5 x vol. EtOH/0.3M NaOAc

The sample was stored at -20°C for at least 1 hour. Next the sample was centrifuged at full speed at 4°C for 30 minutes. After discarding the supernatant the pellet was washed with 70 % EtOH, dried for 10 minutes at room temperature and resuspended in 20µl of ddH_2O. The RNA concentration was measured with an UV/VIS spectrometer (e.g. Nanodrop).

Materials:

- Additional reagents: EtOH / 0.3M NaOAc (pH 5)
  70 % EtOH
  0.5M EDTA (pH 8)
  glycogen (10mg/ml)

13.2. MEGAscript® Kit (Ambion)

The *in vitro* transcription was performed using the MEGAscript® Kit (Ambion), according to the manufacturer's manual.

13.3. MEGAclear™ Kit (Ambion)

The sample cleanup was performed using the MEGAclear™ Kit (Life Technologies) as described in the manufacturer's manual. Afterwards, the sample was precipitated using 2.5 x vol. EtOH/ 0.3M NaOAc, 1µl of glycogen (10mg/ml) and 1µl of 0.5M EDTA (pH 8) and stored at -20°C o/n. The next day it was centrifuged at full speed at 4°C for 30 minutes. The supernatant was discarded, the pellet washed with 70 % EtOH and dried

for 10 minutes at room temperature. The pellet was resuspended in 20µl of ddH_2O and the RNA concentration measured with an UV/VIS spectrometer (e.g. Nanodrop).

Materials:

- Additional reagents: EtOH / 0.3M NaOAc (pH 5)
  70 % EtOH
  0.5M EDTA (pH 8)
  glycogen (10mg/ml)

13.4. ATPase assay

Different conditions were performed to determine whether Mss116 is capable of hydrolyzing ATP and if RNA or CBP2 have an influence on this activity.

	only CBP2	only Mss116	RNA/CBP2	RNA/Mss116
200nM Mss116	-	17.65µl	-	17.65µl
200nM CBP2	1.07µl	-	1.07µl	-
400nM CBP2	-	-	-	-
RNAse inhibitor (40U/µl)	1µl	1µl	1µl	1µl
11.53µM pbI5 [f.c. 0.5µM]	-	-	2.6µl	2.6µl
Proteinase K (20mg/ml)	-	-	-	-
incubate 10' at 30°C				
500mM NaCl	30µl	-	30µl	-
40mM HEPES (pH 7.5)	2.4µl	2.4µl	2.4µl	2.4µl
1mM DTT	6µl	6µl	6µl	6µl
ddH_2O	10.53µl	25.72µl	7.93µl	21.35µl
incubate 10' at 30°C				
20mM $MgCl_2$ [f.c. 1mM]	3µl	3µl	3µl	3µl
10mM ATP [f.c. 1mM]	6µl	6µl	6µl	6µl
	60µl	60µl	60µl	60µl

	RNA/CBP2+Mss116 1:1	RNA/CBP2+Mss116 2:1	RNA/CBP2+Mss116 1:1 + Proteinase K
200nM Mss116	17.65µl	17.65µl	17.65µl
200nM CBP2	1.07µl	-	1.07µl
400nM CBP2	-	2.15µl	-
RNAse inhibitor (40U/µl)	1µl	1µl	1µl
11.53µM pbI5 [f.c. 0.5µM]	2.6µl	2.6µl	2.6µl
Proteinase K (20mg/ml)	-	-	0.5µl
incubate 10' at 30°C			
500mM NaCl	-	-	-
40mM HEPES (pH 7.5)	2.4µl	2.4µl	2.4µl
1mM DTT	6µl	6µl	6µl
ddH_2O	20.28µl	19.2µl	19.78µl
incubate 10' at 30°C			
20mM $MgCl_2$ [f.c. 1mM]	3µl	3µl	3µl
10mM ATP [f.c. 1mM]	6µl	6µl	6µl
	60µl	60µl	60µl

The reaction starts with the addition of ATP. 5µl aliquots of each reaction mix were taken at the following time points 0 / 5 / 10 / 20 / 30 / 45 / 60 / 90 / 120 / 150 / 180 minutes. For determining the amount of hydrolysed ATP in each aliquot, the Malachite Green Phosphate Detection Kit (R&D Systems) was used and all steps were performed in a µclear 96 well plate and at room temperature. First 45µl of ddH_2O were added to each 5µl aliquot. 10µl of reagent A was added to each sample and incubated for 10 minutes. Then 10µl of reagent B was pipetted to the sample and incubated for further 20 minutes. The absorbance was measured at 620nm with the Infinite F500 microplate reader (Tecan). The data was analysed with Microsoft Excel.

Materials:

- 1M Dithiothreitol (DTT)

  154 mg DTT

  Add 1ml of ddH_2O, resuspend and store at -20°C.

- Additional reagents: Proteinase K (20mg/ml)
  1M NaCl
  1M Hepes (pH 7.5)
  1M $MgCl_2$
  10mM ATP

14. Sequencing

To determine the sequences of the plasmid or of PCR products, the samples were sent to LGC Genomics or Microsynth Austria. The samples were prepared in accordance with the company's manual.

Results

To obtain the first insights into how the co-factor CBP2 and RNA helicase Mss116 co-opt to facilitate bI5 folding and in turn splicing *in vitro,* the proteins have to be purified and their activity confirmed. We therefore established a protocol for producing recombinant CBP2 protein. The activity of Mss116, which was kindly provided by S.Handl, was measured with the ATPase assay, and the effect of CBP2 on Mss116 was also tested in this way. After achieving the purification of active proteins, it was possible to determine the efficiency of splicing *in vitro* under near-physiological conditions (7mM Mg^{2+}) in the absence and presence of the proteins. We performed the splicing assays under different conditions, taking into account the time-shifted addition of the proteins. In addition, constructs were created containing different variations of the full-length bI5 intron.

1. Creation of different bI5 intron constructs

To observe efficient splicing of the bI5 intron *in vitro*, it was necessary to delete several larger peripheral extensions to allow proper folding of the intron RNA (Weeks & Cech, 1995a). In other words this bI5 variant maintained the intron core structure and was named accordingly (bI5core). The deleted regions did not alter the splicing mechanism (Weeks & Cech, 1995a). However, to gain information on the role of Mss116 and CBP2 in bI5 folding, it is necessary to have different bI5 constructs at hand varying in their intron length and presence and length of flanking exons. Our aim is to gain information about the splicing activity of the bI5core construct and consequently to create the original full-length intron as well as other three constructs with varying exon lengths (Figs. 17 and 18). The full intron is obtained by RT-PCR of total RNA from a yeast strain expressing bI5. We aimed to create a construct containing just the full length intron without exons (pCW76), and one construct with a shorter version of the ribozyme clone without exons (pCW75). The third construct was expected to contain the full length intron and 25nts exons at each end (pCW77). The fourth construct was also expected to contain the full length intron though a 50nts exon at the 5’ end and a 100nts exon at the 3’ end (pCW78). In order to achieve this we use a two step reverse transcription - PCR process. This process is based on a non-specific reverse transcription, followed by a specific PCR.

At the beginning we purified the RNA of three different yeast strains (provided by Nora Sachsenmaier) using the RiboPure™- Yeast kit (Life Technologies). We examined which strain is the most adequate to use for the experiments. After completing the first experiments we decided to use total RNA extracted from the yeast strain yCW07 for our construct creation, as only bI5 pre-RNA should be present in this sample.

A

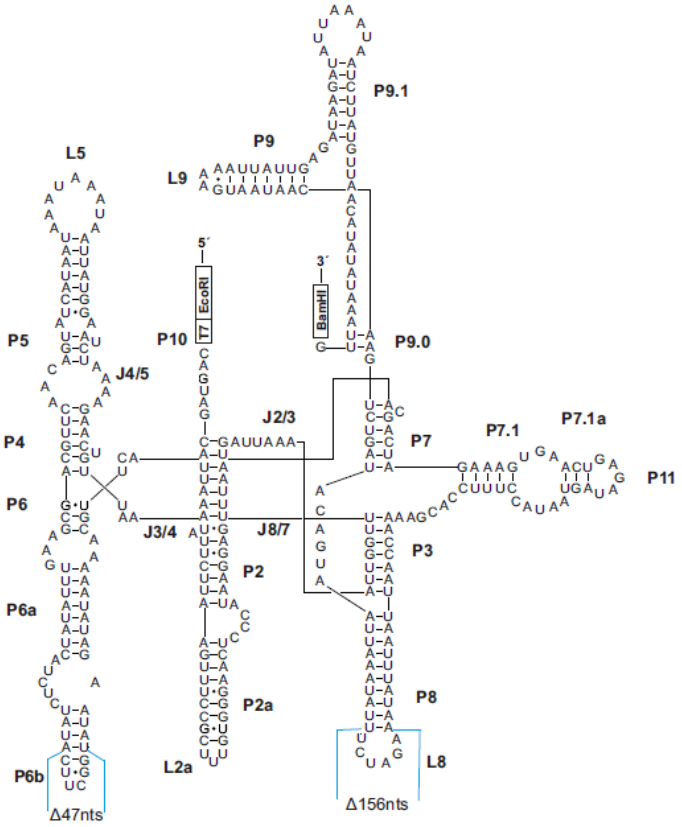

B

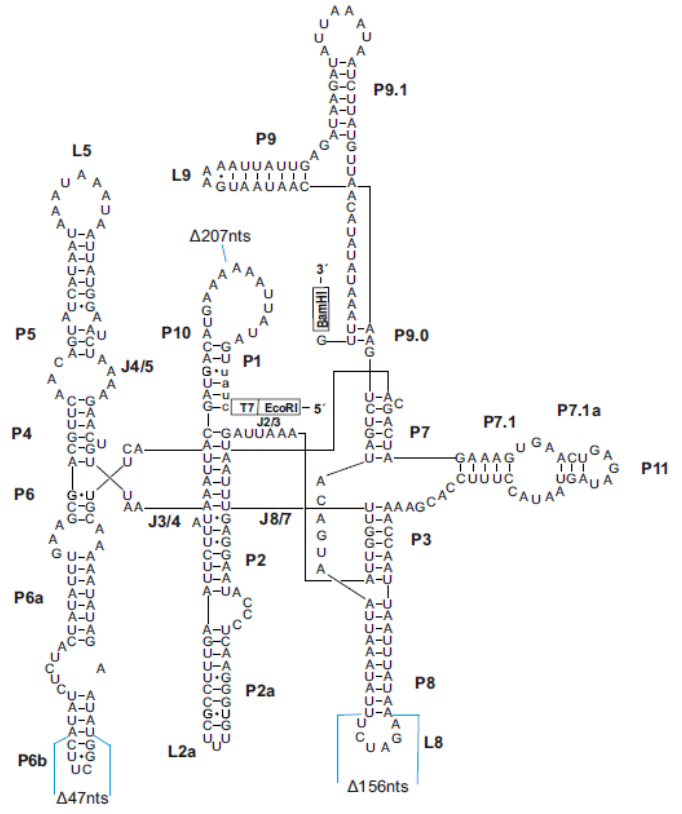

Fig. 17. Secondary structure of the bI5 variants.
Panel A shows bI5 variant of pCW75 containing a short version of the ribozyme clone. Panel B shows bI5 variant of pCW76 with the full intron. Both constructs have the T7 promoter as well as both restriction enzymes (EcoRI and BamHI) indicated.

A

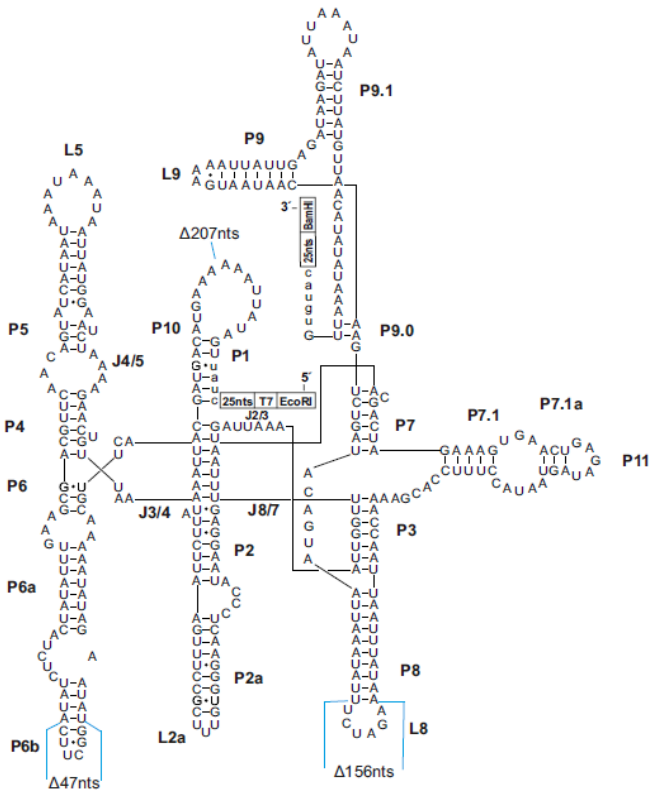

B

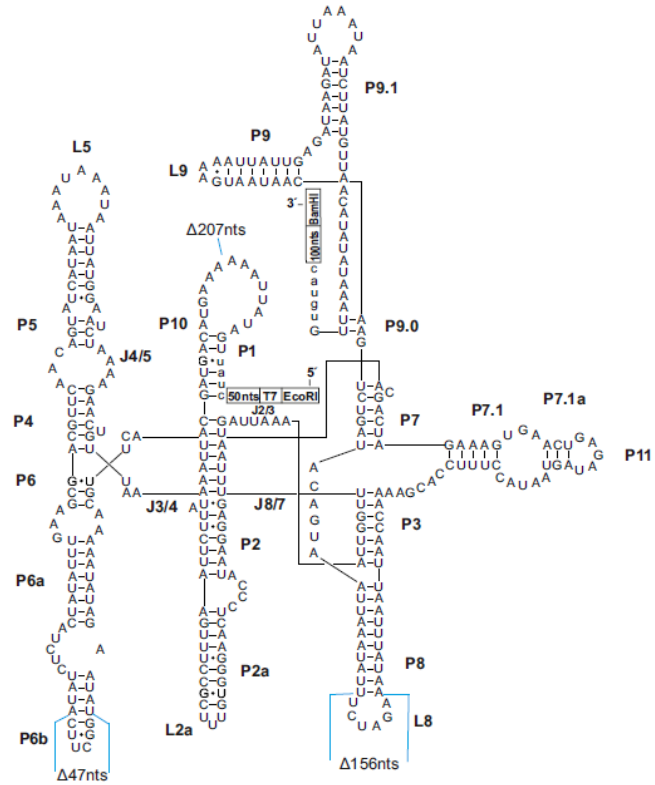

Fig. 18. Secondary structure of bI5 variants with exons.
Panel A shows the bI5 structure with 25nts long exons at both ends. Panel B shows the bI5 structure with a 5' exon of 50nts in length and a 3' exon of 100nts Both constructs have the T7 promoter and both restriction enzymes (EcoRI and BamHI) indicated.

1.1. Random reverse transcription – gene-specific PCR

As the two-step process which is used for creating the constructs is based on randomly primed reverse transcription, a random hexamer mix was used (Promega). The random hexamers are oligonucleotides of 6 bases which are randomly synthesized. The random synthesis provides a large potential for the oligonucleotides to anneal randomly to RNA. The moloney murine leukemia virus reverse transcriptase (MMLV-RT) was used for the reverse transcription (Promega). MMLV-RT is an RNA-dependent DNA polymerase mostly used for cDNA synthesis of longer length. The reverse transcription was performed at 40°C.

With the obtained cDNA we performed a PCR using gene-specific primers. For this PCR, we used the primer pair CW75F and CW75R for the rc construct, the CW76F and CW76R primer pair for the fi construct, the CW77F and CW77R primer pair for the 25/25 construct and the CW78F and CW78R primer pair for the 50/100 construct. The forward (F) primers contain an EcoRI restriction site, followed by a T7-promoter sequence. The reverse (R) primers contain a BamHI restriction site at the end. We used a combination of Pfu/GoTaq polymerase for PCR. GoTaq polymerase (Promega) is a robust DNA polymerase, whereby the Pfu polymerase (Promega) has proofreading activity.

As no PCR products were obtained, we modified the reaction set up, but the results did not improve (data not shown).

1.2. Gene-specific reverse transcription and PCR

Due to unsuccessful unspecific reverse transcription, we decided to change our approach. The reverse transcription protocol was optimized by adding DMSO to the reverse transcription reaction mix, using just GoTaq polymerase and varying the PCR annealing temperature between 45°C and 50°C. As the specific primers for the PCR reaction contain a T7 promoter sequence and different restriction sites, we designed shorter new primers specifically for the RT with just the exon or intron sequence (no dangling ends). For the gene-specific PCR we also designed new primers. The new primers have a longer sequence complementary to the template RNA. Using a shorter primer (CW75R_3) for the reverse transcription at 45°C and the longer primer pair (CW75F_2 & CW75R_2) for a gradient PCR we received a fragment for the rc construct (pCW75) of correct length (554bp). An additional reverse transcription with primer CW78R_2 at 40°C and subsequent gradient PCRs with the specific primer pairs CW77F_2 & CW77R_2, CW78F_2 & CW78R_2 and CW76F_2 & CW75R_2 for each of the remaining construct sequences resulted in PCR products of proper length – fi construct (pCW76) 781bp; 25/25 construct (pCW77) 829bp; 50/100 construct (pCW78) 923bp (Fig. 19). The products were cut with EcoRI and BamHI and ligated into the previously cut and dephosphorylated vector pBS-ΔT7. The vector is a BlueSkript vector lacking the original T7 promoter and carrying an ampicillin resistance. The ligated vector was then transformed into KCM cells (provided by Georgeta Zemora). After successful colony growth on LB-Amp-plates, colonies where picked and colony PCRs performed using GoTaq polymerase, to confirm the insertion of the wanted DNA sequence. Colonies showing the successful integration of the intron DNA were sent for sequencing to LGC Genomics.

Unfortunately only the 25/25 construct showed the correct sequence of a 829nts long bI5 pre-RNA gene without mutation (see Appendix for sequence). The other three constructs contained too many mutations. This

is explained by the use of the GoTaq polymerase which has no proofreading ability and therefore is more prone to introduce mutations in the PCR.

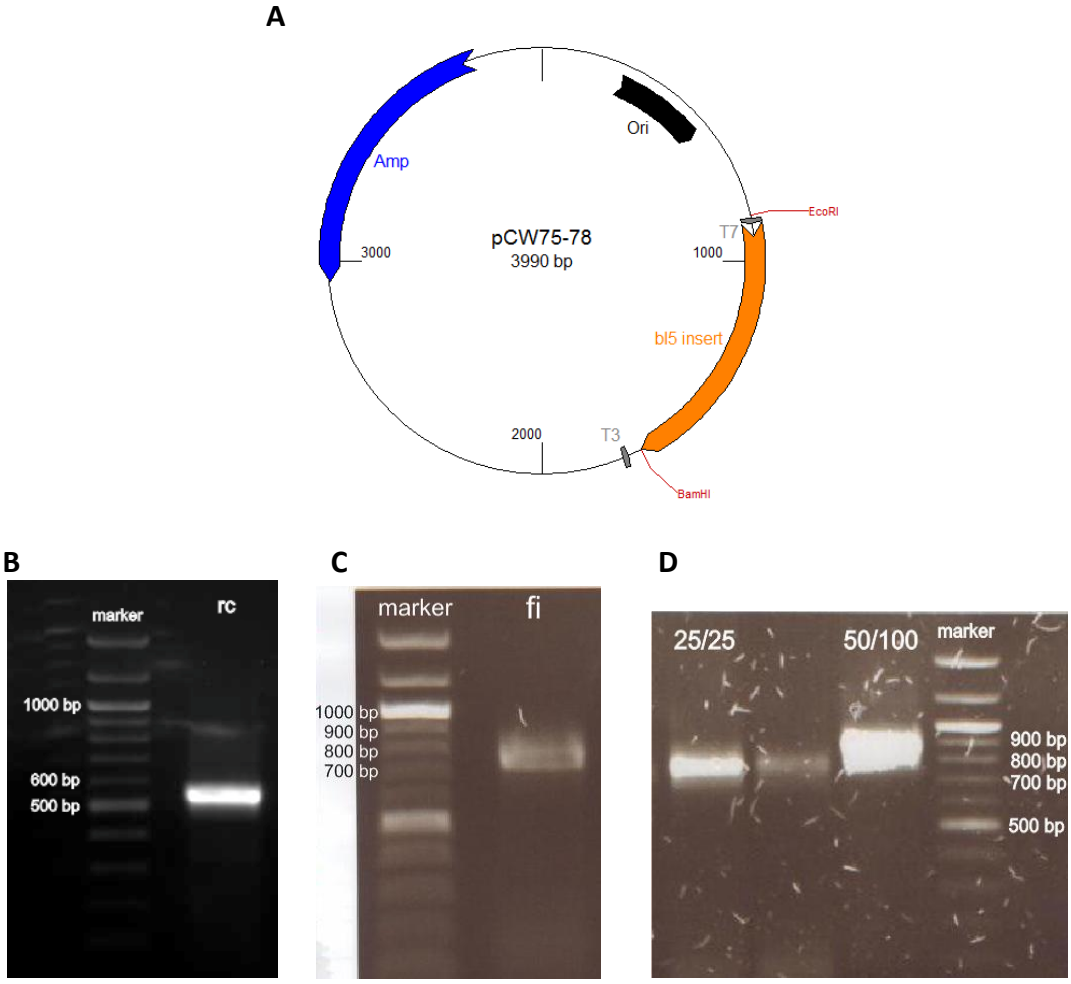

Fig. 19. Construct structure and PCR fragments
In panel A the structure of the plasmids CW 75-78 containing the bI5 inserts, the restriction sites and the ampicillin resistance gene is shown. Panel B shows the PCR fragment of the ribozyme clone (pCW75) of 554bp. In panel C the full intron fragment (781bp) of pCW76 is shown. Panel D shows the gained PCR fragments with exons. On the left PCR fragment (829bp) with exons of 25nts in length is shown. On the right the fragment (923bp) with 50nts 5' exon and 100nts 3' exon is shown.

1.3. Using the 25/25 construct as template for the preparation of remaining three bI5 constructs

Having the construct containing the full-length intron flanked by 25 nt of exonic sequence at both ends at hand led us to a new approach for preparing the other three constructs.

The 25/25 construct was used as our template for PCR with the gene-specific primers for the three constructs. This time the Pfu polymerase was used, because of its proof-reading capacity. At the temperatures previously used for the gene-specific primers, no product was obtained (data not shown), so consequently the reaction was repeated using a PCR gradient (data not shown). The gradient PCR did not lead to any results (data not shown).

Using various PCR conditions, e.g. varying the concentration of Mg^{2+} (2mM Mg^{2+} - 3.5mM Mg^{2+}) in the reaction mixes, gradient PCRs were performed between 50 – 60°C. The GoTaq polymerase at different Mg^{2+} as well as the GoTaq/Pfu mix was used. A positive result was achieved with the GoTaq polymerase alone implying that the primer design was correct. Due to mutations which had occurred previously, we did not use these PCR products for cloning.

The decision was made to try out new polymerases, Pfu Turbo and Pfu Ultra II Fusion HS (Agilent/ Stratagene), in addition to the other polymerases. In contrast to the Pfu Turbo the Pfu Ultra II Fusion HS polymerase successfully amplified the rc construct with a size of 554nts and an fi construct of 781nts (Fig. 20) (see Appendix for construct sequences). These fragments were successfully cloned into pBS-ΔT7, and a clone with the correct sequence was identified as well.

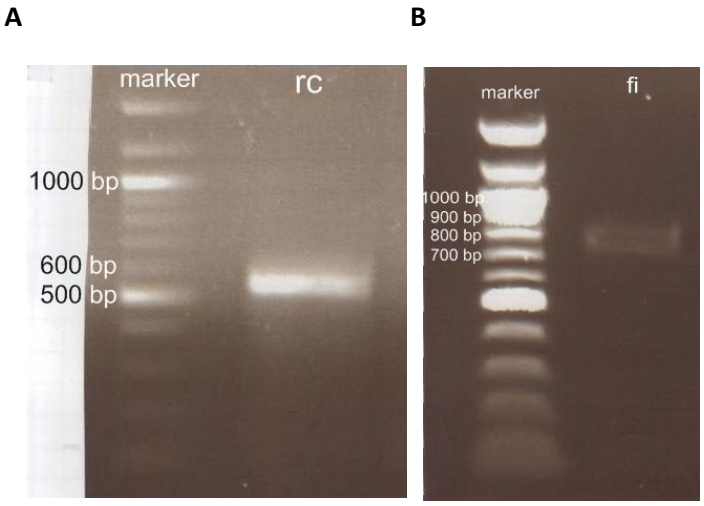

Fig. 20. bI5 inserts gained by using Pfu Ultra II Fusion HS polymerase
In panel A the rc-fragment of 554bp is shown. Panel B shows the fi-fragment (781 bp).

1.4. Construction of the 50/100 nts exon containing construct

Since it was not possible to obtain the longest of the targeted constructs with the primers tried so far, new primers were designed. This time the long primers used so far were split in two forward primers and three reverse primers. The Pfu Ultra II Fusion HS polymerase was used.

In the first PCR reaction, we amplified a product with the primer pair CW78F_3 & CW78R_5. The product was purified from a 0.8% agarose gel and used as a template for a second PCR round with the primer pair CW78F & CW78R_4. The obtained product was used as a template for the last PCR round. Notably, the third PCR was only necessary to further extend the 3' end of the construct (to yield a 100nts exon), while the extension of the 5' end (50nts exon) was already finalized in the second PCR. As such, we used the primer pair CW78F & CW78R_3 in the last PCR. Indeed, this strategy yielded a PCR product of 923nts in length (Fig. 21). This fragment was ligated into the pBS-ΔT7 vector. Transformation into KCM cells was performed and insert was confirmed through colony PCR. Plasmids from the positive clones were sent for sequencing.

Unfortunately we obtained a sequence that had the desired extended exon sequences but the sequence in-between the exons does not share any homology to the bI5 intron, nor to the yeast genome. A BLAST of the sequence did not lead to any specific conclusion about the origin of the sequence, as a variety of bacterial sequences showed up. The sequence was checked to determine whether an inverted variation of the targeted sequence or a combination resulting from incorrect integration into the vector had occurred, but this was not the case.

The same approach was repeated, using new PCR solutions and filter tips to avoid any contamination. Each PCR round product was sent for sequencing before conducting the next round. A correct product was obtained from the first PCR. The second PCR round showed a band of the correct size on the gel, although sequencing revealed that the incorrect sequence flanked by the correct exons was introduced at this step. The third PCR round demonstrated a fragment of correct size, but of incorrect sequence (see Appendix for incorrect sequence).

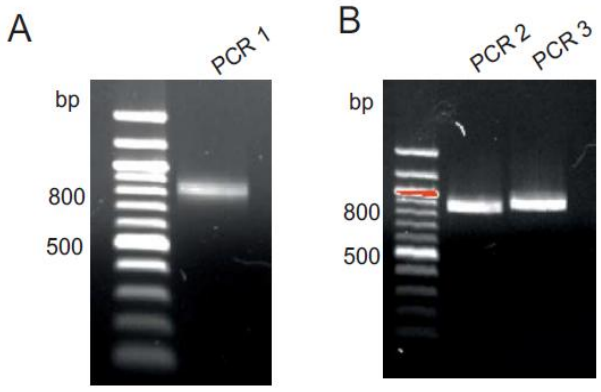

Fig. 21. Construction of 50/100 construct
Panel A shows the PCR product of the first PCR round. The product band is shown at 800bp, which indicates the right size for the product of 845bp.
Panel B shows the second (PCR 2) and the third (PCR3) PCR rounds and the obtained product bands with a size of 894bp and 924bp.

Due to lack of time it was not possible to conduct further approaches to achieve the last construct. As all attempts failed so far, a possibility would be to start at the beginning by conducting RT-PCR to obtain the insert for cloning.

2. CBP2 expression and purification

The plasmid containing the CBP2 coding sequence was generously provided by K. M. Weeks (University of North Carolina, Chapel Hill, USA). Before starting the expression of the protein, the plasmid was sent for sequencing to LGC Genomics to confirm that the correct gene sequence is found on the plasmid (see Appendix for sequence). The protein was fused to a 6 x His-tag at its C-terminus, though the first His is part of the CBP2 sequence.

To successfully express and purify the protein from *E. coli* we employed the method used by Weeks and Cech (Weeks & Cech, 1995a). CBP2 was overexpressed in *Escherichia coli* Rosetta and gene expression was induced with IPTG; after cell lysis CBP2 is purified via affinity chromatography using Ni-NTA. At the beginning, different expression conditions had to be tested. The plasmid contained ampicillin and tetracycline resistance genes. We transformed the plasmid into *E. coli* Rosetta and plated it on selective LB-plates. We decided to use just ampicillin as a selective antibiotic, because slow growth was observed on LB-Tet-plates. This may be due to the higher toxicity of tetracycline. In addition, the most adequate protein expression temperature had to be chosen. The highest yield of the protein was obtained by inducing CBP2 expression with 1mM IPTG at 22°C overnight.

It is important to note that the molecular weight of CBP2 was calculated to be 74kDa, although the apparent molecular mass determined by sedimentation is 55 ± 7 kDa (Weeks & Cech, 1995a). In our gels the protein migrated between 58 and 80 kDa in the SDS-PAGE; this is in accordance with the mentioned results. The solubility of the protein is important for reaching a high-yield. Therefore it is important to choose a method of purification where the protein is soluble. The solubility can depend on the protein expression conditions or the cell breakage method. At high-yield protein purifications, the protein can turn out to be insoluble and found in the bacterial cell debris or aggregate in inclusion bodies, reducing the protein amount for further steps of experiments. We therefore compared the level of protein found in the cell pellet and the supernatant after cell lysis. The results (Fig. 22) showed that most of the protein is found in the supernatant and therefore is in a soluble state, while in the cell pellet a low amount of protein is present.

To follow the different expression and purification step, each fraction was analyzed on a SDS-PAGE (Fig. 22). In panel A of Fig. 22 the protein expression in the cell before and after induction with IPTG is shown in the first two lanes. The expression of the protein was clearly visible compared with the sample before induction. Lane 4 and 5 showed the amount of protein in the supernatant and in the cell pellet after sonication. The majority of the protein was found in the supernatant. This indicated that the protein was soluble and cell lysis by sonication was a favourable method to gain a high yield of protein. The flow-through of the Ni-NTA column (lane 6) showed significant amounts of the induced protein, implying that the column matrix was saturated. Lanes 7-10 were the first washing steps of the column with the column buffer. In Fig. 17B the second washing steps with column buffer containing 20mM imidazole were shown in lane 2-6. A slight elution of the CBP2 protein (or protein of same size) was observed already, though other cell components were still visible in the first fractions. This implied that 20mM imidazole were not enough to elute CBP2, though are efficient at eluting cell remains that are still bound to the Ni-NTA column. Lane 7-10 showed the elutions of CBP2 with column buffer supplemented with 80mM imidazole. CBP2 protein was eluted in a high amount, made visible as the thick band between 50 – 80 kDa. 80mM imidazole was efficient to elute the protein from the column. In Fig. 17C the last elution fraction with 80mM imidazole was seen in lane 2, followed by 5 elution fractions with 200mM imidazole in lane 3-7. 200mM imidazole still eluted some moiety of CBP2 protein, though most of it was already eluted with 80mM imidazole, indicated by the decreasing band intensity. The gel runs after the purification from the Ni-NTA column showed that the majority of the pure protein was achieved at the elution steps with the column buffer containing 80mM imidazole. As such, only a rather small amount of CBP2 could be

eluted with 200mM imidazole. No degradation of CBP2 was seen, although a second band indicated a protein double the size of CBP2 thus, a potential CBP2 dimer. This protein was also released from the column when washed with the column buffer containing 80mM imidazole, although the intensity was by far weaker than the band seen between 58 – 80 kDa.

To make sure that the protein band obtained in the different elution steps is CBP2, we performed a Western blot analysis (Fig. 23). Therefore we used a mouse α-His-tag antibody as the primary antibody and an anti-mouse antibody as the secondary antibody. Even after only short exposure time an intense signal appeared on the film, confirming that the obtained protein has a His-tag and might be CBP2. Interestingly, the band seen at ~ 174 kDa was also visible on the film. This indicated that it also contains a His-tag.

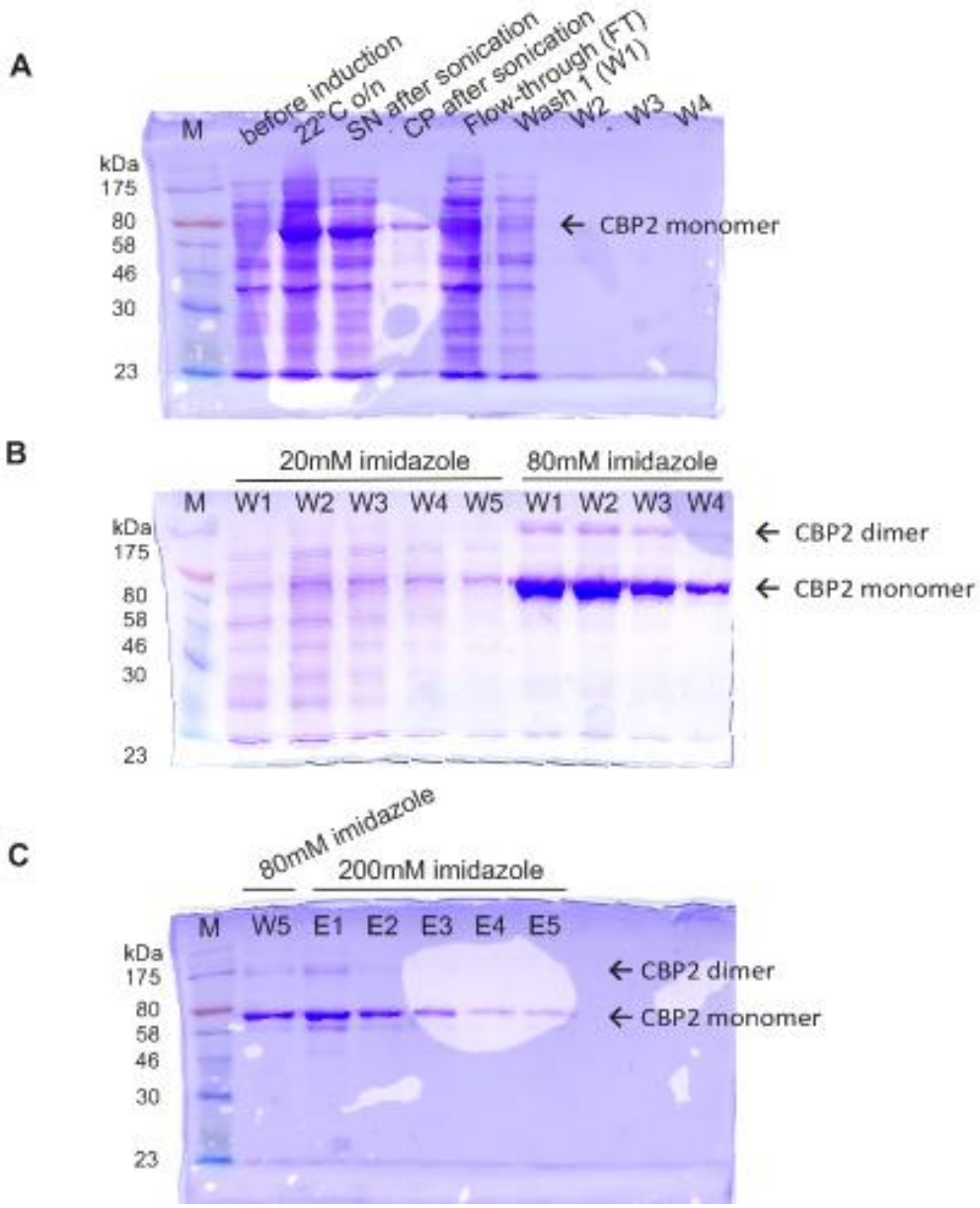

Fig. 22. CBP2 purification SDS-PAGE gels.
The first gel (A) shows the protein expression before and after IPTG induction as well as the moiety of CBP2 found in the cell pellet and supernatant after sonication. The flow-through sample and the first washing steps are as well seen in panel A. All wash and elution fraction samples are shown in panel B and C.

To assess if a pure CBP2 batch was prepared and to get more information about the second band we observed, both observed bands were cut out from a SDS-PAGE gel and sent for mass spectrometry analysis to the Mass Spectrometry Facility of the Max F. Perutz Laboratories. The results received confirmed that both bands contained the CBP2 protein (data not shown). The band at ~174 kDa could indicate a dimer formed during the purification step or in the cell, as it mostly consists of the CBP2 protein. Evidence for dimer formation of CBP2 could not be found in previous publications.

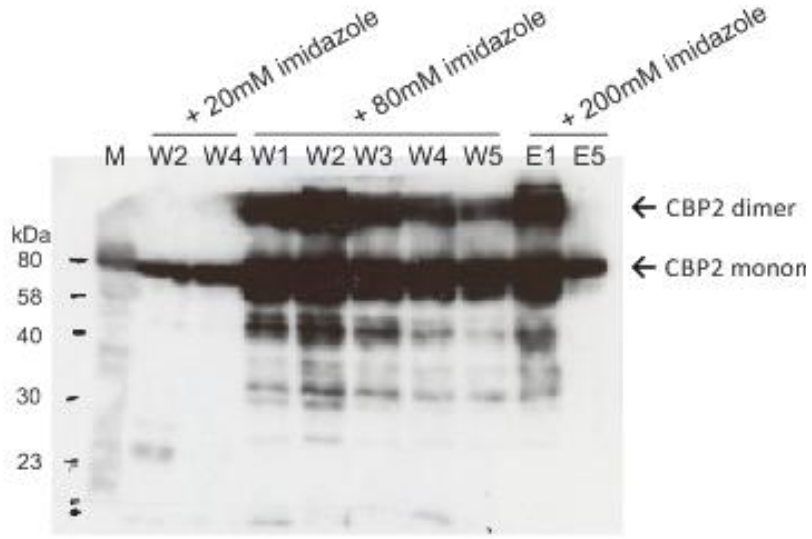

Fig. 23. Western blot analysis of CBP2 elutions.
The CBP2 is purified by using a His-tag at the C-terminus of the protein. To confirm that the elutions contain CBP2, a Western blot was performed using an anti-His-antibody.

To eliminate small proteins, which were also identified during mass spectrometry and to obtain very pure CBP2, we used centrifugal unit devices with a cut-off of 30kDa and dialysis overnight. It is important to note that removal of the His-tag is not needed.

The concentration of the purified protein was measured via the Bradford assay. As already indicated from the SDS-PAGE gel run, the concentration of the CBP2 protein was very high, namely ~333µM at the first purification attempt and twice as much performing the purification for a second time (670µM). The protein was stored at -20°C and showed no decrease in activity within 1 year.

3. The influence of CBP2 on the ATPase activity of Mss116

S. cerevisiae DEAD-box protein Mss116 is essential for *in vivo* splicing of group I and group II introns (Halls et al, 2007; Huang et al, 2005; Solem et al, 2006). To stimulate intron splicing Mss116 depends on its ATPase activity (Cao et al, 2011; Halls et al, 2007; Huang et al, 2005; Mohr et al, 2006). The hypothesis that Mss116 has an

RNA-dependent ATPase activity has been proven previously by Halls et al. Almost no ATPase activity was measured in the absence of RNA. Halls et al. showed that the efficiency of ATP hydrolysis varies in the presence of different RNAs (Halls et al., 2007). Cao et al. also showed that RNA enhances the ATPase activity of Mss116 ~7 fold by promoting the rate-limiting ATP hydrolysis step (Cao et al, 2011).

To determine the ATPase activity of Mss116, the Malachite Green Phosphate Detection Kit (R&D Systems) was used. The kit measures the concentration of free inorganic phosphate by forming complexes with malachite green and molybdate under acidic conditions (Van Veldhoven & Mannaerts, 1987). The protocol (see Methods section 13.4.) was adapted from E. M. Steiner (Steiner, 2012). Mss116 was purified and provided by Stefan Handl from the Waldsich group. The main point of interest was the influence of CBP2 on the ATPase activity correlation of Mss116. Therefore we not only performed experiments involving Mss116 only, but also added CBP2 and determined Mss116's ATPase activity. CBP2 has no ATPase activity and is needed to stabilize the structure of bI5, to which it binds with high affinity (Weeks & Cech, 1995a).

The results (Fig. 24) show that Mss116 is active and hydrolyses ATP; this activity is enhanced in the presence of bI5 RNA. Almost the same activity is observed when CBP2 is added in an equimolar ratio to the reaction, as well as when adding a 2-fold molar excess of CBP2. This indicates that CBP2 does not have any effect on the ATPase activity of Mss116. This implies that CBP2 does not sequester bI5 RNA on Mss116, as this would reduce ATP hydrolysis. Thus, it is possible that both proteins have similar affinities to bI5 and may bind simultaneously to bI5 at different sites.
Previous publications (Halls et al, 2007) showed that reduced ATPase activity is observed by Mss116 without RNA. This agrees with our results and the activity of Mss116 was increased in presence of bI5; however this increase in ATPase activity is smaller than previously determined (Steiner, 2012). An explanation for our results could be the purification of the Mss116 protein. Despite of excessive washing steps and dialysis used during purification of the protein, it is still conceivable that a small quantity of the RNA that was already bound to the protein at the expression state is still present and could not be removed during purification. This small quantity of RNA could be the reason that the supposed reaction without bI5 contains RNA and shows somewhat higher ATPase activity. Additionally, our results confirmed that CBP2 alone, and also when mixed together with bI5 intron, has no ATPase activity. As a control reaction equimolar amounts of Mss116 and CBP2 supplemented with RNA were treated with Proteinase K. Proteinase K digests proteins, therefore no ATPase reaction should be achieved as both proteins should be degraded. As expected the control reaction showed no activity, implying that the detected ATPase activity is attributable to Mss116.

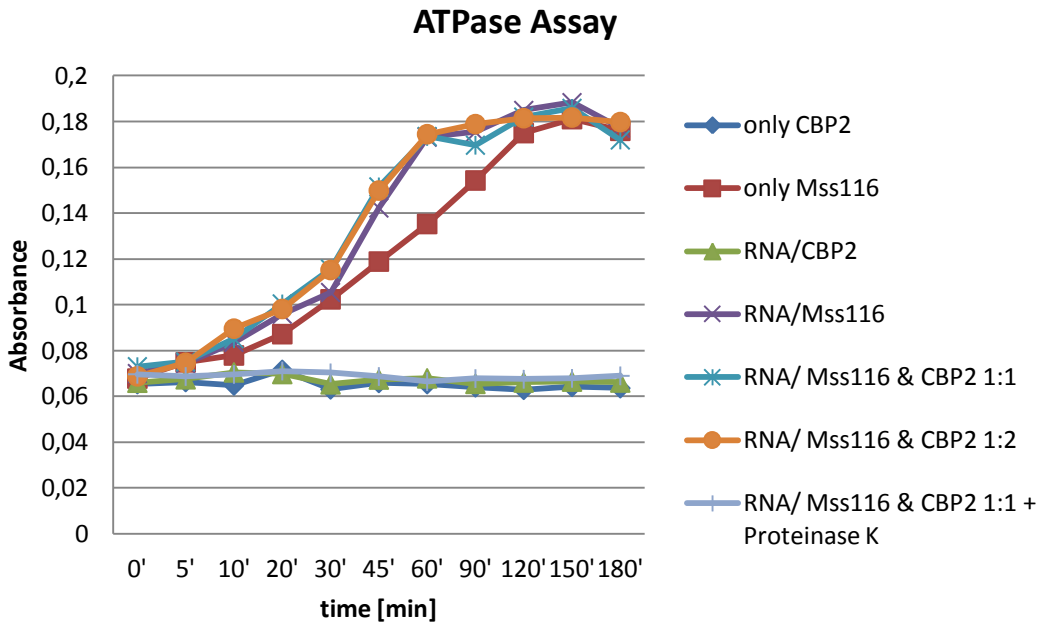

Fig. 24. ATPase activity of Mss116 and CBP2
The ATPase activity of the proteins is measured by the conversion of ATP to inorganic phosphate. On the right, different conditions used for the assay are shown.

4. Splicing activity of bI5 intron in combination with CBP2 and Mss116

CBP2 as well as Mss116 are both needed *in vivo* for efficient splicing of the bI5 group I intron (Halls et al, 2007; Huang et al, 2005). *In vitro* bI5 can splice efficiently under near-physiological conditions (7mM Mg^{2+}) in the presence of CBP2, while Mss116 appears to be dispensable – at least for an intron construct with large deletions in some peripheral extensions and with short exons (Weeks & Cech, 1995a; Zingler et al, 2010). Here we determine the splicing efficiency in the absence and presence of Mss116 and CBP2 proteins and their influence on each other.

4.1. Establishing and optimizing the bI5 splicing assay *in vitro*

To perform the splicing assays we body-labelled the bI5 intron radioactively using α-^{32}P-UTP. Using this method, a radioactively labelled UTP is incorporated during the transcription reaction, producing body-labelled bI5 pre-mRNA. For all conducted splicing assays the bI5core construct received from K. M. Weeks (University of North Carolina, Chapel Hill, USA) was used, if not otherwise indicated.

In the experiments 2µl of the body-labelled RNA stock were initially used. However, the signal we obtained was too strong and needed a lot of adjustment during analysis with Image Quant. Consequently, we decreased the RNA amount steadily, choosing in the end 0.25µl of RNA stock as a suitable amount to conduct the experiments.

Initially, splicing assays were performed with a high amount of CBP2. 1200nM of CBP2 [f.c.] were used to stimulate splicing under near-physiological conditions and an aliquot of the splicing reaction at the following time points taken: 0/ 15/ 30/ 60 minutes. After adjusting the conditions, we chose to perform our experiments using 25nM and 50nM of CBP2 [f.c.]. For the Mss116 protein, 50nM and 100nM [f.c.] of protein were chosen as reaction conditions. The first results showed that the splicing reaction of bI5 is very efficient and in the presence of CBP2 bI5 splices rapidly (data not shown). Consequently, our time intervals had to be reduced, as most of the pre-RNA was already spliced after 10 minutes. We tested various intervals but chose to take samples of each reaction at 0/ 1/ 3/ 5/ 10/ 20/ 30/ 60/ 120 minutes.

Group I intron splicing reaction results in the gain of a linear intron, ligated exons, 5' exon and 3' exon and the first step intermediate in which the intron is still flanked by the 3' exon. To distinguish between the bands observed on the gels we used an RNA ladder. We labelled the ladder according to the manufacturer's protocol with ^{32}P-ATP. In this way we were able to differentiate the products. In addition to the mentioned products, circular intron was observed on the gels. The sizes of the splice product are shown in Table 1. On the gels all relevant splicing products can be observed. The splice products are separated depending on their size. Due to the size of just 45nts, the 3' exon ran out and cannot be observed on the gels and used for analysis of our results.

We also added RNase Inhibitor to the splicing reaction mixture to prevent degradation of the RNA. This was of importance in particular for the reactions with Mss116, as during purification of their protein nuclease contamination cannot be avoided fully. CBP2 (in absence and presence of Mss116) accelerates bI5 folding very efficiently, as can be observed in the samples taken as the 0 time point, at which splice products were already detected. Although just seconds passed between the addition of GTP to start the reaction and taking the first aliquot, we observed some splicing in almost every experiment. To quench the splicing reaction we added first Proteinase K to degrade the proteins and subsequently destroyed the intron stucture with the stop buffer containing denaturing agents and EDTA to chelate Mg^{2+} ions. Proteinase K degrades the proteins quickly and efficiently and thus inhibits their function.

bI5core size	
pre-RNA	562nts
linear intron + 3' exon	389nts
linear intron	344nts
ligated exons	218nts
5' exon	173nts
3' exon	45nts

Table 1.The length of the bI5 intron containing pre-RNA and of the different splicing products.

To be certain that the splicing reaction occurred correctly and is indeed stimulated by the proteins, a positive and a negative control were conducted each time. In the negative control the bI5 intron was folded at near-physiological conditions (7mM Mg^{2+}) in the absence of either protein. As such the bI5 intron is not capable to

form the native state stably (equilibrium shifted towards collapsed state). For the positive control, the bI5 intron was folded at non-physiological conditions (40mM Mg^{2+}), at which the intron folds to the native, splicing-competent structure. These conditions were previously established by Weeks and Cech (Weeks & Cech, 1995a)

Once all conditions were established and the splicing assay optimized, we aimed at understanding the role of Mss116 in bI5 and/or CBP2-assisted bI5 folding.

4.2. CBP2-assisted bI5 splicing

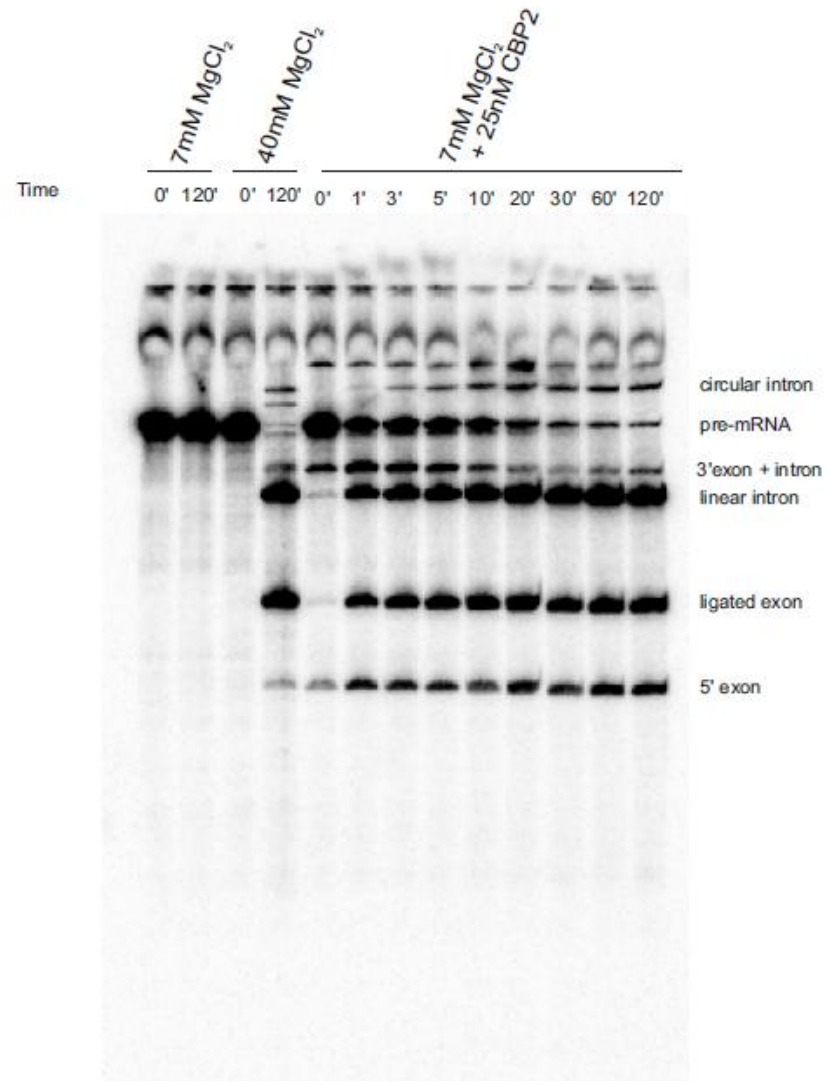

Fig. 25. CBP2-promoted splicing of the bI5 group I intron.
The pre-RNA was folded with 7mM Mg^{2+} in the presence of 25nM CBP2. A negative control (7mM Mg^{2+}) without protein and a positive control (40mM Mg^{2+}) were included.

The addition of 25nM CBP2 [f.c.] already results in efficient splicing of bI5 under near-physiological conditions (7mM Mg^{2+} / 35°C) (Fig. 25, Table 2). Already at time point 0, which is taken immediately after starting the

reaction with 1mM GTP, the first splicing step is carried out. Faint bands further indicate that some pre-mRNA is fully spliced producing linear intron and ligated exons. After 20 minutes, more than half of the pre-mRNA is spliced.

From the beginning, we can see a band appearing above the pre-mRNA. We suppose that this band is a circular form of the intron and it increases with the time course. Thus, the pre-mRNA is spliced to linear introns and subsequently a circular intron is formed. The ratio of the linear intron still attached to the 3' exon decreases about 50% after 120 minutes. Overall, we observe that 80 – 90% of the pre-mRNA is fully spliced after 120 minutes, which agrees well with previously data (Weeks & Cech, 1995a).

As expected, no splicing was observed without CBP2 at near-physiological conditions (7mM Mg^{2+}). The positive control (40mM Mg^{2+}) showed nearly full splicing activity and confirmed previously published data (Weeks & Cech, 1995a), stating that a high amount of divalent ion concentration is necessary and sufficient for self-splicing of the bI5 group I intron. Importantly, the products of self-splicing and of protein-assisted splicing appear to be identical.

The data was analysed with Image Quant and we fitted the results using Kaleidagraph (Table 2). In Fig. 26 the fractions of the precursor (pre-mRNA) and the fractions of the linear intron were fit to single-exponential equation and all other splice products are shown as well. The quantification revealed an average k_{obs} of 0.41 min^{-1} for bI5 splicing when following the precursor decay.

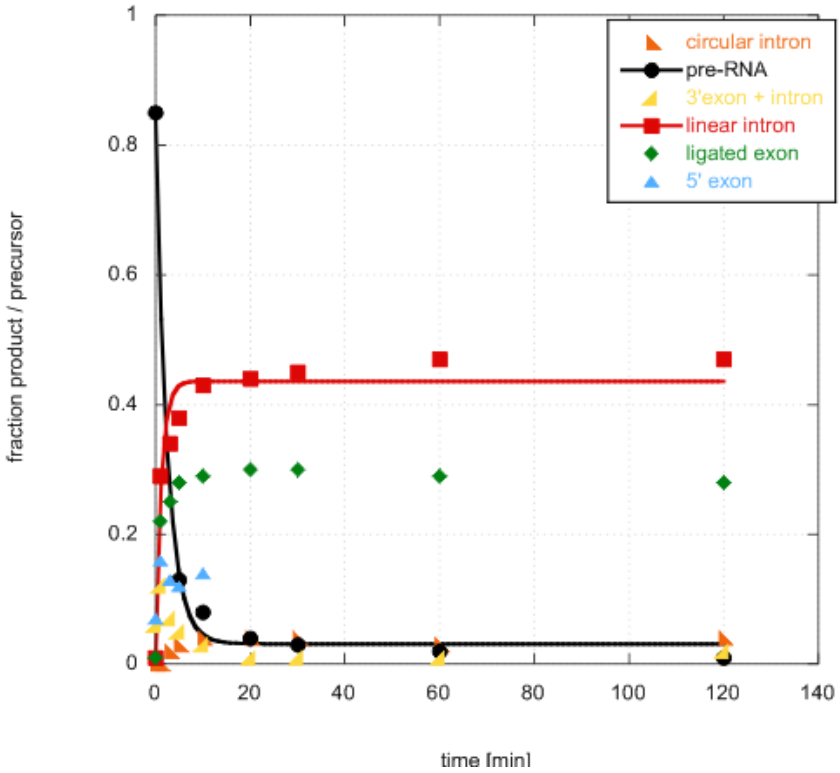

Fig. 26. Splicing of bI5 promoted by CBP2.
The pre-RNA was folded in the presence of 7mM Mg^{2+} and 25nM CBP2. The data from the gel runs was analysed by Image Quant and fitted with Kaleidagraph. Kinetic progress curves were fit to single-exponential equations and are shown for the pre-RNA decay in black and for the linear intron evolution in red.

precursor decay	k_{obs} [min^{-1}]	st.d.	amplitude [%]	st.d.
25 nM Cbp2	0.41		82	
50 nM Cbp2	0.55	0.17	59	28
50 nM Mss116	n.a.		n.a.	
25 nM Cbp2 + 25 nM Mss116	1.49	0.59	78	3
25 nM Cbp2 + 50 nM Mss116	2.33		67	
50 nM Cbp2 + 100 nM Mss116	1.22	0.09	53	11
25 nM Cbp2 / 25 nM Mss116	2.24	0.06	65	3
25 nM Cbp2 / 50 nM Mss116	0.45		23	
50 nM Cbp2 / 50 nM Mss116	1.32	0.03	51	1
50 nM Cbp2 / 100 nM Mss116	1.22	0.36	60	4

Table 2. The effect of proteins on bI5 splicing.
Splicing was tested in the absence and presence of either CBP2 or Mss116 or both proteins. The average was calculated from at least two independent experiments. As the k_{obs} derived from fitting the precursor decay or evolution of linear intron which were within error, the latter values were not included. The outlier is marked in grey. + refers to concomitant addition of Mss116 and CBP2 to the denatured bI5 RNA; / indicates that Mss116 was added to the preformed CBP2-bI5 complex; n.a. stands for not active.

To assess whether 25nM CBP2 is saturating, bI5 folding and splicing was tested at higher CBP2 concentration.

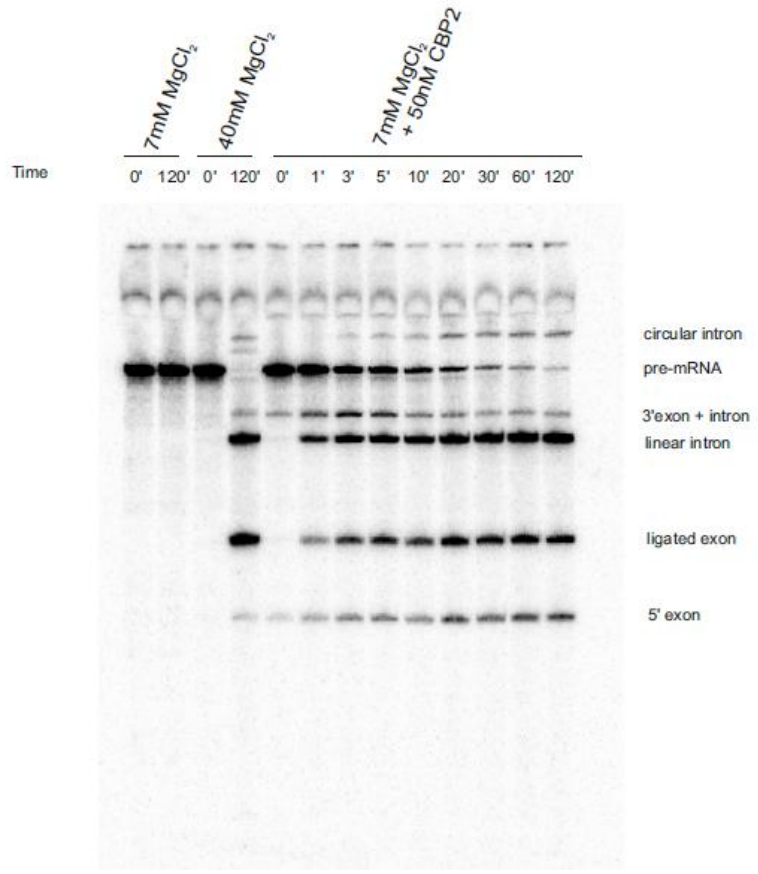

Fig. 27. CBP2-promoted splicing of the bI5 intron.
The pre-RNA was folded with 7mM Mg^{2+} in the presence of 50nM CBP2. A negative control without protein at 7mM Mg^{2+} and a positive control with 40mM Mg^{2+} were included.

When conducting the splicing reactions with 50nM CBP2 (Fig. 27, Table 2), the turnover of pre-mRNA into its products was within error to that measured in the presence of 25nM CBP2. It can be seen that already after 10 minutes, more than half of the pre-mRNA is fully spliced. After 120 minutes almost the entire precursor pool is spliced. The splice products are again comparable to the positive control, which represents by self-splicing at a high magnesium concentration. The negative control shows no splicing activity at all. We obtained a k_{obs} of 0.55 ± 0.17 min^{-1} for the precursor decay (Fig. 28, Table 2).

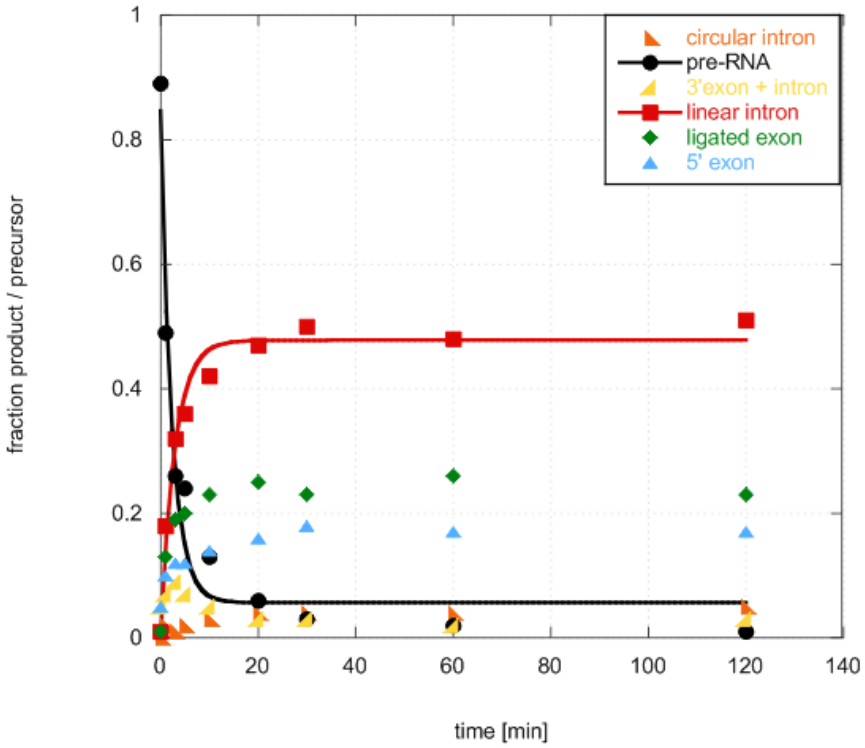

Fig. 28. Splicing of bI5 promoted by 50nM CBP2.
The kinetic progress curve for the pre-RNA is shown with the black graph and the increase of the linear intron is shown in red.

Although a higher CBP2 concentration may have an effect on the circularization of the linear intron, the overall precursor conversion is similar at both CBP2 concentrations. Thus, it can be assumed that these concentrations are saturating.

In brief, as previously reported (Weeks & Cech, 1995a), CBP2 facilitates folding of a shortened bI5 intron flanked by short exons efficiently. Thus, the quality of my CBP2 preparation is excellent.

4.3. The DEAD-box helicase is not sufficient to induce the native, splicing-competent state of bI5

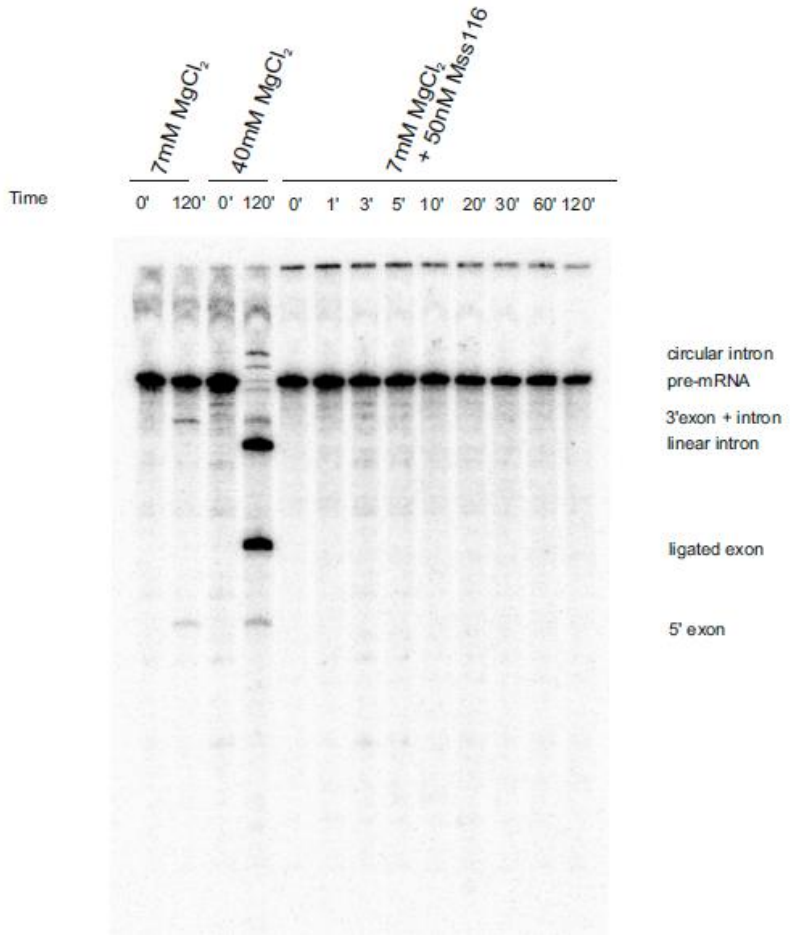

Fig. 29. Mss116-assisted splicing of the bI5 group I intron.
The pre-RNA was folded with 7mM Mg^{2+} in the presence of 50nM Mss116. A negative control without protein and a positive control with high amount of Mg^{2+} are included.

To determine whether Mss116 has a redundant function with CBP2, we tried to stimulate bI5 splicing *in vitro* at near-physiological conditions and in the presence of Mss116. The RNA helicase Mss116 is needed for efficient splicing of group I and group II introns *in vivo* and can promote splicing of ai5γ under near physiological conditions *in vitro*. Our results show no splicing activity of the bI5 intron in the presence of 50nM Mss116 (Fig. 29, Table 2). To be certain that mistakes are avoided during the experiment, a negative and positive control were performed as well. In the positive lane, efficient bI5 splicing induced by high amount of magnesium is achieved, while 7mM Mg^{2+} is insufficient for native state formation. The kinetic results are also confirmed through the data of the Kaleidagraph analysis (Fig. 30, Table 2).

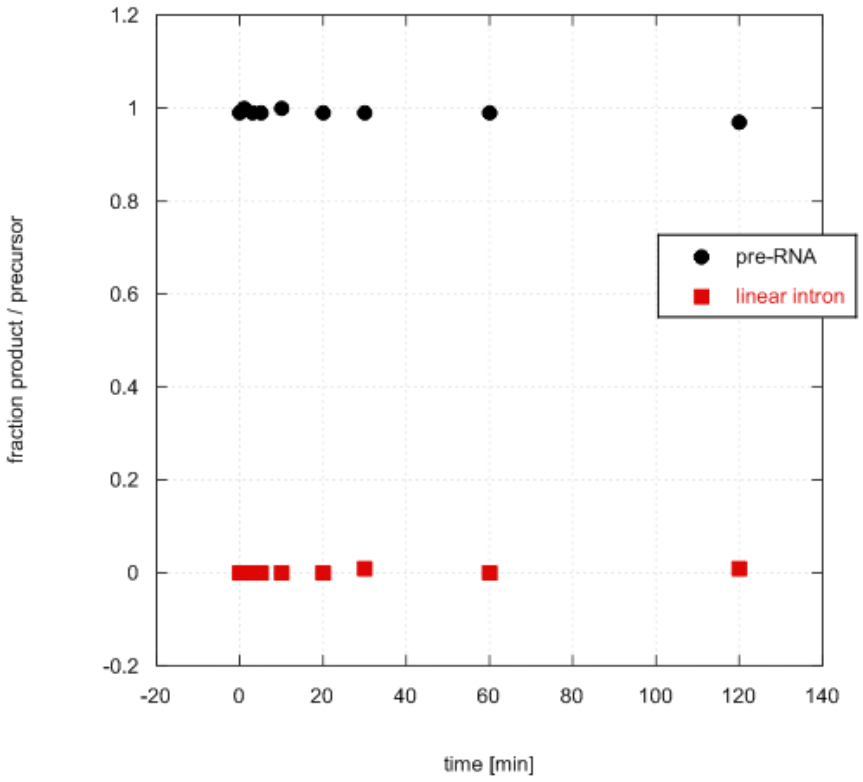

Fig. 30. Splicing of bI5 promoted by Mss116.
Red data points indicate the evolution of the linear intron and black data points are indicate the pre-RNA decay.

The results demonstrated that Mss116 itself cannot induce folding an in turn splicing of the group I intron bI5 under near-physiological conditions. This is in strong contrast to the observations made for the group II intron ai5γ, whose splicing is efficiently stimulated by Mss116 alone at near-physiological conditions (Halls et al, 2007; Huang et al, 2005; Solem et al, 2006).

4.4. Do CBP2 and Mss116 co-opt to promote efficient splicing of the bI5 pre-mRNA?

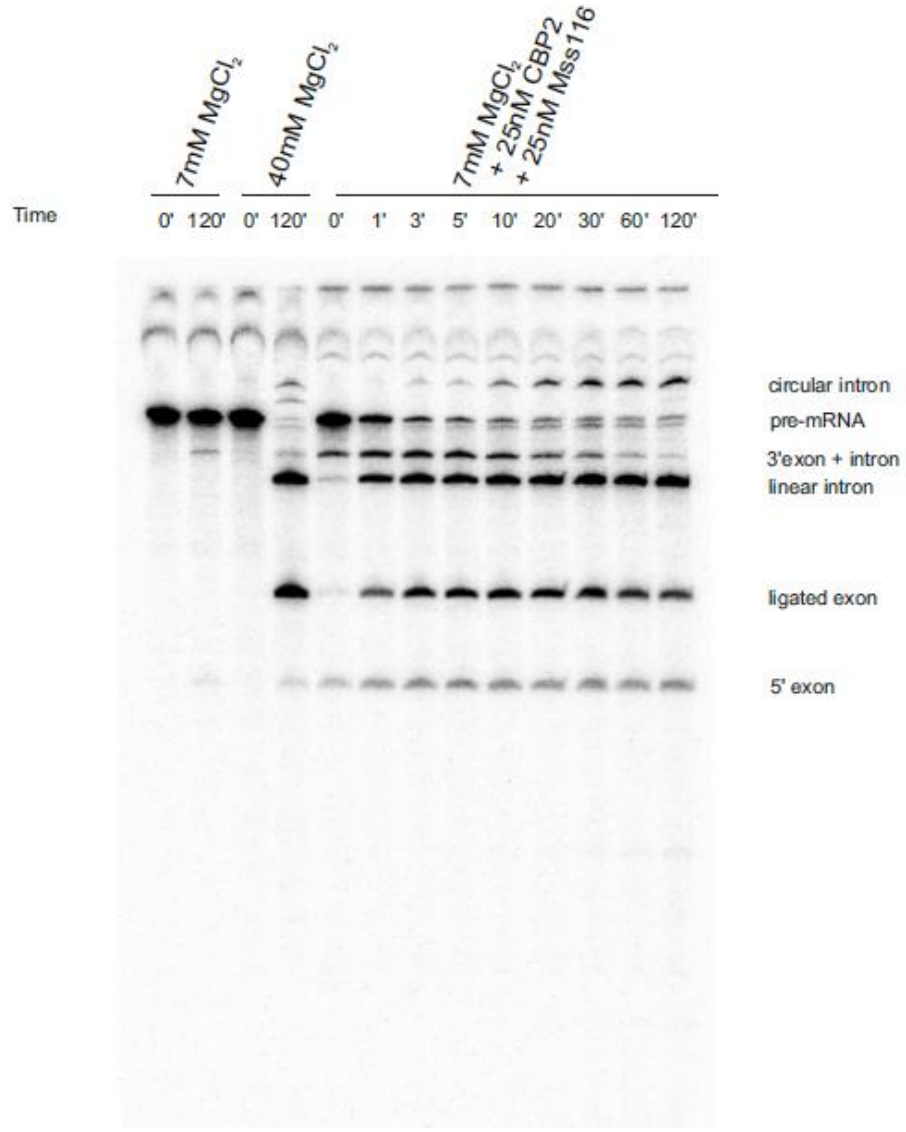

Fig. 31. Splicing promoted by addition of CBP2 and Mss116.
The pre-RNA was folded at 7mM Mg2+ with both proteins added. A negative control and positive control were included.

To gain more insights on the influence of CBP2 and Mss116 on each other and in turn on the bI5 intron, we performed the splicing assay by adding both proteins. CBP2 is known to stabilize the bI5 structure and is needed during the last step along the bI5 folding pathway. Mss116 *in vitro* did not stimulate splicing of bI5 (Figs. 29 and 30, Table 2)

The combination of both proteins at a concentration of 25nM [f.c.] seems to slightly speed up bI5 splicing compared to CBP2 alone (Fig. 31, Table 2). After ~3 minutes more than half of the pre-mRNA is spliced into its products. In addition, a second band is seen slightly beneath the pre-mRNA band. The band may be a by-

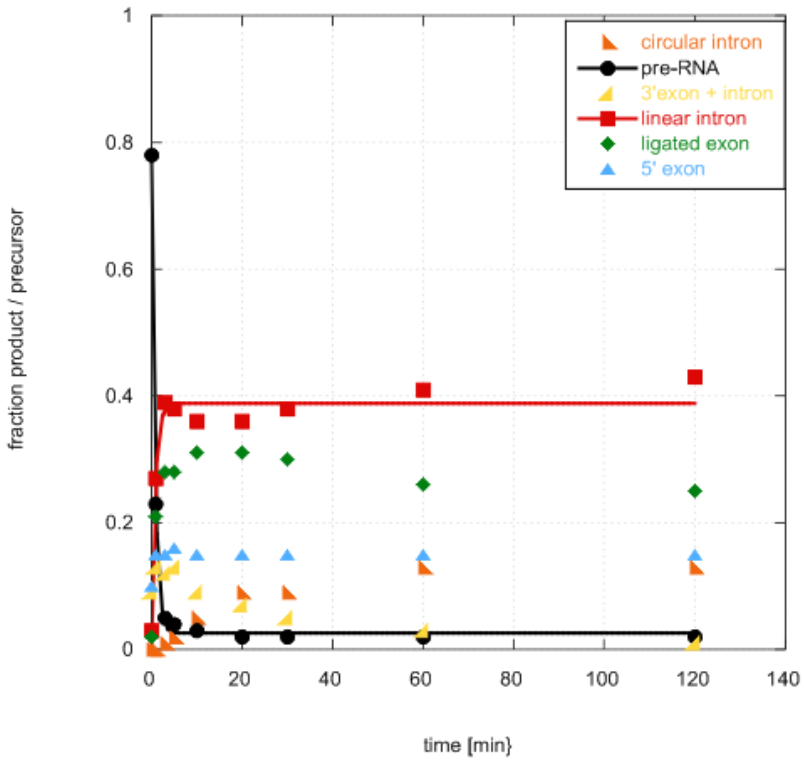

Fig. 32. Splicing of bI5 promoted by CBP2 and Mss116.
In the graphic, the decrease of the pre-RNA is shown in black and the linear intron evolution in red.

product during the splicing reaction as it increases with time. After 120 minutes, nearly all pre-mRNA is spliced, showing similar results to the positive control. We obtained a k_{obs} of 1.49 ± 0.59 min^{-1} for the precursor. These results indicate that Mss116 increases the observed rate constant 3.6-fold compared to CBP2 alone, as the k_{obs} increases from 0.41 min^{-1} to 1.49 min^{-1} (Fig. 32, Table 2). This finding suggests that Mss116 accelerates folding steps prior to CBP2 binding.

At next, we tested whether the effect of Mss116 on CBP2-assisted splicing further increases if a molar excess of the DEAD-box protein is used.

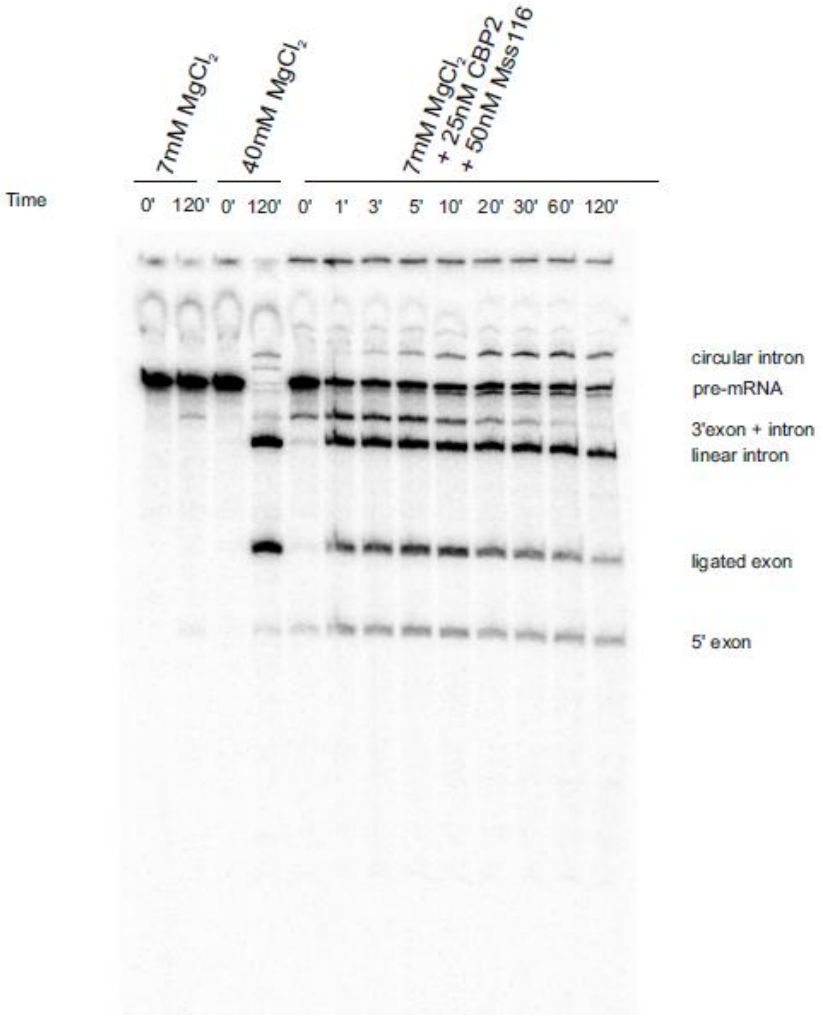

Fig. 33. Splicing promoted by CBP2 and Mss116 with a 1:2 ratio.
The pre-RNA was folded at 7mM Mg^{2+} in the presence of both proteins added in a 1:2 ratio concomitant. A negative control without protein and a positive control with high amount of Mg^{2+} were included.

Indeed, increasing the amount of Mss116 protein led to a further enhancement of the k_{obs}, i.e. it is 5.7-fold increased (0.41 min^{-1} vs. 2.33 min^{-1}) (Fig. 33, Table 2).

Again half of the bI5 population is spliced after 3 minutes. 80 – 90% of the pre-mRNA is efficiently spliced after 120 minutes. The k_{obs} of the precursor is 2.33 min^{-1} and for the linear intron a k_{obs} of 2.6 min^{-1} (Fig. 34). The calculated kinetic results are also comparable to the splicing assays with an equimolar amount of protein when looking at the precursor decay. However, at equimolar amounts of CBP2 and Mss116 the k_{obs} derived from linear intron evolution is 1.5-fold enhanced compared to CBP2-assisted bI5 splicing and increasing the Mss116 concentration lead to a 3.1-fold increase of that k_{obs}.

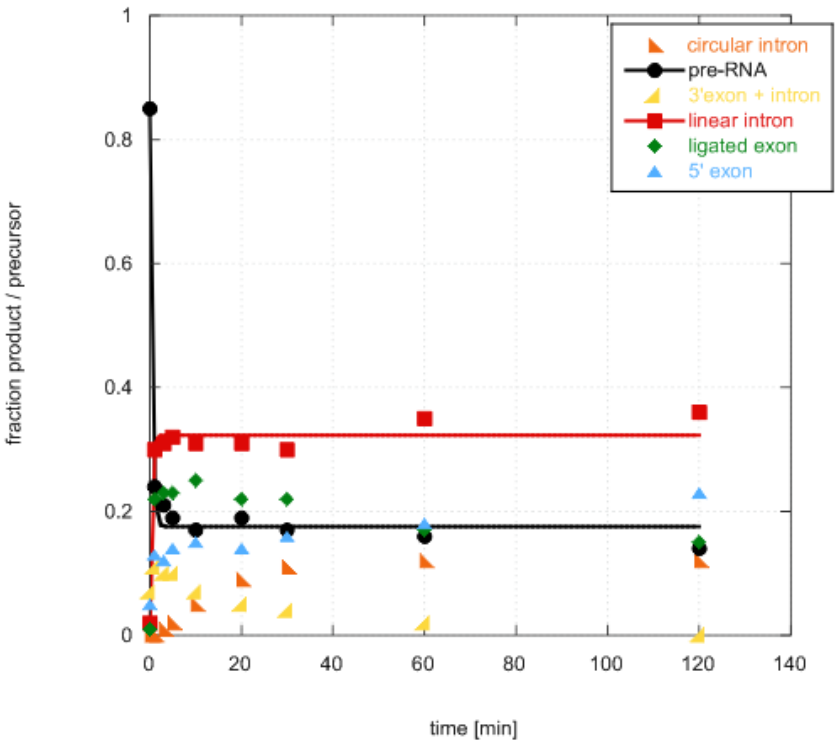

Fig. 34. Splicing of bI5 promoted by CBP2 and Mss116.
The kinetic progress curve of the pre-RNA decay are shown in black, while the evolution of the linear intron is shown in red.

Upon doubling the concentration of CBP2 and Mss116 in 1:2 molar ratios a similar result was obtained (Figs. 35 and 36, Table 2). The average k_{obs} of the precursor here is 1.22 ± 0.09 min^{-1}. Thus when compared to the k_{obs} obtained for bI5 splicing in presence of 50nM CBP2 alone (0.55 ± 0.17 min^{-1}, Table 2), Mss116 enhances bI5 splicing but only by 2-fold. Possibly the higher Mss116 concentration has an aberrant effect on bI5 folding by dissociating CBP2 from bI5 due to its helicase activity, among other potential explanations for this finding. Although the results indicate that Mss116 enhances the population of splicing-competent bI5 molecules, further experiments have to be performed to determine the underlying reason. Possible explanations could be that Mss116 accelerates the bI5 collapse and in turn facilitates the tertiary capture mechanism of CBP2, among other scenarios.

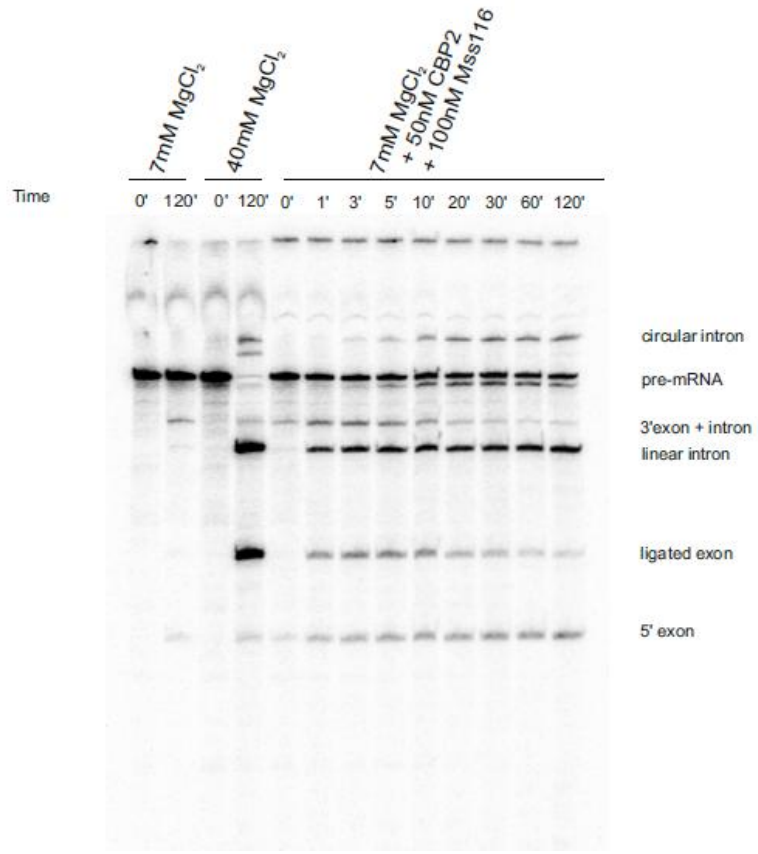

Fig. 35. Splicing promoted by 50nM CBP2 and 100nM Mss116.
The pre-RNA was folded with 7mM Mg2+ in the presence of both proteins. A negative control and a positive control were included.

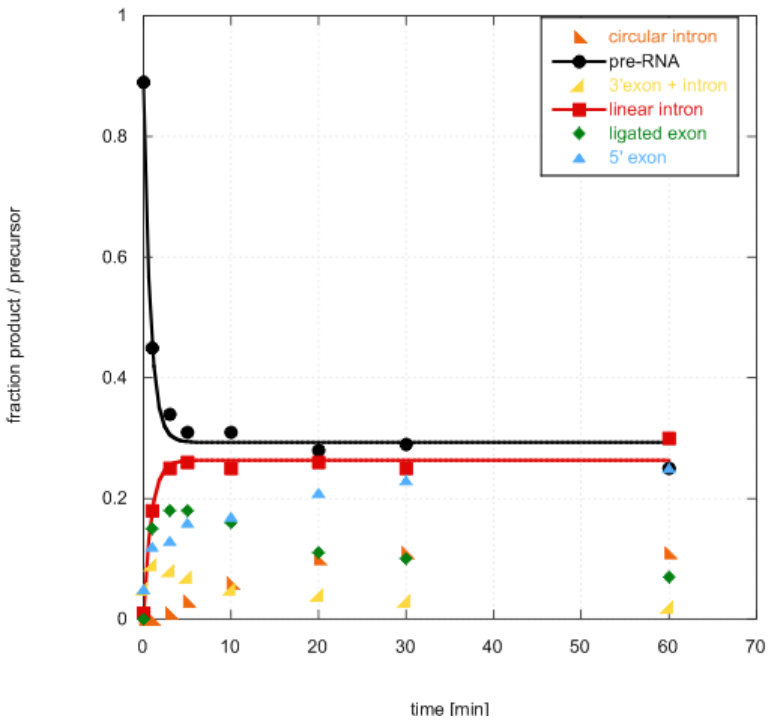

Fig. 36. Splicing of bI5 promoted by 50nM CBP2 and 100nM Mss116.
The pre-RNA was folded at 7mM Mg^{2+} with both proteins in a 1:2 ratio. The pre-RNA decay is indicated in black, the linear intron evolution in red.

4.5. Adding Mss116 to the native, splicing-competent CBP2-bI5 complex

So far, bI5 folding and splicing was studied by adding both proteins at the same time to the denatured bI5 intron. To see if Mss116 interferes with CBP2 binding, we decided to add the proteins at different step during bI5 folding. We therefore first added CBP2 to the reaction mix and incubated it for 30 minutes at 35°C. This is sufficient time for the RNA to fold into its active fold. After the incubation we also added Mss116 to investigate if it has any effect on the native folded bI5. These experiments were performed at various protein concentrations.

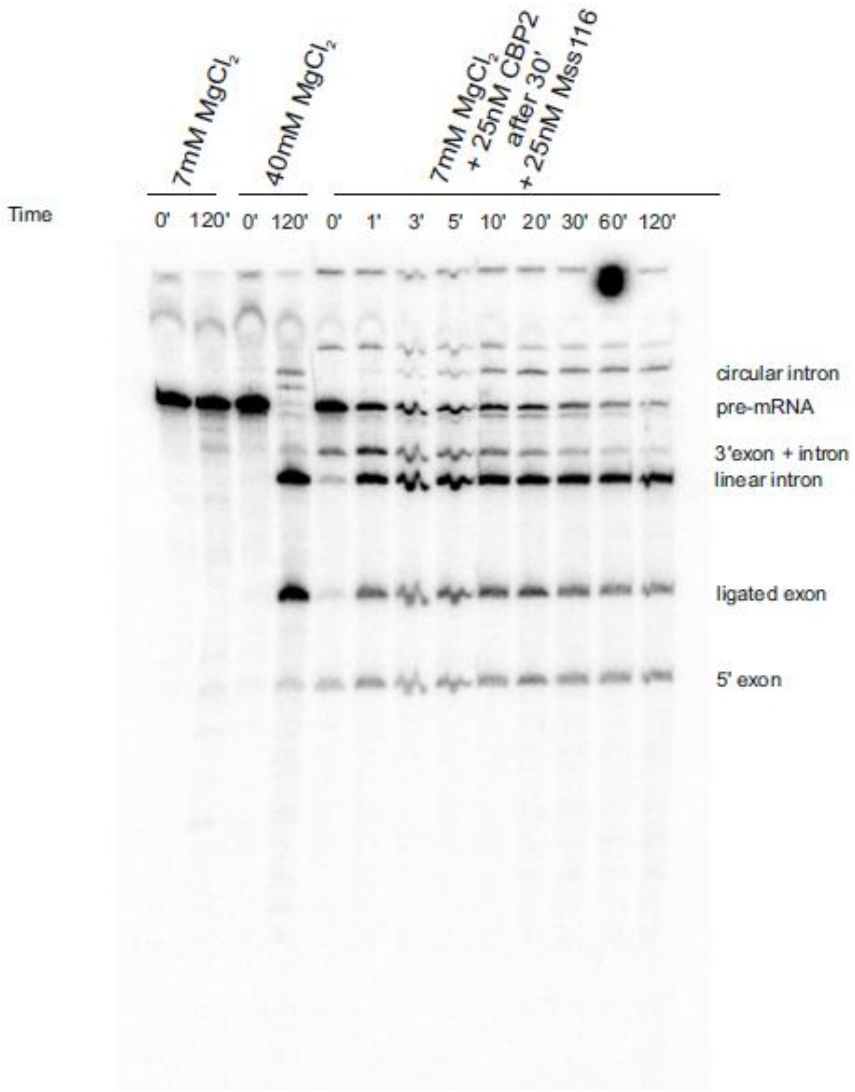

Fig. 37. The effect of Mss116 on splicing of a preformed CBP2-bI5 complex.
The pre-RNA was folded with 7mM Mg^{2+} in the presence of 25nM CBP2 with addition of 25nM Mss116 after 30 minutes. A negative control (7mM Mg^{2+}) without proteins and a positive control (40mM Mg^{2+}) were included.

To see if Mss116 affects CBP2-facilitated splicing of the intron, we folded the bI5 intron to the native state with the help of CBP2 and subsequently Mss116 was added (Fig. 37, Table 2).

To affirm the possibility that splicing is facilitated by the proteins and the correct splice products are obtained, we performed a negative and a positive control respectively.

We obtained a k_{obs} of 2.24 ± 0.06 min^{-1} for the precursor decay (Fig. 38, Table 2). Both proteins were added at equimolar ratio.

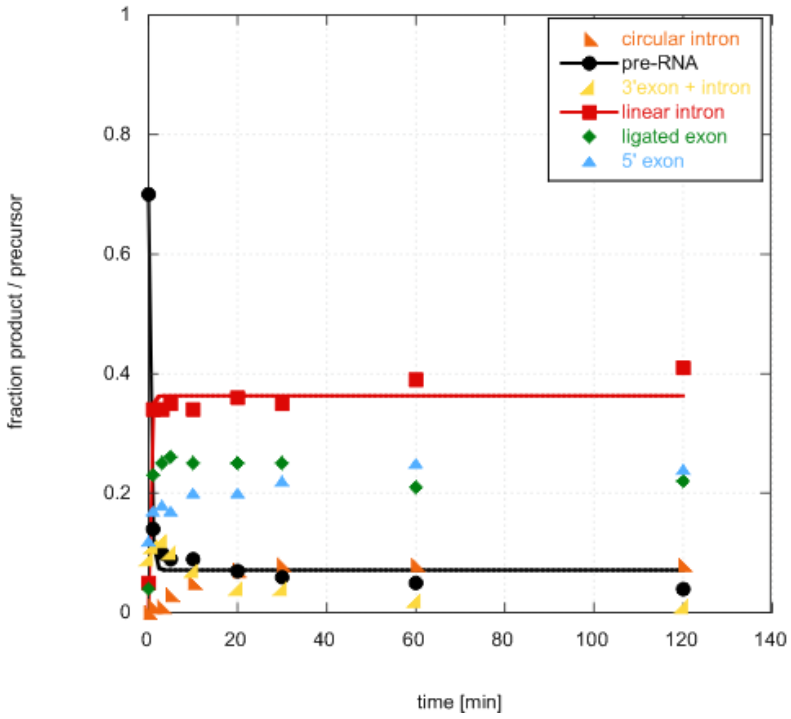

Fig. 38. Splicing of preformed CBP2-bI5 complex with Mss116 addition.
The kinetic data gained after fitting with Kaleidagraph show the linear intron evolution in red and the pre-RNA decay in black.

Importantly, applying the same reaction set up but with 2-fold increased protein concentration did not alter the outcome. A k_{obs} of 1.32 ± 0,03 min^{-1} was observed following the pre-RNA decay (Fig. 39 and 40, Table 2). However, the increased protein concentration enhanced bI5 splicing as well, but only by 2.4 compared to 5.5-fold at 25nM of both Mss116 and CBP2 (Figs. 31 and 32, Table 2 and 3).

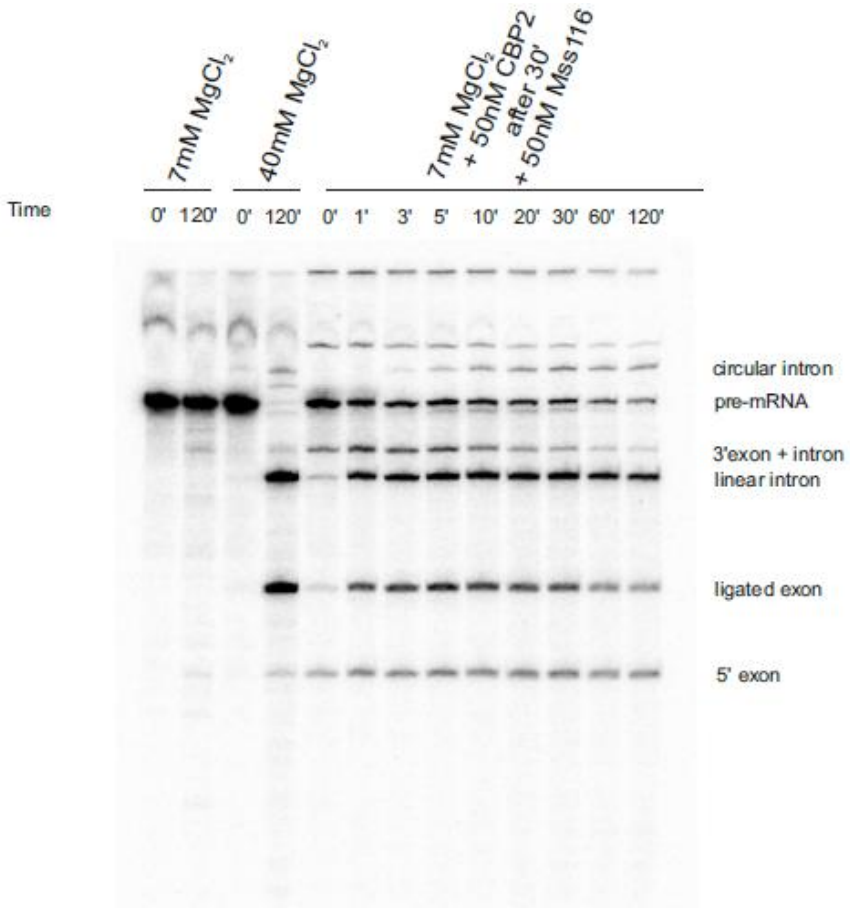

Fig. 39. Splicing of preformed CBP2-bI5 complex at addition of 50nM Mss116.
The pre-RNA was folded at 7mM Mg^{2+} and with 50nM CBP2. 50nM Mss116 was added after 30 minutes to the preformed complex. A negative control and a positive control are included.

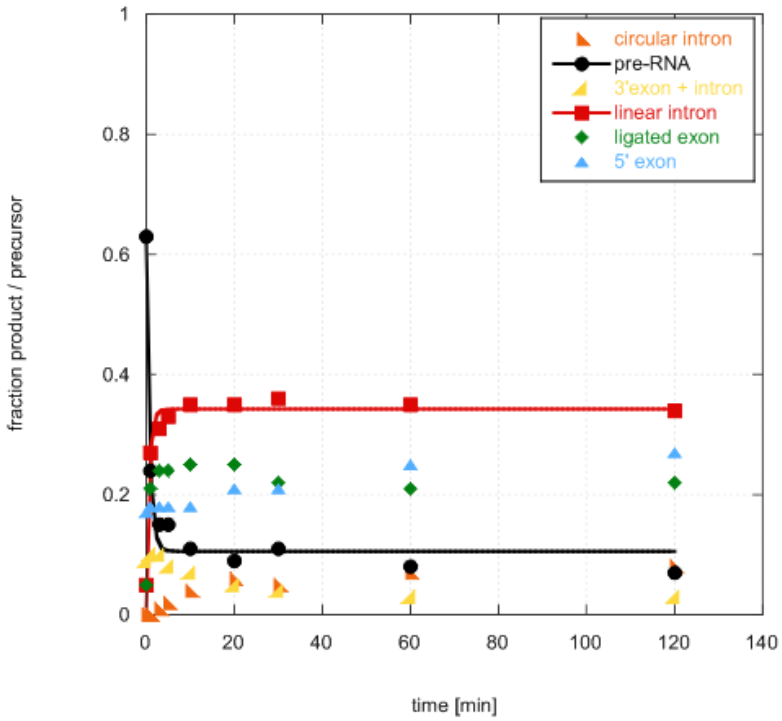

Fig. 40. The addition of Ms116 to a preformed CBP2-bI5 complex.
The kinetic progress curve for the pre-RNA decay is shown in black, the linear intron evolution in red.

At next, it was tested whether Mss116 influences CBP2-assisted bI5 splicing, if Mss116 is used at a 2-fold molar excess over CBP2, i.e. 25nM CBP2 and 50nM Mss116 (Fig. 41, Table 2).

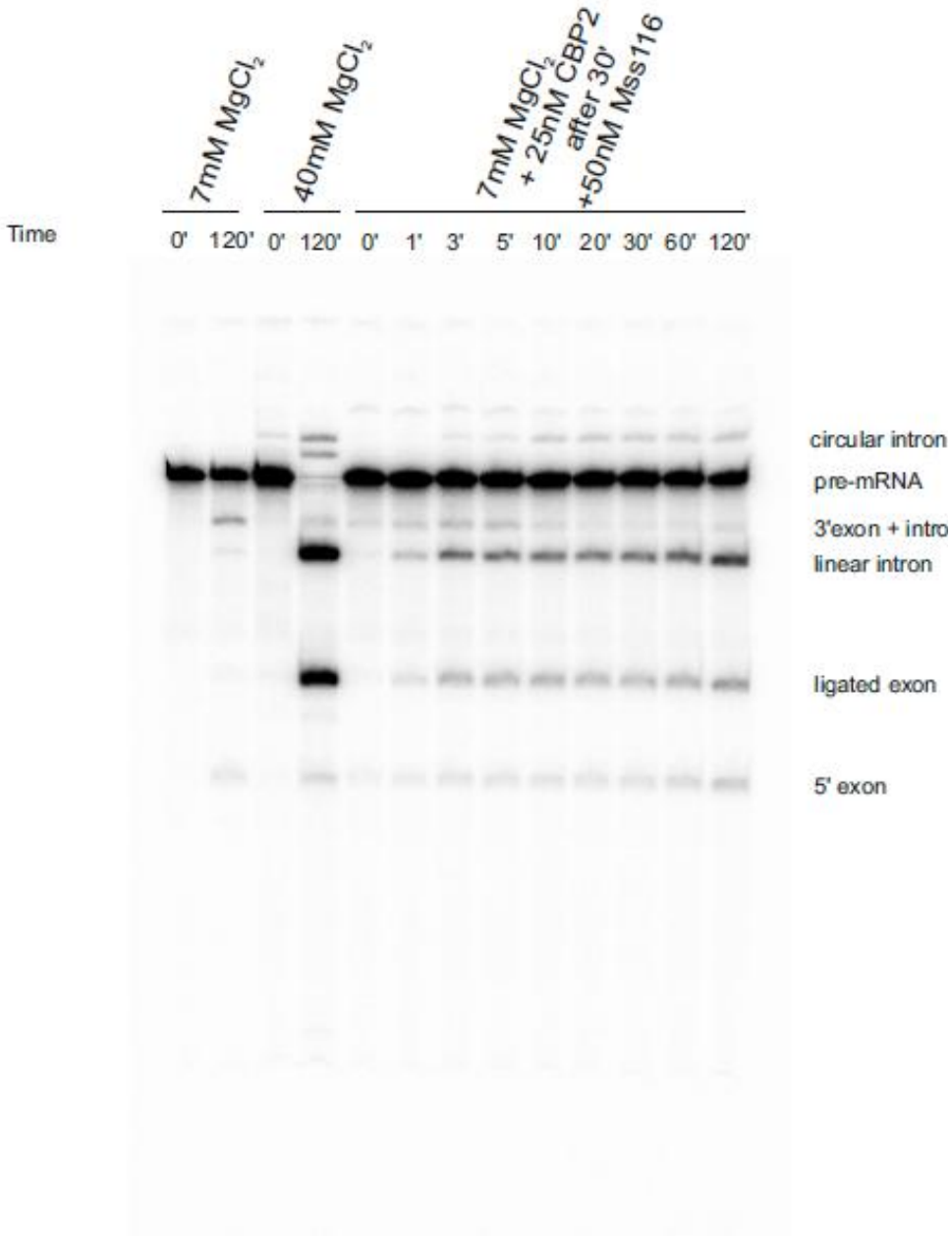

Fig. 41. The effect of Mss116 on a preformed CBP2-bI5 complex by using a 1:2 protein ratio.
The pre-RNA was folded at 7mM Mg^{2+} with 25nM CBP2. After 30 minutes 50nM Mss116 was added.
A negative control (7mM Mg^{2+}) without proteins and a positive control (40mM Mg^{2+}) are included.

The k_{obs} derived from the precursor decay is 0.45 min^{-1} (Fig. 42, Table 2). These numbers indicate that the k_{obs} is reduced compared to bI5 splicing in the presence of CBP2 only. However, the strongest effect is seen at the severely reduced amplitude, as only ~ 20% of the pre-RNA were spliced and only ~10% of linear intron were observed. One possibility could be that Mss116 dissociates the CBP2-RNA complex and binds to the RNA. Due

to the formation of Mss116-RNA complex, the intron cannot splice. In light of the so far observed stimulatory effect of Mss116 on the rate constant for bI5 splicing, this result was truly surprising.

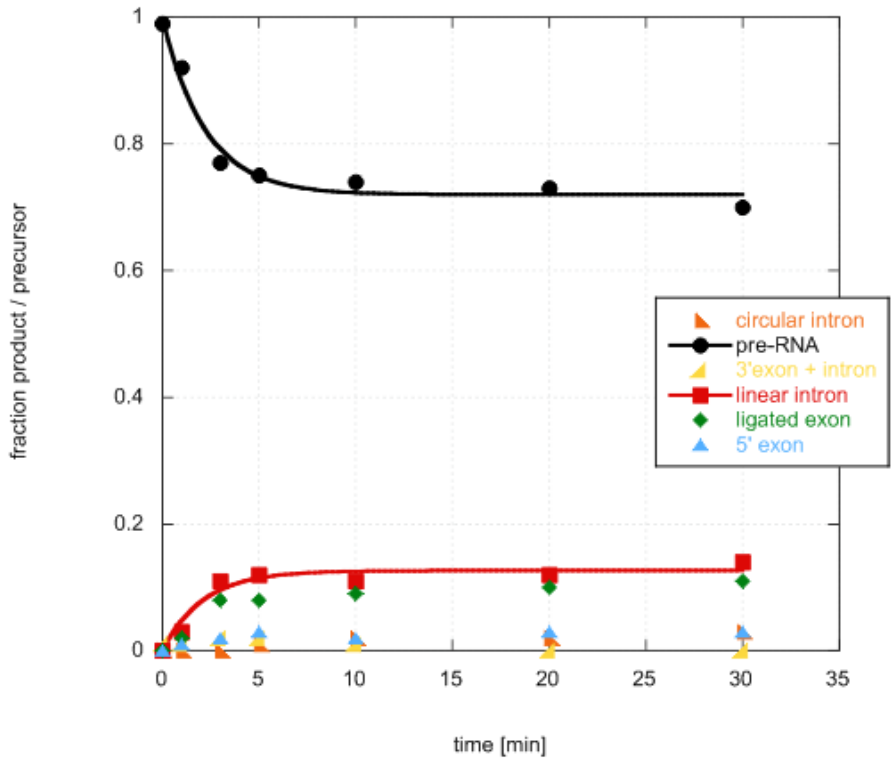

Fig. 42. Splicing of a preformed CBP2-bI5 complex after addition of Mss116.
The gained kinetic data was fit to single exponential equations with Kaleidagraph. The pre-RNA decay is indicated in black, the linear intron evolution in red.

A such, we increased the amount of both proteins two-fold (i.e. 50nM/100nM) and using a 1:2 ratio of CBP2 to Mss116 we again detected a 2-fold increase in the observed rate constants (Fig. 43, Table 2). We obtained a k_{obs} of 1.22 ± 0.36 min^{-1} from the precursor decay (Fig. 44, Table 2). Most strikingly, these data are in strong contrast with those seen at the two-fold reduced concentration of both proteins (Fig. 41 and 42, Table 2), suggesting that an error must have occurred when testing the effect of Mss116 (50nM) on the pre-formed CBP2-bI5 complex (using 25nM CBP2).

Importantly, our data show that adding 100nM Mss116 either together with CBP2 to the unfolded bI5 intron or to the pre-formed CBP2-bI5 complex enhances bI5 splicing to the same degree, namely 2-fold. This effect is significantly smaller than at lower protein concentration.

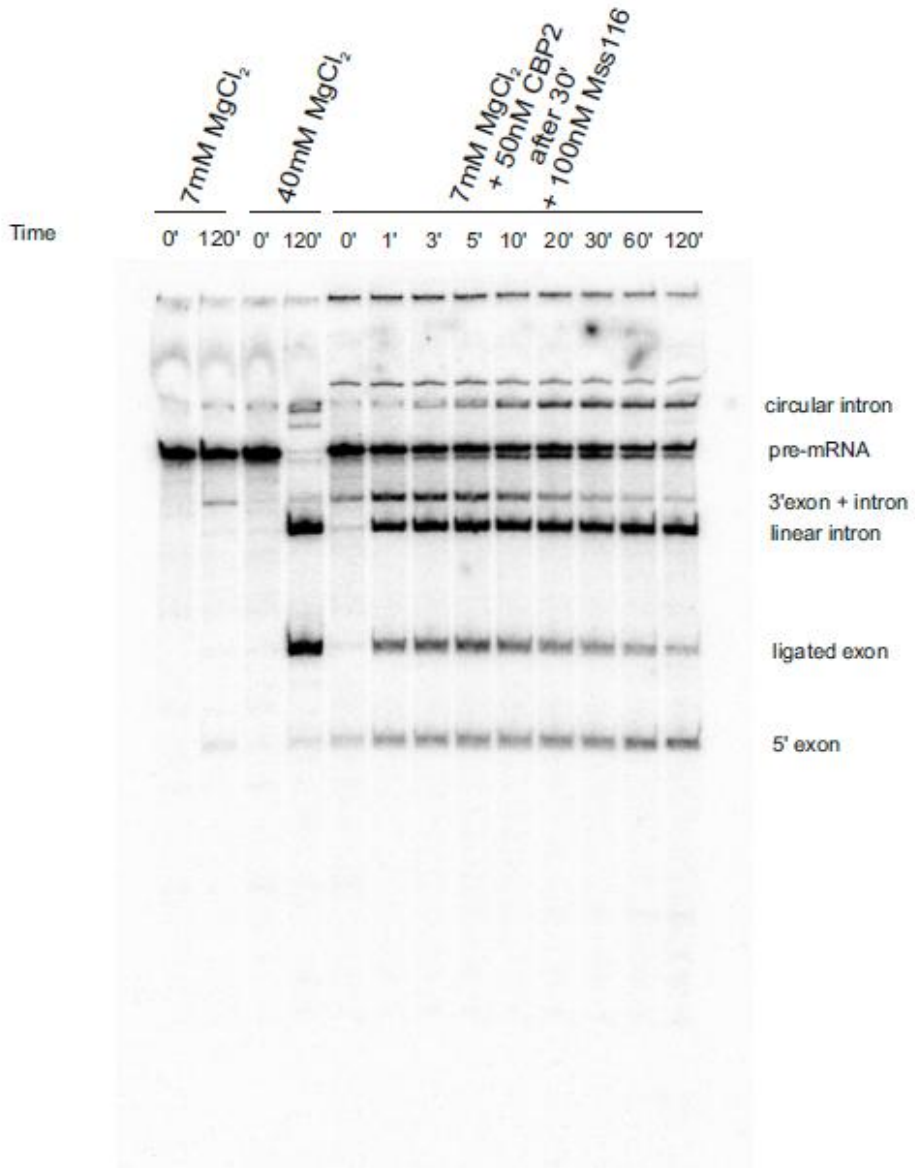

Fig. 43. Splicing of preformed CBP2-bI5 complex with addition of 100nM Mss116.
The pre-RNA was folded at 7mM Mg^{2+} and 50nM CBP2 with further addition of 100nM Mss116 after 30 minutes. A negative control without proteins and a positive control at a high Mg^{2+} concentration are included.

Taken together, out data indicate that independent of the time point at which Mss116 is added to the CBP2-promoted bI5 folding reaction, Mss116 does stimulate the intron's observed rate constant 2-5.7 -fold (Table 3). However, additional data are required to strengthen this hypothesis.

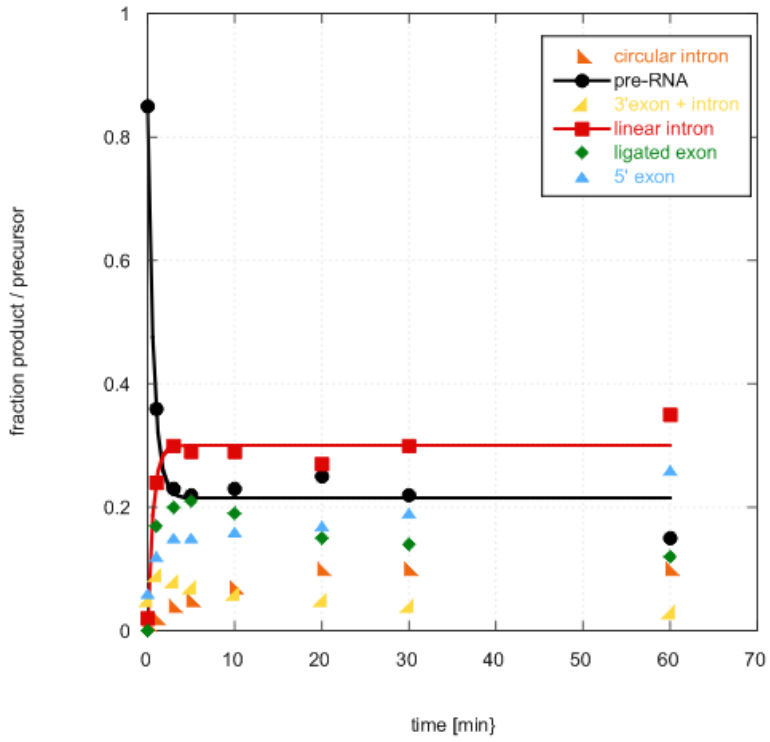

Fig. 44. The effect of Mss116 on a preformed CBP2-bI5 complex.
The kinetic curve progress for the pre-RNA decay is shown in black and for the linear intron evolution in red.

4.6. Is Mss116 necessary to promote splicing of the full-length bI5 intron?

Since CBP2 is only capable of assisting folding and in turn splicing of a "minimal" bI5 pre-RNA and as Mss116 does only 2-fold enhance this folding process, it remains possible that the DEAD-box protein (together with CBP2) is only essential to facilitate proper folding of the full-length bI5. To test this hypothesis we had prepared different bI5 pre-RNAs and aimed at the studying their splicing efficiency in the presence of both proteins. To start with we created a construct that contains the full length bI5 intron without any deletions and flanked by 25nts exons (see Appendix for sequence). We performed the splicing assay under the same conditions as with the bI5core construct, which has large deletions in L1, L6 and L8 but is flanked by 25nts exons as well.

First, we confirmed that CBP2 cannot promote splicing of a pre-RNA containing the full-length bI5 intron. Increasing the CBP2 concentration to 100nM [f.c.], did not facilitate bI5 splicing. We further tested the combination of both CBP2 and Mss116 to facilitate splicing of the bI5 intron. However, also under these conditions no splicing was observed (Fig. 45).

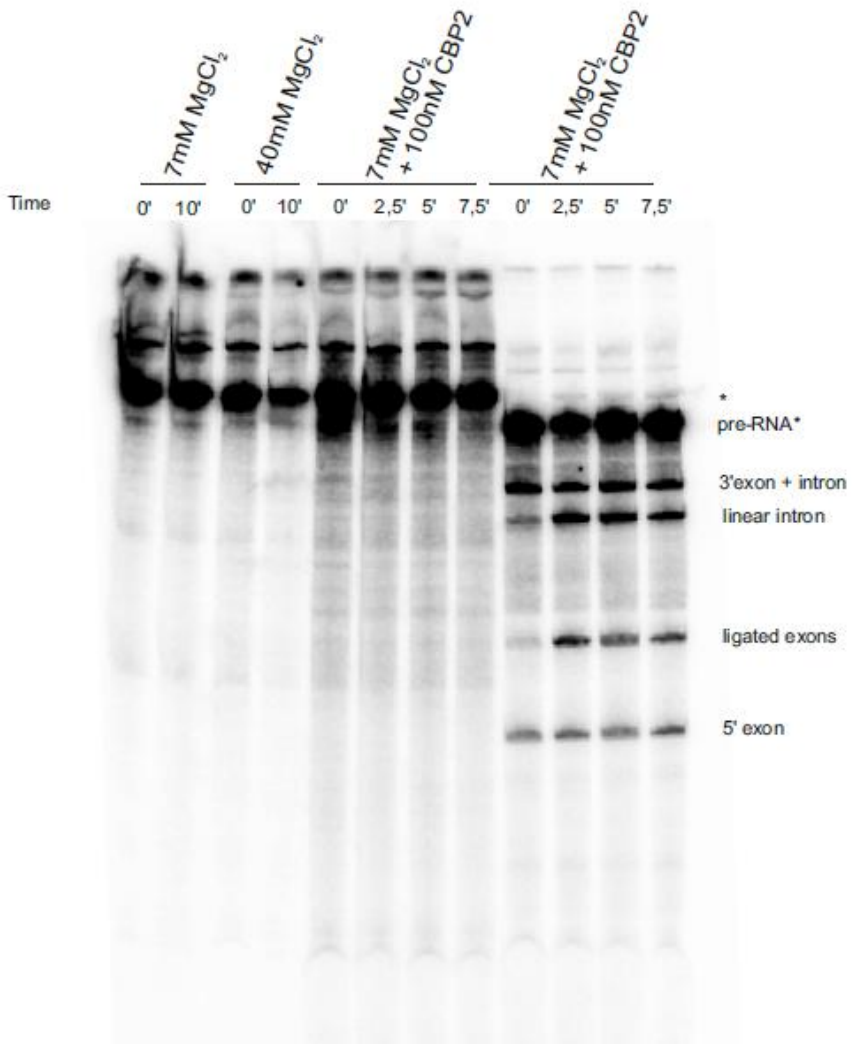

Fig. 45. Monitoring Mss116 and CBP2 facilitated folding of the full-length bI5 intron flanked with short exons and bI5core.
Pre-RNA* is the one harbouring the full-length bI5 intron flanked by 25nts long exons. The asterisk indicates a band of unknown origin. Pre-RNA, contains the bI5core only and was used as a positive control in this experiment.

As expected neither 40mM nor 100mM Mg^{2+} was sufficient to induce self-splicing. Similarly, we tested whether elevated temperature and an increased concentration of monovalent ions during bI5 folding allow self-splicing (Fig. 46). This was however not the case.

Due to time constraints we were unable to continue modifying the reaction conditions and analyzing if Mss116 and CBP2 together might stimulate folding of the natural bI5 intron under any condition.

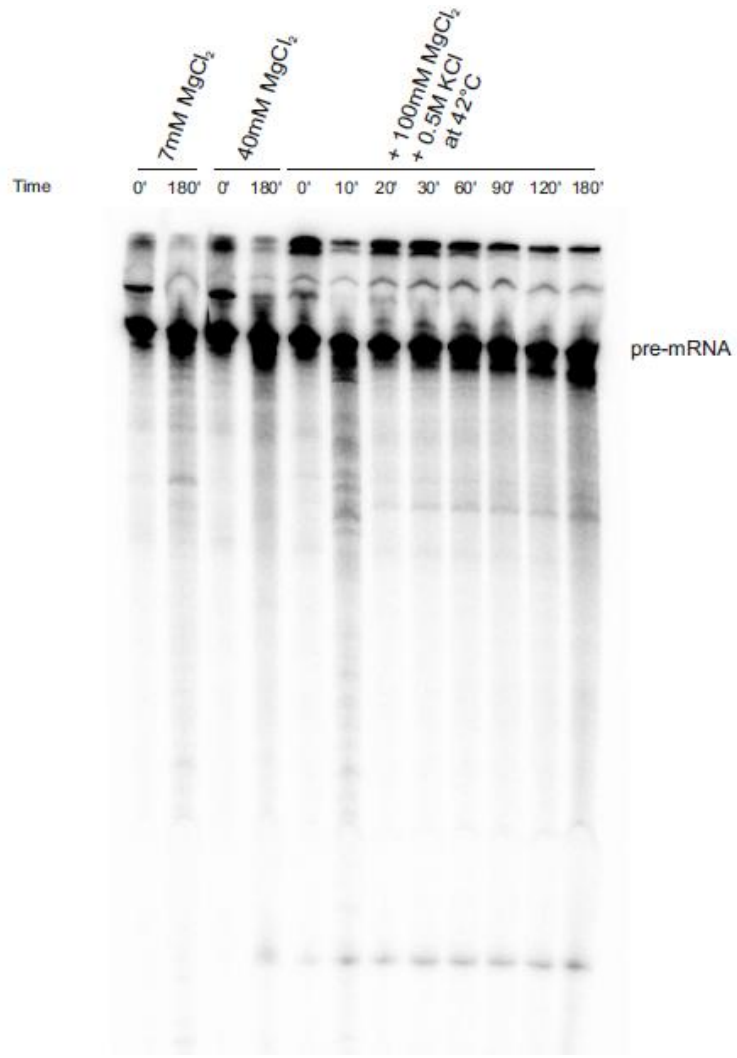

Fig. 46. Assessing the self-splicing ability of the full-length bI5 intron flanked with short exons folded at high salt conditions.
The pre-RNA was folded in the presence of 0.5M KCl and 100mM Mg^{2+}, as lower salt conditions did not allow self-splicing.

4.7. Evaluation of Mg^{2+} concentration that is sufficient to start splicing reaction

While conducting the above described experiments, we observed some splicing products in the negative control, namely those of the first step of group I splicing (5' exon and intron-3' exon intermediate), although bI5 was folded with 7mM Mg^{2+} only. This concentration was chosen in accordance with previously published results of Weeks et al. They stated that at 7mM Mg^{2+}, bI5 can only form its native state with the help of CBP2, while without stabilizing co-factor, bI5 can collapse to a compact intermediate, but not maintain the native state (Weeks & Cech, 1995a; Webb et al, 2001). Nevertheless, after two hours of incubation, out data show that already at 7mM Mg^{2+} the first splicing step of the splicing reaction can be carried out. At the first splicing step, the exogenous GTP binds to the G-binding site of the intron and attacks the phosphorus atom at the 5' splice site. This step leads to the release of the 5' exon covalently linked to the guanosine, while the intron is still flanked by the 3' exon (Cech, 1990). In the majority of our experiments, we can see both products of the

first splicing step. To determine whether one of the reagents used in the splicing reaction is contaminated with a significant amount of CBP2 or Mg^{2+}, the bI5 intron was folded at varying Mg^{2+} concentrations and in the absence of proteins (Fig. 47). As splice products of the first step were only observed at 6 and 7mM Mg^{2+} but not at lower Mg^{2+} concentrations, such contaminations can be ruled out. This reassured that the before described data are specific for the protein studied.

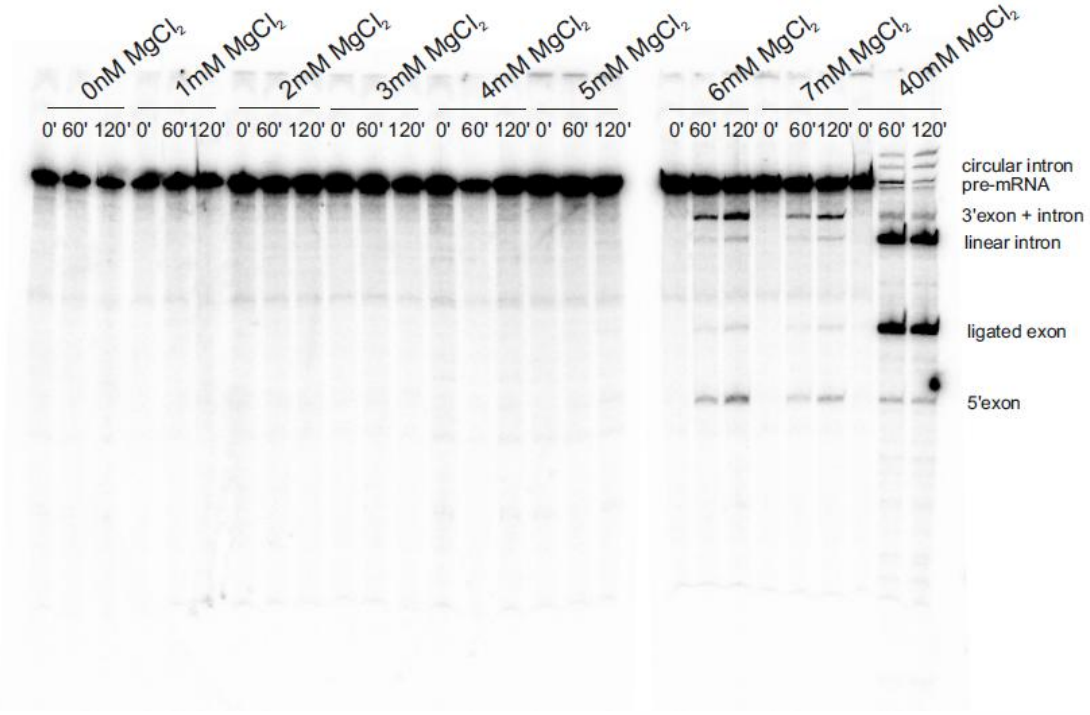

Fig. 47. Splicing assay with different amount of Mg^{2+}
Because most of the time the first splicing reaction step was observed in the negative control lane after 120 minutes, an Mg^{2+} gradient was conducted.

Consequently, it appears that at magnesium concentrations of 6 and 7mM a small fraction of bI5 introns can reach the native state and in turn proceed into the first step of splicing. These concentrations are however too low to allow the second step of splicing to occur.

Discussion

Group I introns have a self-splicing ability *in vitro* under high magnesium conditions, but often need a protein co-factor under near-physiological conditions to reach their stable fold and to splice (Gampel & Tzagoloff, 1987; Shaw & Lewin, 1995). For example, CBP2 is a stabilizing co-factor exclusively needed by the bI5 group I intron. However, *in vivo* bI5 depends on a second protein, Mss116, for efficient splicing (Halls et al, 2007; Huang et al, 2005). Mss116 is a *S. cerevisiae* DEAD-box protein extensively studied in connection with group II introns (Fedorova et al, 2010; Liebeg et al, 2010; Zingler et al, 2010). The aim of the project was to provide the first insights into the role of Mss116 in CBP2-assisted folding of the bI5 group I intron *in vitro*. As such, recombinant Mss116 and CBP2 proteins were produced first. This allowed us to study the efficiency of bI5 splicing in the absence and presence of either or both proteins.

Recombinant CBP2 does not interfere with ATP hydrolysis by Mss116

The purification procedure for recombinant CBP2 was optimized yielding large quantities of the protein in excellent quality. Therefore we recommend the use of the protocol established here for further purifications.
The use of sonication for cell disruption seems very efficient, as does the use of a Ni-NTA agarose resin for the purification. The Ni-NTA method appeared to be effective as it binds the protein by its His-tag and is easy to handle. During purification, CBP2 appeared to be a very stable protein and storage at -20°C does not reduce its activity, as experiments performed 1 year after purification showed strong activity. Nevertheless, we recommend performing the purification at 4°C.
Mss116 protein used was received in purified condition and we only determined its activity by an ATPase assay using a Malachite Green Phosphate detection kit. CBP2 activity cannot be measured in this way as it has no ATPase activity. The ATPase assay confirmed that Mss116 bound to RNA is active and CBP2 does not affect the ATPase activity of Mss116.
Thus CBP2 seems not to affect the binding of Mss116 to bI5.

Mss116 does play a role in CBP2-assisted bI5 splicing *in vitro*

While CBP2-assisted bI5 folding has been studied in great detail (Webb & Weeks, 2001; Weeks & Cech, 1996), the role of Mss116 in bI5 splicing remains elusive. At first, we confirmed the ability of CBP2 to promote bI5 splicing under near physiological conditions (7mM Mg^{2+} and 35°C). 25nM CBP2 [f.c.] were sufficient to obtain nearly full splicing of the existent pre-RNA. In contrast, Mss116 did not promote bI5 splicing, suggesting that CBP2 and Mss116 do not have redundant functions in bI5 folding.
CBP2 is known to be a stabilizing factor of the bI5 group I intron by capturing the tertiary structure of the intron (Shaw & Lewin, 1995; Weeks & Cech, 1995b; Weeks & Cech, 1996). By contrast, Mss116 was shown to accelerate the collapse of the ai5γ group II intron *in vitro* (Fedorova et al, 2010). To shed light on the role of an RNA helicase in bI5 folding, we determined the bI5 splicing efficiency by adding Mss116 and CBP2 concomitantly to the denatured bI5 pre-RNA or Mss116 to the native CBP2-bI5 complex. In both cases, the DEAD-box protein did enhance CBP2-assisted bI5 splicing. This is indicated by the fact that the observed rate

constant of splicing is 2-fold – 5.5-fold increased, when compared to that of CBP2-mediated bI5 splicing in the absence of Mss116 (Table 3). When Mss116 and CBP2 were present at higher concentrations during the bI5 folding, the splicing efficiency was only two-fold enhanced. Among other explanations, it is possible that Mss116 disrupts the CBP2-RNA complex to some extent, thereby reducing the splicing efficiency. Importantly, similar results were obtained, when bI5 was pre-folded with CBP2 and Mss116 was added afterwards or both proteins were added concomitantly to the unfolded bI5 intron except for one reaction set up whose data are more ambiguous.

	k_{obs} [min^{-1}]	amplitude [%]
25 nM Cbp2	1	1
25 nM Cbp2 + 25 nM Mss116	3.6	1.0
25 nM Cbp2 + 50 nM Mss116	5.7	0.8
25 nM Cbp2 / 25 nM Mss116	5.5	0.8
25 nM Cbp2 / 50 nM Mss116	1.1	0.3
50 nM Cbp2	1	1
50 nM Cbp2 + 100 nM Mss116	2.2	0.9
50 nM Cbp2 / 50 nM Mss116	2.4	0.9
50 nM Cbp2 / 100 nM Mss116	2.2	1.0

Table 3. Protein-facilitated bI5 splicing.
This summary is based on the k_{obs} values obtained from following the precursor decay (Fig. 25-44, Table 2). The outlier is marked in grey. n.a. stands for not active.

Thus, the time point of Mss116 addition is not a critical determinant; it may influence both earlier and later steps along the CBP2-assisted bI5 folding pathway.

At last, we considered that Mss116 is only required to facilitate folding of the full-length intron. Accordingly, we attempted to identify conditions that allow self-splicing of the natural bI5 intron flanked by short exons in the presence of both splicing factors. So far, splicing of this constructs has not been observed under a variety of conditions. It is well possible that Mss116 is not necessary for proper folding of the large peripheral extensions, but to resolve inhibitory structures within the exons. Such a role has also been proposed for the ai5γ group II intron when embedded within long exons (Fedorova et al, 2010). Due to time constraints, we were not able to follow up on this hypothesis.

Perspectives

In order to determine how CBP2 and Mss116 co-opt to facilitate bI5 splicing, additional experiments have to be conducted. First of all some of the conditions used in this project have to be repeated to gain statistically significant value. Of course, it would also be interesting to reveal if the splicing activity is affected if Mss116 is added to bI5 before CBP2. This set of experiments would further elucidate whether Mss116 indeed enhances CBP2's splicing of bI5 under near physiological conditions *in vitro*.

Investigating the splicing behaviour of the three new constructs will provide more data and help to determine whether the introduced exons or the full intron interferes with the correct fold and therefore influences splicing activity. Mapping of the constructs with bound CBP2 or Mss116 could also shed more light onto the binding specificity and folding of bI5.

To obtain mechanistically relevant data it is essential to assess whether Mss116 is crucial for folding of the large insertion in the loops L1, L6 and L8 or for resolving inhibitory structures in the exons to allow efficient bI5 splicing. In this regard, one has to keep in mind that Mss116 is required for efficient splicing of all 13 yeast mitochondrial introns, thus the downstream exon of one intron is the upstream exon of the neighbouring intron. As such Mss116 may play a role in functional timing of the splicing events of such neighbouring introns, which are bI4 and bI5 in this case.

Literature

1. http://www.emdmillipore.com/

2. http://openwetware.org/wiki/E._coli_genotypes

Abrahams JP, van den Berg M, van Batenburg E, Pleij C (1990) Prediction of RNA secondary structure, including pseudoknotting, by computer simulation. *Nucleic acids research* **18:** 3035-3044

Adams PL, Stahley MR, Kosek AB, Wang J, Strobel SA (2004) Crystal structure of a self-splicing group I intron with both exons. *Nature* **430:** 45-50

Barfod ET, Cech TR (1989) The conserved U.G pair in the 5' splice site duplex of a group I intron is required in the first but not the second step of self-splicing. *Molecular and cellular biology* **9:** 3657-3666

Bass BL, Cech TR (1984) Specific interaction between the self-splicing RNA of Tetrahymena and its guanosine substrate: implications for biological catalysis by RNA. *Nature* **308:** 820-826

Birgisdottir AB, Johansen S (2005) Site-specific reverse splicing of a HEG-containing group I intron in ribosomal RNA. *Nucleic acids research* **33:** 2042-2051

Bokinsky G, Nivon LG, Liu S, Chai G, Hong M, Weeks KM, Zhuang X (2006) Two distinct binding modes of a protein cofactor with its target RNA. *Journal of molecular biology* **361:** 771-784

Buchmueller KL, Webb AE, Richardson DA, Weeks KM (2000) A collapsed non-native RNA folding state. *Nature structural biology* **7:** 362-366

Buchmueller KL, Weeks KM (2003) Near native structure in an RNA collapsed state. *Biochemistry* **42:** 13869-13878

Burke JM (1988) Molecular genetics of group I introns: RNA structures and protein factors required for splicing--a review. *Gene* **73:** 273-294

Butcher SE, Pyle AM (2011) The molecular interactions that stabilize RNA tertiary structure: RNA motifs, patterns, and networks. *Accounts of chemical research* **44:** 1302-1311

Cao W, Coman MM, Ding S, Henn A, Middleton ER, Bradley MJ, Rhoades E, Hackney DD, Pyle AM, De La Cruz EM (2011) Mechanism of Mss116 ATPase reveals functional diversity of DEAD-Box proteins. *Journal of molecular biology* **409:** 399-414

Cate JH, Gooding AR, Podell E, Zhou K, Golden BL, Kundrot CE, Cech TR, Doudna JA (1996) Crystal structure of a group I ribozyme domain: principles of RNA packing. *Science* **273:** 1678-1685

Cech TR (1990) Self-splicing of group I introns. *Annual review of biochemistry* **59:** 543-568

Cech TR (2002) Ribozymes, the first 20 years. *Biochemical Society transactions* **30:** 1162-1166

Cech TR (2009) Crawling out of the RNA world. *Cell* **136:** 599-602

Cech TR (2012) The RNA worlds in context. *Cold Spring Harbor perspectives in biology* **4:** a006742

Cech TR, Damberger SH, Gutell RR (1994) Representation of the secondary and tertiary structure of group I introns. *Nature structural biology* **1:** 273-280

Chamberlin SI, Weeks KM (2003) Differential helix stabilities and sites pre-organized for tertiary interactions revealed by monitoring local nucleotide flexibility in the bI5 group I intron RNA. *Biochemistry* **42:** 901-909

Chen JL, Greider CW (2004) Telomerase RNA structure and function: implications for dyskeratosis congenita. *Trends in biochemical sciences* **29:** 183-192

Clancy S. (2008) RNA Functions. http://www.nature.com/scitable/topicpage/rna-functions-352

Del Campo M, Lambowitz AM (2009) Structure of the Yeast DEAD box protein Mss116p reveals two wedges that crimp RNA. *Molecular cell* **35:** 598-609

Del Campo M, Mohr S, Jiang Y, Jia H, Jankowsky E, Lambowitz AM (2009) Unwinding by local strand separation is critical for the function of DEAD-box proteins as RNA chaperones. *Journal of molecular biology* **389:** 674-693

Del Campo M, Tijerina P, Bhaskaran H, Mohr S, Yang Q, Jankowsky E, Russell R, Lambowitz AM (2007) Do DEAD-box proteins promote group II intron splicing without unwinding RNA? *Molecular cell* **28:** 159-166

Doetsch M, Gstrein T, Schroeder R, Furtig B (2010) Mechanisms of StpA-mediated RNA remodeling. *RNA biology* **7:** 735-743

Doherty EA, Doudna JA (1997) The P4-P6 domain directs higher order folding of the Tetrahymena ribozyme core. *Biochemistry* **36:** 3159-3169

Doonan S, Royal Society of Chemistry (Great Britain) (2004) *Nucleic acids*, Cambridge: Royal Society of Chemistry.

Doudna JA, Cech TR (1995) Self-assembly of a group I intron active site from its component tertiary structural domains. *Rna* **1:** 36-45

Draper DE (2004) A guide to ions and RNA structure. *Rna* **10:** 335-343

Draper DE, Grilley D, Soto AM (2005) Ions and RNA folding. *Annual review of biophysics and biomolecular structure* **34:** 221-243

Engelhardt MA, Doherty EA, Knitt DS, Doudna JA, Herschlag D (2000) The P5abc peripheral element facilitates preorganization of the tetrahymena group I ribozyme for catalysis. *Biochemistry* **39:** 2639-2651

Fairman-Williams ME, Guenther UP, Jankowsky E (2010) SF1 and SF2 helicases: family matters. *Current opinion in structural biology* **20:** 313-324

Fedorova O, Solem A, Pyle AM (2010) Protein-facilitated folding of group II intron ribozymes. *Journal of molecular biology* **397:** 799-813

Gampel A, Cech TR (1991) Binding of the CBP2 protein to a yeast mitochondrial group I intron requires the catalytic core of the RNA. *Genes & development* **5:** 1870-1880

Gampel A, Nishikimi M, Tzagoloff A (1989) CBP2 protein promotes in vitro excision of a yeast mitochondrial group I intron. *Molecular and cellular biology* **9:** 5424-5433

Gampel A, Tzagoloff A (1987) In vitro splicing of the terminal intervening sequence of Saccharomyces cerevisiae cytochrome b pre-mRNA. *Molecular and cellular biology* **7:** 2545-2551

Garcia I, Weeks KM (2003) Small structural costs for evolution from RNA to RNP-based catalysis. *Journal of molecular biology* **331:** 57-73

Garcia I, Weeks KM (2004) Structural basis for the self-chaperoning function of an RNA collapsed state. *Biochemistry* **43:** 15179-15186

Garriga G, Lambowitz AM (1984) RNA splicing in neurospora mitochondria: self-splicing of a mitochondrial intron in vitro. *Cell* **39:** 631-641

Golden BL, Kim H, Chase E (2005) Crystal structure of a phage Twort group I ribozyme-product complex. *Nature structural & molecular biology* **12:** 82-89

Guerrier-Takada C, Gardiner K, Marsh T, Pace N, Altman S (1983) The RNA moiety of ribonuclease P is the catalytic subunit of the enzyme. *Cell* **35:** 849-857

Guo F, Gooding AR, Cech TR (2004) Structure of the Tetrahymena ribozyme: base triple sandwich and metal ion at the active site. *Molecular cell* **16:** 351-362

Halls C, Mohr S, Del Campo M, Yang Q, Jankowsky E, Lambowitz AM (2007) Involvement of DEAD-box proteins in group I and group II intron splicing. Biochemical characterization of Mss116p, ATP hydrolysis-dependent and -independent mechanisms, and general RNA chaperone activity. *Journal of molecular biology* **365:** 835-855

Haugen P, Simon DM, Bhattacharya D (2005) The natural history of group I introns. *Trends in genetics : TIG* **21:** 111-119

Herschlag D (1995) RNA chaperones and the RNA folding problem. *The Journal of biological chemistry* **270:** 20871-20874

Hill J, McGraw P, Tzagoloff A (1985) A mutation in yeast mitochondrial DNA results in a precise excision of the terminal intron of the cytochrome b gene. *The Journal of biological chemistry* **260:** 3235-3238

Huang HR, Rowe CE, Mohr S, Jiang Y, Lambowitz AM, Perlman PS (2005) The splicing of yeast mitochondrial group I and group II introns requires a DEAD-box protein with RNA chaperone function. *Proceedings of the National Academy of Sciences of the United States of America* **102:** 163-168

Ikawa Y, Shiraishi H, Inoue T (2000) Minimal catalytic domain of a group I self-splicing intron RNA. *Nature structural biology* **7:** 1032-1035

Jaeger L, Westhof E, Michel F (1991) Function of P11, a tertiary base pairing in self-splicing introns of subgroup IA. *Journal of molecular biology* **221:** 1153-1164

Jarmoskaite I, Russell R (2011) DEAD-box proteins as RNA helicases and chaperones. *Wiley interdisciplinary reviews RNA* **2:** 135-152

Kruger K, Grabowski PJ, Zaug AJ, Sands J, Gottschling DE, Cech TR (1982) Self-splicing RNA: autoexcision and autocyclization of the ribosomal RNA intervening sequence of Tetrahymena. *Cell* **31:** 147-157

Laggerbauer B, Murphy FL, Cech TR (1994) Two major tertiary folding transitions of the Tetrahymena catalytic RNA. *The EMBO journal* **13:** 2669-2676

Lehmann K, Schmidt U (2003) Group II introns: structure and catalytic versatility of large natural ribozymes. *Critical reviews in biochemistry and molecular biology* **38:** 249-303

Leontis NB, Stombaugh J, Westhof E (2002) The non-Watson-Crick base pairs and their associated isostericity matrices. *Nucleic acids research* **30:** 3497-3531

Leontis NB, Westhof E (1998) Conserved geometrical base-pairing patterns in RNA. *Quarterly reviews of biophysics* **31:** 399-455

Leontis NB, Westhof E (2001) Geometric nomenclature and classification of RNA base pairs. *Rna* **7:** 499-512

Liebeg A, Mayer O, Waldsich C (2010) DEAD-box protein facilitated RNA folding in vivo. *RNA biology* **7:** 803-811

Linder P, Jankowsky E (2011) From unwinding to clamping - the DEAD box RNA helicase family. *Nature reviews Molecular cell biology* **12:** 505-516

Long MB, Jones JP, 3rd, Sullenger BA, Byun J (2003) Ribozyme-mediated revision of RNA and DNA. *The Journal of clinical investigation* **112:** 312-318

Mathews DH, Moss WN, Turner DH (2010) Folding and finding RNA secondary structure. *Cold Spring Harbor perspectives in biology* **2:** a003665

McGraw P, Tzagoloff A (1983) Assembly of the mitochondrial membrane system. Characterization of a yeast nuclear gene involved in the processing of the cytochrome b pre-mRNA. *The Journal of biological chemistry* **258:** 9459-9468

Michel F, Ferat JL (1995) Structure and activities of group II introns. *Annual review of biochemistry* **64:** 435-461

Michel F, Hanna M, Green R, Bartel DP, Szostak JW (1989) The guanosine binding site of the Tetrahymena ribozyme. *Nature* **342:** 391-395

Michel F, Netter P, Xu MQ, Shub DA (1990) Mechanism of 3' splice site selection by the catalytic core of the sunY intron of bacteriophage T4: the role of a novel base-pairing interaction in group I introns. *Genes & development* **4:** 777-788

Michel F, Westhof E (1990) Modelling of the three-dimensional architecture of group I catalytic introns based on comparative sequence analysis. *Journal of molecular biology* **216:** 585-610

Moghaddam S, Caliskan G, Chauhan S, Hyeon C, Briber RM, Thirumalai D, Woodson SA (2009) Metal ion dependence of cooperative collapse transitions in RNA. *Journal of molecular biology* **393:** 753-764

Mohr G, Del Campo M, Mohr S, Yang Q, Jia H, Jankowsky E, Lambowitz AM (2008) Function of the C-terminal domain of the DEAD-box protein Mss116p analyzed in vivo and in vitro. *Journal of molecular biology* **375:** 1344-1364

Mohr G, Del Campo M, Turner KG, Gilman B, Wolf RZ, Lambowitz AM (2011) High-throughput genetic identification of functionally important regions of the yeast DEAD-box protein Mss116p. *Journal of molecular biology* **413:** 952-972

Mohr S, Matsuura M, Perlman PS, Lambowitz AM (2006) A DEAD-box protein alone promotes group II intron splicing and reverse splicing by acting as an RNA chaperone. *Proceedings of the National Academy of Sciences of the United States of America* **103:** 3569-3574

Mohr S, Stryker JM, Lambowitz AM (2002) A DEAD-box protein functions as an ATP-dependent RNA chaperone in group I intron splicing. *Cell* **109:** 769-779

Moore PB (1999) Structural motifs in RNA. *Annual review of biochemistry* **68:** 287-300

Muller J (2010) Functional metal ions in nucleic acids. *Metallomics : integrated biometal science* **2:** 318-327

Murphy FL, Cech TR (1994) GAAA Tetraloop and Conserved Bulge Stabilize Tertiary Structure of a Group I Intron Domain. *Journal of molecular biology* **236:** 49-63

Nielsen H, Fiskaa T, Birgisdottir AB, Haugen P, Einvik C, Johansen S (2003) The ability to form full-length intron RNA circles is a general property of nuclear group I introns. *Rna* **9:** 1464-1475

Nielsen H, Johansen SD (2009) Group I introns: Moving in new directions. *RNA biology* **6:** 375-383

Nobrega FG, Tzagoloff A (1980) Assembly of the mitochondrial membrane system. DNA sequence and organization of the cytochrome b gene in Saccharomyces cerevisiae D273-10B. *The Journal of biological chemistry* **255:** 9828-9837

Ohuchi SJ, Ikawa Y, Shiraishi H, Inoue T (2002) Modular engineering of a Group I intron ribozyme. *Nucleic acids research* **30:** 3473-3480

Pan C, Russell R (2010) Roles of DEAD-box proteins in RNA and RNP Folding. *RNA biology* **7:** 667-676

Pan J, Deras ML, Woodson SA (2000) Fast folding of a ribozyme by stabilizing core interactions: evidence for multiple folding pathways in RNA. *Journal of molecular biology* **296:** 133-144

Pan J, Woodson SA (1998) Folding intermediates of a self-splicing RNA: mispairing of the catalytic core. *Journal of molecular biology* **280:** 597-609

Partono S, Lewin AS (1988) Autocatalytic activities of intron 5 of the cob gene of yeast mitochondria. *Molecular and cellular biology* **8:** 2562-2571

Peebles CL, Perlman PS, Mecklenburg KL, Petrillo ML, Tabor JH, Jarrell KA, Cheng HL (1986) A self-splicing RNA excises an intron lariat. *Cell* **44:** 213-223

Pyle AM, Murphy FL, Cech TR (1992) RNA substrate binding site in the catalytic core of the Tetrahymena ribozyme. *Nature* **358:** 123-128

Rajkowitsch L, Chen D, Stampfl S, Semrad K, Waldsich C, Mayer O, Jantsch MF, Konrat R, Blasi U, Schroeder R (2007) RNA chaperones, RNA annealers and RNA helicases. *RNA biology* **4:** 118-130

Rocak S, Linder P (2004) DEAD-box proteins: the driving forces behind RNA metabolism. *Nature reviews Molecular cell biology* **5:** 232-241

Roman J, Rubin MN, Woodson SA (1999) Sequence specificity of in vivo reverse splicing of the Tetrahymena group I intron. *Rna* **5:** 1-13

Roman J, Woodson SA (1998) Integration of the Tetrahymena group I intron into bacterial rRNA by reverse splicing in vivo. *Proceedings of the National Academy of Sciences of the United States of America* **95:** 2134-2139

Russell R (2008) RNA misfolding and the action of chaperones. *Frontiers in bioscience : a journal and virtual library* **13:** 1-20

Russell R, Zhuang X, Babcock HP, Millett IS, Doniach S, Chu S, Herschlag D (2002) Exploring the folding landscape of a structured RNA. *Proceedings of the National Academy of Sciences of the United States of America* **99:** 155-160

Sachsenmaier N, Waldsich C (2013) Mss116p: a DEAD-box protein facilitates RNA folding. *RNA biology* **10:** 71-82

Schmelzer C, Schweyen RJ (1986) Self-splicing of group II introns in vitro: mapping of the branch point and mutational inhibition of lariat formation. *Cell* **46:** 557-565

Schroeder R, Barta A, Semrad K (2004) Strategies for RNA folding and assembly. *Nature reviews Molecular cell biology* **5:** 908-919

Sclavi B, Sullivan M, Chance MR, Brenowitz M, Woodson SA (1998) RNA folding at millisecond intervals by synchrotron hydroxyl radical footprinting. *Science* **279:** 1940-1943

Sclavi B, Woodson S, Sullivan M, Chance MR, Brenowitz M (1997) Time-resolved synchrotron X-ray "footprinting", a new approach to the study of nucleic acid structure and function: application to protein-DNA interactions and RNA folding. *Journal of molecular biology* **266:** 144-159

Semrad K, Schroeder R (1998) A ribosomal function is necessary for efficient splicing of the T4 phage thymidylate synthase intron in vivo. *Genes & development* **12:** 1327-1337

Seraphin B, Boulet A, Simon M, Faye G (1987) Construction of a yeast strain devoid of mitochondrial introns and its use to screen nuclear genes involved in mitochondrial splicing. *Proceedings of the National Academy of Sciences of the United States of America* **84:** 6810-6814

Seraphin B, Simon M, Boulet A, Faye G (1989) Mitochondrial splicing requires a protein from a novel helicase family. *Nature* **337:** 84-87

Shaw LC, Lewin AS (1995) Protein-induced folding of a group I intron in cytochrome b pre-mRNA. *The Journal of biological chemistry* **270:** 21552-21562

Shaw LC, Lewin AS (1997) The Cbp2 protein stimulates the splicing of the omega intron of yeast mitochondria. *Nucleic acids research* **25:** 1597-1604

Singleton MR, Dillingham MS, Wigley DB (2007) Structure and mechanism of helicases and nucleic acid translocases. *Annual review of biochemistry* **76:** 23-50

Solem A, Zingler N, Pyle AM (2006) A DEAD protein that activates intron self-splicing without unwinding RNA. *Molecular cell* **24:** 611-617

Solem A, Zingler N, Pyle AM, Li- Pook-Than J (2009) Group II Introns and Their Protein Collaborators. In *Non-Protein Coding RNAs*, Dr. Nils G. Walter DSAW, Dr. Robert T. Batey (ed), Vol. 13, 8, pp 167-182. Springer Berlin Heidelberg

Stahley MR, Strobel SA (2006) RNA splicing: group I intron crystal structures reveal the basis of splice site selection and metal ion catalysis. *Current opinion in structural biology* **16:** 319-326

Steiner EM (2012) The activity of recombinant DEAD-Box protein Mss116p : towards its role in the collapse of the Ai5gamma Group II Intron. Zentrum für Molekulare Biologie, Universität Wien, Wien

Strobel SA, Cech TR (1993) Tertiary interactions with the internal guide sequence mediate docking of the P1 helix into the catalytic core of the Tetrahymena ribozyme. *Biochemistry* **32:** 13593-13604

Strobel SA, Ortoleva-Donnelly L, Ryder SP, Cate JH, Moncoeur E (1998) Complementary sets of noncanonical base pairs mediate RNA helix packing in the group I intron active site. *Nature structural biology* **5:** 60-66

Su LJ, Waldsich C, Pyle AM (2005) An obligate intermediate along the slow folding pathway of a group II intron ribozyme. *Nucleic acids research* **33:** 6674-6687

Sullenger BA, Cech TR (1994) Ribozyme-mediated repair of defective mRNA by targeted, trans-splicing. *Nature* **371:** 619-622

Tanner MA, Cech TR (1997) Joining the two domains of a group I ribozyme to form the catalytic core. *Science* **275:** 847-849

Tanner NK, Cech TR (1987) Guanosine binding required for cyclization of the self-splicing intervening sequence ribonucleic acid from Tetrahymena thermophila. *Biochemistry* **26:** 3330-3340

Theimer CA, Feigon J (2006) Structure and function of telomerase RNA. *Current opinion in structural biology* **16:** 307-318

Thirumalai D (1998) Native secondary structure formation in RNA may be a slave to tertiary folding. *Proceedings of the National Academy of Sciences of the United States of America* **95:** 11506-11508

Thirumalai D, Woodson SA (2000) Maximizing RNA folding rates: a balancing act. *Rna* **6:** 790-794

van der Veen R, Kwakman JH, Grivell LA (1987) Mutations at the lariat acceptor site allow self-splicing of a group II intron without lariat formation. *The EMBO journal* **6:** 3827-3831

Van Veldhoven PP, Mannaerts GP (1987) Inorganic and organic phosphate measurements in the nanomolar range. *Analytical biochemistry* **161:** 45-48

Vicens Q, Cech TR (2006) Atomic level architecture of group I introns revealed. *Trends in biochemical sciences* **31:** 41-51

Vicens Q, Cech TR (2009) A natural ribozyme with 3',5' RNA ligase activity. *Nature chemical biology* **5:** 97-99

Waldsich C, Grossberger R, Schroeder R (2002a) RNA chaperone StpA loosens interactions of the tertiary structure in the td group I intron in vivo. *Genes & development* **16:** 2300-2312

Waldsich C, Masquida B, Westhof E, Schroeder R (2002b) Monitoring intermediate folding states of the td group I intron in vivo. *The EMBO journal* **21:** 5281-5291

Waldsich C, Semrad K, Schroeder R (1998) Neomycin B inhibits splicing of the td intron indirectly by interfering with translation and enhances missplicing in vivo. *Rna* **4:** 1653-1663

Webb AE, Rose MA, Westhof E, Weeks KM (2001) Protein-dependent transition states for ribonucleoprotein assembly. *Journal of molecular biology* **309:** 1087-1100

Webb AE, Weeks KM (2001) A collapsed state functions to self-chaperone RNA folding into a native ribonucleoprotein complex. *Nature structural biology* **8:** 135-140

Weeks KM, Cech TR (1995a) Efficient protein-facilitated splicing of the yeast mitochondrial bI5 intron. *Biochemistry* **34:** 7728-7738

Weeks KM, Cech TR (1995b) Protein facilitation of group I intron splicing by assembly of the catalytic core and the 5' splice site domain. *Cell* **82:** 221-230

Weeks KM, Cech TR (1996) Assembly of a ribonucleoprotein catalyst by tertiary structure capture. *Science* **271:** 345-348

Woodson SA (2002) Folding mechanisms of group I ribozymes: role of stability and contact order. *Biochemical Society transactions* **30:** 1166-1169

Woodson SA (2005) Metal ions and RNA folding: a highly charged topic with a dynamic future. *Current opinion in chemical biology* **9:** 104-109

Woodson SA (2010) Taming free energy landscapes with RNA chaperones. *RNA biology* **7:** 677-686

Woodson SA (2011) RNA folding pathways and the self-assembly of ribosomes. *Accounts of chemical research* **44:** 1312-1319

Woodson SA, Cech TR (1989) Reverse self-splicing of the tetrahymena group I intron: implication for the directionality of splicing and for intron transposition. *Cell* **57:** 335-345

Yang Q, Del Campo M, Lambowitz AM, Jankowsky E (2007) DEAD-box proteins unwind duplexes by local strand separation. *Molecular cell* **28:** 253-263

Zarrinkar PP, Williamson JR (1994) Kinetic intermediates in RNA folding. *Science* **265:** 918-924

Zaug AJ, Grabowski PJ, Cech TR (1983) Autocatalytic cyclization of an excised intervening sequence RNA is a cleavage-ligation reaction. *Nature* **301:** 578-583

Zaug AJ, Kent JR, Cech TR (1984) A labile phosphodiester bond at the ligation junction in a circular intervening sequence RNA. *Science* **224:** 574-578

Zemora G, Waldsich C (2010) RNA folding in living cells. *RNA biology* **7:** 634-641

Zingler N, Solem A, Pyle AM (2010) Dual roles for the Mss116 cofactor during splicing of the ai5gamma group II intron. *Nucleic acids research* **38:** 6602-6609

Appendix

Abstract

RNA has to fold into its native fold to carry out its proper functions. The folding pathways vary for different types of RNA. So far, RNA folding principles have mostly derived from catalytic RNA, in particular from group I introns, as native state formation can be measured as a function of catalysis. Group I introns are catalytically active and have self-splicing ability under high magnesium concentrations *in vitro*. At near physiological conditions they require the addition of protein co-factors to promote intron folding and in turn self-splicing. For example, the yeast mitochondrial bI5 group I intron requires the cytochrome b pre-mRNA processing protein 2, CBP2, as an essential co-factor for efficient splicing both *in vitro* and in *S. cerevisiae*. CBP2 stabilizes the bI5 structure by binding in a specific manner to the intron and capturing tertiary interactions. This allows bI5 to reach its native fold and to carry out splicing. *In vivo,* a second protein Mss116 is needed to promote efficient bI5 splicing. Mss116 is a DEAD-box helicase promoting splicing of all mt introns, group I and group II introns, as well as showing unwinding and strand-annealing activity. Both proteins are needed *in vivo* to stimulate efficient splicing. The aim of this diploma thesis was to provide the first insights into the role of Mss116 in CBP2-assisted folding of the bI5 intron *in vitro*. Accordingly, we first adapted the previously published expression and purification protocol for CBP2. After confirming the ability of CBP2 to promote bI5 splicing *in vitro* under near-physiological conditions, we were able to show that CBP2 does not affect the ATPase activity of the DEAD-box helicase Mss116. This allowed us to study the efficiency of bI5 splicing in the absence and presence of either or both proteins. We determined the bI5 splicing efficiency by adding Mss116 and CBP2 concomitantly to the denatured bI5 pre-RNA or Mss116 to the native CBP2-bI5 complex. In both cases, the DEAD-box protein did enhance CBP2-assisted bI5 splicing. This is indicated by the fact that the observed rate constant of splicing is 2-fold – 5.5-fold increased, when compared to that of CBP2-mediated bI5 splicing in the absence of Mss116. When Mss116 and CBP2 were present at higher concentrations during the bI5 folding, the splicing efficiency was only 2-fold enhanced. Among other explanations, it is possible that Mss116 disrupts the CBP2-RNA complex to some extent, thereby reducing the splicing efficiency. Thus, the time point of Mss116 addition is not a critical determinant; it may influence both earlier and later steps along the CBP2-assisted bI5 folding pathway. At last, we considered that Mss116 is only required to facilitate folding of the full-length intron. Accordingly, we attempted to identify conditions that allow self-splicing of the natural bI5 intron flanked by short exons in the presence of both splicing factors. So far, splicing of this constructs has not been observed under a variety of conditions. It is well possible that Mss116 is not necessary for proper folding of the large peripheral extensions, but to resolve inhibitory structures within the exons. Such a role has also been proposed for the ai5γ group II intron when embedded within long exons.

Zusammenfassung

Um ihre Funktionen korrekt ausführen zu können muss RNA in ihrer nativen Faltungsform vorhanden sein. Der Faltungsweg hängt von der jeweiligen RNA-Art ab. Bisher wurden RNA-Faltung an katalytisch aktiven RNAs, besonders an Gruppe I Introns untersucht, da die Ausbildung ihres natürlichen Faltungszustandes als katalytische Funktion gemessen werden kann. Introns der Gruppe I sind katalytisch aktiv und können *in vitro*, in Verbindung mit hoher Magnesiumkonzentration, selbst-spleißen. Unter nahezu physiologischen Bedingungen benötigen sie zusätzlich Protein Co-Faktoren, welche die Intronfaltung begünstigen und damit auch das Selbst-spleißen. Zum Beispiel benötigt das mitochondriale bI5 Gruppe I Intron aus Hefe zusätzlich das Cytochrom B pre-mRNA Prozessierungsprotein 2, CBP2, als Co-Faktor für effizientes Spleißen *in vitro* und in *S.cerevisiae*. CBP2 stabilisiert die Struktur von bI5, wenn es spezifisch an das Intron bindet und ermöglicht die Ausbildung von Tertiärstrukturen. Diese Bindung ermöglicht bI5 seine natürliche Faltungsform zu erreichen wodurch das Intron spleißen kann. *In vivo* wird ein weiteres Protein, Mss116, benötigt um ein effektives Spleißen einzuleiten. Mss116 gehört zu der Gruppe von DEAD-box Helikasen, die das Spleißen aller mitochondrialen Introns, Gruppe I und Gruppe II begünstigt, sowie für das Aufwinden und Strang-Annealing benötigt wird. Beide Proteine gemeinsam werden zum Spleißen *in vivo* benötigt. Das Ziel dieser Diplomarbeit ist erste Erkenntnisse über die Rolle von Mss116 bei CBP2-unterstützter Faltung vom bI5 Intron *in vitro* zu gewinnen. Dementsprechend haben wir zuerst das Expressions- und Aufreinigungsprotokoll für CBP2 angepasst. Nach erfolgreicher Bestätigung, dass CBP2 das bI5 Spleißen *in vitro* unter nahezu physiologischen Bedingungen begünstigt, haben wir gezeigt, dass CBP2 keinen Einfluss auf die ATPase Aktivität von Mss116 hat. Dies erlaubte uns weiter das Spleißverhalten von bI5 in Abwesenheit sowie Anwesenheit von einem oder beiden Proteinen zu untersuchen. Wir bestimmten die Spleißeffizienz von bI5 durch gleichzeitige Zugabe von Mss116 und CBP2 zu der denaturierten bI5 pre-RNA oder durch Zugabe von Mss116 zum CBP2-bI5 Komplex. In beiden Fällen förderte Mss116 das CBP2-unterstütze bI5 Spleißen. Dies wird durch die 2-fach – 5.5-fach erhöhte Geschwindigkeitskonstante, verglichen mit CBP2-unterstütztem bI5 Spleißen in Abwesenheit von Mss116, gezeigt. Wenn sowohl Mss116 als auch CBP2 in höherer Konzentration vorhanden waren, stieg die Spleißrate nur 2-fach an. Eine Erklärung dafür wäre, dass Mss116 den CBP2-RNA Komplex bis zu einem gewissen Grad stört und somit die Spleißeffizienz senkt. Folglich ist der Zeitpunkt der Mss116-Zugabe kein entscheidender Faktor; Mss116 dürfte sowohl frühere als auch spätere Faltungsschritte während dem CBP2-unterstützten bI5 Faltungsweg beeinflussen. Zuletzt erwogen wir die Möglichkeit, dass Mss116 nur benötigt wird um die Faltung von vollständigem Intron zu begünstigen. Dementsprechend untersuchten wir verschiedene Bedingungen, welche das Selbst-spleißen des vollständigen bI5 Introns mit kurzen Exons in Anwesenheit beider Spleißfaktoren ermöglichen würden. Bisher wurde aber kein Spleißen dieses Konstruktes unter verschiedensten Bedingungen beobachtet. Es ist möglich, dass Mss116 nicht unbedingt für die korrekte Faltung von großen peripheren Verlängerungen notwendig ist, jedoch für die Auflösung inhibitorischer Strukturen in den Exons. Solch eine Rolle wurde auch beim ai5γ Gruppe II Intron, welches lange Exons enthält, vorgeschlagen.

Sequences

All sequences are shown in 5'→ 3' direction.

- CBP2 ORF

ATGGTGAATTGGCAAACATTGTTCATGGTCTCATTGAGGAGACAGGGCAGTTCCTCTCGTTACAGGTATAAGTTCAACATGGAGA
ATATCACACATCAGGTGTTCCCTCGCTGTAAGCAAGCGTTTAAGAAGACAAACTTATCTTATGAATATTGTGATCTTGAAGGAGTA
CTGTATAATATTTCACTCACGGACTTGCAAAAACTGCTATTACGTGATATAAACGCCCCTCGCGAACACGCATTCAAGATTGTTAG
AACAGATCTAACTCAAAAATCCTCGAAGAAGAGGATCCAACACTGGGAACGGATTGCGCCTATGTTTGACCACCCCTTAAGTCTC
TACGAGAAGTTGTTCAGCGAAATGGATGAGGACTTCAAGCCATCTTTCGAGTGGCAACAATTAATAAGGGTACGATGCAAAGAT
GATAAGTTGAAACTGCAGCGTGTAATTTGGCCTAAGTCGATATTTTCAAACTTTTGTCGGGGAATCGGGGTTAAGAAGAGCACTT
ACGATAGACTCTTGGAACAAAATAATGGTGAGGTACCCATGTTTGTAAACCCAGCTAATGCAAAGCCCTTGCCTCTTTTCCAGGTT
TCCGATGAGGCGATGATTGGGGAATTCGATGGAATTGGTATTTTCCCTTACTTTGTAGATAAACATAGAGAATTTTTCGTTACTGA
GGTAGACAAATTGAAGACCAAGATAGCTTCGCCACTTTGCACCTTGAATGAACGAAAGCGCATTGAGAAGGCTAACGCTGGTCG
GATACTGGCGAACGAAGAGGGTAAACCATTCTATCTGGATGCAAACAGTGCCACAACTCGAATCGCTGGTGGTAATGTCGTCACT
TTGAAGCAACTTTTAGAAAGATCGGTTAGCCATAAGACATTGTGGAGCAAACAATCAAACAAAGACAGAACGTGCCCTGGAGAC
ATTTTAAGAGCTACAATATTATCAAACGACTTCTCCATCCGGCAATTGAGGGCTGAATTTTGCAAAAATTTCATTCTCTACAATATA
TTCACCATTTTACAACGTAACAAGAAAAGCATCCGTTCCTTCTCTGGTAACGATAATGCGCCTTCCTTTCAATTTAGTTGGAATGTT
TGGGACTCATATATATGGAAGCAATATCAAGAGACCGAGTCCATGAAAATACCCACGGACCAAGCTTCTCTGATCAACTACAAGA
CAAAATACGACTCTTTTCTTCATGACCTACAAACATATTCCGCACTGGTAATTTCAGAAATGAAATGGAACCAATTCTCTATTTTCC
AAAATGATGAAACGACTTTATCAAGATTTGAACACATCACATTAATTTTGCAAACCGTGCTGACAAAATCGAAAATGATTAGAATT
TTCCAGCCAAACTTGTACAAGTTTATGCAAGATGATTTAAGACCAACTTTAATGGAGTTGGTGGGTTTCACTGAGTCAATAAATGC
AACAATAGAACCTGGTTTTGCGAATGAACAATCGCTACAATCTGCAAACGGATTAAAGAAATTGGCCAACCAACTTTTATACTTCG
AACAGGAAATATATGGCGAAAAGTTCCGCGTAAATAGGCCCATCCAGCTTCGTCCAATAACATTATCAGCAAACTACAAAATTGT
TATTCTGGATAAGAAGAACGCCATACCCGAAATATTTCAAACCCTACTGAAATTCATGACACAAATAACGACATATTTTGTTAAAG
ATTTGTCGGAGGTAGAACTTCATGGGCACATGCATTGTATTGATAAAAAAATGCTGGACAAGTCGAAATTCATGTATTTATACGA
AGAGAAAAGCAACGAGGAAGTGAAAGCAGCTTCTCCTCAAAAGGAGAAGATAGTAGATAATATCATTGGCCTATTATCAAATGA
TGAAGAACATTAA

- bI5core construct received from K. M. Weeks

TAATACGACTCACTATAGGGAATTCGAGCTCGCCCGGGGATCATTAAACATGATTGAAGAAATAATAATAGTTTATGAAAT
AAGATAGTGTAATATAAATTTTTATGAAGATATAGTCCATTTTATATTTATTATAAAAGCATCCTGATAACTATATTCCTGGT
AATCCTTTAGTAACACCAGCATCTATTGATATTAAAAAAGTACAGTAGCATTAAATATTCTTAAGTTTCCGCTTTGTGGGAA
CTCCCATAAGGAGTTTAATGATTAAAATTGGTTAATTGTCAAGAAAATCTAAGGTATTAATAAATAAATAATACTATGACAA
CTTGCAGCGAAGTTTATATCATCTCTATACTTCGGTATAAGATATAAAAACGTTCAACGACTAGAAAGTGAACTGAGATAG
TAATACCTTTCCACGAAAACCAATTAATTTATAAAGATCTTTATAAATTAATGACATAGTCTGAACAATAATGAAAATTATTG
AGATAAGATATTAAATAATCTTATGTTAACATATATAAATTGTGTACCTGAATGATACTTATTACCATTCTATGCTATTTTAA
GATC

flanking exons

T7-promotor sequence

intron

IGS (and complementary exon sequences)

- Ribozyme construct (rc)

GAATTCCGTAATACGACTCACTATAGGGCAGTAGCATTAAATATTCTTAAGTTTCCGCTTTGTGGGAACTCCCATAAGGAGT
TTAATGATTAAAATTGGTTAATTGTCAAGAAAATCTAAGGTATTAATAAATAAATAATACTATGACAACTTGCAGCGAAGTT
TATATCATCTCTATATTATATATTAATATATATATAATAATAATAATAATATTAATATAATATAAGATATAAAAACGTTCA
ACGACTAGAAAGTGAACTGAGATAGTAATACCTTTCCACGAAAACCAATTAATTTATAAATTATTTTTAAATAAAGAATAGA
TTATTAATTTTTTTTTATATAGTTCCGGGCCCCGGCCACGGGAGCCGGAACCCCGGAAGGAGTAATATATATTATATATAAA
ATAAAAAATATATATATATATATTATAAAATATCAAAAGTTTTAATCTTTTATTATAAATTAATGACATAGTCTGAACAATAA
TGAAAATTATTGAGATAAGATATTAAATAATCTTATGTTAACATATATAAATTGGATCC

Insertions in L6b and L8 (deleted in the ribozyme construct used for *in vitro* studies –(Weeks & Cech, 1995a)

restriction site

- Full intron (fi) construct

GAATTCCGTAATACGACTCACTATAGGGCTATTGATATTAAAAATATTAATAAAATTATTATTATTTAATCTTATTTATTTTAT
ATAAAAAAAATAAATAATAATTATTAATAAAAATATATTATTTATTTCTCCTTTCGGGGTTATTTATATATATTCCTTTATAAT
TTATATTTAATATATTATATTAAATATATGAAAAATTATAATAAATAAATTAATTAATTAATTAATAATAAATAATAATAAAA
AGTACAGTAGCATTAAATATTCTTAAGTTTCCGCTTTGTGGGAACTCCCATAAGGAGTTTAATGATTAAAATTGGTTAATTG
TCAAGAAAATCTAAGGTATTAATAAATAAATAATACTATGACAACTTGCAGCGAAGTTTATATCATCTCTATATTATATATTA
ATATATATATATAATAATAATAATAATTATTAATATAATATAAGATATAAAAACGTTCAACGACTAGAAAGTGAACTGAGATA
GTAATACCTTTCCACGAAAACCAATTAATTTATAAATTATTTTTAAATAAAGAATAGATTATTAATTTTTTTTTATATAGTTCC
GGGCCCCGGCCACGGGAGCCGGAACCCCGGAAGGAGTAATATATATTATATATAAAATAAAAAATATATATATATATATT
ATAAAATATCAAAAGTTTTAATCTTTTATTATAAATTAATGACATAGTCTGAACAATAATGAAAATTATTGAGATAAGATAT
TAAATAATCTTATGTTAACATATATAAATTGGATAAGATATTAAATAATCTTATGTTAACATATATAAATTGTGTACCTGAAT
GATACTTATTACCATTCGGATCC

Insertions in L1, L6b and L8 (deleted in the ribozyme construct used for *in vitro* studies –(Weeks & Cech, 1995a)

- 25/25 nts exon (25/25) construct sequence

GAATTCCGTAATACGACTCACTATAGGGTCCTTTAGTAACACCAGCATCTATTGATATTAAAAATATTAATAAAATTATTATT
ATTTAATCTTATTTATTTTATATAAAAAAAATAAATAATAATTATTAATAAAAATATATTATTTATTTCTCCTTTCGGGGTTAT
TTATATATATTCCTTTATAATTTATATTTAATATATTATATTAAATATATGAAAAATTATAATAAATAAATTAATTAATTAATT
AATAATAAATAATAATAAAAAGTACAGTAGCATTAAATATTCTTAAGTTTCCGCTTTGTGGGAACTCCCATAAGGAGTTTAA
TGATTAAAATTGGTTAATTGTCAAGAAAATCTAAGGTATTAATAAATAAATAATACTATGACAACTTGCAGCGAAGTTTATA
TCATCTCTATATTATATATTAATATATATATAATAATAATAATAATTAATATAATATAAGATATAAAAACGTTCAACGA
CTAGAAAGTGAACTGAGATAGTAATACCTTTCCACGAAAACCAATTAATTTATAAATTATTTTTAAATAAAGAATAGATTAT
TAATTTTTTTTTTATATAGTTCCGGGCCCCGGCCACGGGAGCCGGAACCCCGGAAGGAGTAATATATATTATATATAAAATA
AAAAATATATATATATATATTATAAAATATCAAAAGTTTTAATCTTTTATTATAAATTAATGACATAGTCTGAACAATAATGA
AAATTATTGAGATAAGATATTAAATAATCTTATGTTAACATATATAAATTGTGTACCTGAATGATACTTATTACCATTCGGAT
CC

- 50/100 nts exon (50/100) construct sequence

GAATTCCGTAATACGACTCACTATAGGGCATCCTGATAACTATATTCCTGGTAATCCTTTAGTAACACCAGCATCTATTGATATTA
AAAATATTAATAAAATTATTATTATTTAATCTTATTTATTTTATATAAAAAAAATAAATAATAATTATTAATAAAAATATATTA
TTTATTTCTCCTTTCGGGGTTATTTATATATATTCCTTTATAATTTATATTTAATATATTATATTAAATATATGAAAAATTATAA
TAAATAAATTAATTAATTAATTAATAATAAATAATAATAAAAGTACAGTAGCATTAAATATTCTTAAGTTTCCGCTTTGTGG
GAACTCCCATAAGGAGTTTAATGATTAAAATTGGTTAATTGTCAAGAAAATCTAAGGTATTAATAAATAAATAATACTATG
ACAACTTGCAGCGAAGTTTATATCATCTCTATATTATATATTAATATATATATAATAATAATAATAATATTAATATAATAT
AAGATATAAAAACGTTCAACGACTAGAAAGTGAACTGAGATAGTAATACCTTTCCACGAAAACCAATTAATTTATAAATTA
TTTTTAAATAAAGAATAGATTATTAATTTTTTTTTATATAGTTCCGGGCCCCGGCCACGGGAGCCGGAACCCCGGAAGGAG
TAATATATATTATATATAAAATAAAAAATATATATATATATATTATAAAATATCAAAAGTTTTAATCTTTTATTATAAATTAAT
GACATAGTCTGAACAATAATGAAAATTATTGAGATAAGATATTAAATAATCTTATGTTAACATATATAAATTGTGTACCTGA
ATGATACTTATTACCATTCTATGCTATTTTAAGATCTATTCCTGATAAATTATTAGGAGTTATTCTAATGTTTGCAGCTATTTTACGG
GATCC

- Incorrect 50/100 construct sequence

TTAGTAACACCAGCATCACCTGGCGCTTCGCCAGTTTGTGACCGCAGTAAAAGCGGGCGAGCAGGTCATAGCAGCCGTAA
ATCAGATAGCTGACGACCACCAGCCCGACCGCACTAAGCAGCGCAACGCGATTGTAGTCGCGGATGACCTTCCAGACCTC
TTCCCAGTCCACTTTTTTGGCGTAGACCACCAGCAACACAATCACCGCGATAAAAAACAGCCAGGTGAGGATCTTCTTTGCT
AAGCGCCAGCGCGGGTGTGATTTACTCATCAGGGTTTTACCCCCGTGTTTTCAGTTTCTACCCGATCCTGCGTTTCCATTGT
CGGTTGTGCGGGCGGATCAACCTGCGCCAGACGTGGCGTGTGTGCCGGAAGCCAGCCAACCAGCGCCGGGAAGTGGCGT
AAAAAGTGGAACGCCAGCACGCTTTTGGTCAGGTTCCACCAGGTGCGTTTGGGCAGCATGGTTTCATCCACCTGCTGACAA
TCTGCGGCAATAATGCCGTTCAGATTATCGCGCAGCGTCTGGTTAAAATGACGATCGTGGATGATGACATTTGCTTCGAGA
TTCAGTGACAAACTGAGCGGATCGAGATTACTGGACCCTACTGTCGCCCAGTGATCGTCCATCAATGCCACTTTGCCGTGG
AGCGGGCGGCGGCGGTACTCAAAAACCTGAACGCCGCCTTTAACCAGATAGTTATACAGCAAGCGCGCACCGACTCTGAC
AATCGGCATATCCGGTTCGCCCTGAATGATACTTATTACCATTCTATGCTATTTTAAGATCTATTCCTGATAAATTATTAGGA
GTTATTCTAATGTTTGCAGCTATTT

Correct extended exons

Incorrect intron sequence

Curriculum vitae

Personal information

Name:	Franka Debeljak
Address:	Welzergasse 36 2500 Baden Austria
Phone:	+43 664 6322 830
E-mail:	frankadebeljak@hotmail.com
Birthday and –place:	14. December 1987, Zagreb (Croatia)
Nationality:	Austria

Education

October 2006 -	Diplomstudium Molecular biology at the University of Vienna • Field of studies: immunology, molecular medicine, biochemistry
November 2011 – May 2013	Diploma-thesis in the laboratory of Dr.Christina Waldsich at the Institute of Biochemistry and Cell Biology – University of Vienna • Thesis: The influence of the RNA helicase Mss116 on CBP2-assisted splicing of the bI5 group I intron *in vitro*
1998 – 2006	Secondary school BG & BRG Baden Biondekgasse • Humanistic secondary school with Latin and Ancient Greek • Participation at the Austrian Chemistry Olympiad (2006)
1994 – 1998	Primary school in Baden bei Wien

Research Experience

May 2011 – June 2011	Internship in the field of Immunology in the laboratory of Univ.- Prof. Dipl.-Ing. Dr. Barbara Bohle (Department of Pathophysiology and Allergy Research, Medical University Vienna) • Title: Development of new candidates for allergen specific immunotherapy: expression, purification and characterizations
February 2011 – March 2011	Internship in the field of Molecular Medicine in the laboratory of Univ. Prof. Dr. med. univ. Jasminka Godnic- Cvar (Department of Occupational medicine, Medical University Vienna) • Title: DCF use for the detection of oxidative stress
November 2010 – December 2010	Internship in the field of Biochemistry in the laboratory of Dr. Christina Waldsich (Institute of Biochemistry and Cell biology, University of Vienna) • Title: Folding of Telomerase RNA *in vitro*

Research work experience

January 2013	Tutor at practical course in biochemistry • Tasks: Supervision of students during a three week practical course at the University of Vienna
April 2011 – October 2011	Laboratory employee at the Department of Occupational Medicine at the Medical University Vienna • Tasks: Working on the cytotoxicity and genotoxicity of nanoparticles on human fibroblasts *in vitro*

Publications and presentations

- Book
  Sachsenmaier N.; Handl S.; Debeljak F. *In vitro* chemical probing of RNA with DMS, CMCT and Kethoxal. In *RNA Folding: Methods and Protocols (Methods in Molecular Biology)*; Waldsich C., Ed., Humana Press: 2014 *(in press)*

- Poster
  F. Debeljak, A.Girard, K.Klien, A.C.Budinsky, A.Pilger, L.Richter, P.Ertl, J.Godnic-Cvar (2011, November). *Zytotoxische und genotoxische Effekte von Eisen-Cobalt-Bor Nanopartikel auf humane Fibroblasten in vitro* (*engl. Cytotoxicity and genotoxicity effects of iron-cobalt-bor nanoparticles on human fibroblasts in vitro*). Poster presented at Jahrestagung der österreichischen Gesellschaft für Arbeitsmedizin 2011, Wien.

Other work experience

October 2010 – September 2011	Employee at Beethoven-Cinema Baden
May 2007 – January 2008	Employee at Monsoon & Accessorize (Vienna)
October 2005 – October 2011	Employee at Sparkasse Baden • Working in the real estate department and credit department
July 2005	Internship at Sparkasse Baden in the real estate department